



**STUDY ON MECHANICAL AND THERMAL  
BEHAVIOR OF THE LIGHTWEIGHT  
AGGREGATE GEOPOLYMER CONCRETE  
(LWAGC) USING FLY ASH**

**By**

**OMAR A.K.A. ABDULKAREEM**

**(1040410517)**

A thesis submitted  
In fulfillment of the requirements for the degree of  
Doctor of Philosophy

**SCHOOL OF MATERIALS ENGINEERING  
UNIVERSITI MALAYSIA PERLIS**

**2014**

# THESIS DECLARATION

UNIVERSITI MALAYSIA PERLIS

## DECLARATION OF THESIS

Author's full name : **OMAR A.K.A. ABDULKAREEM**  
Date of birth : **18/8/1983**  
Title : **STUDY ON THE MECHANICAL AND THERMAL BEHAVIOR OF THE LIGHTWEIGHT AGGREGATE GEOPOLYMER CONCRETE (LWAGC) USING FLY ASH**  
Academic Session : **2013-2014**

I hereby declare that the thesis becomes the property of Universiti Malaysia Perlis (UniMAP) and to be placed at the library of UniMAP. This thesis is classified as :

- CONFIDENTIAL** (Contains confidential information under the Official Secret Act 1972)\*  
 **RESTRICTED** (Contains restricted information as specified by the organization where research was done)\*  
 **OPEN ACCESS** I agree that my thesis is to be made immediately available as hard copy or on-line open access (full text)

I, the author, give permission to the UniMAP to reproduce this thesis in whole or in part for the purpose of research or academic exchange only (except during a period of \_\_\_ years, if so requested above).

Certified by:

\_\_\_\_\_

**SIGNATURE**

**G2031828**

**(NEW IC NO. / PASSPORT NO.)**

Date:

\_\_\_\_\_

**SIGNATURE OF SUPERVISOR**

**Datuk. Prof. Dr. Kamarudin Hussin**

**NAME OF SUPERVISOR**

Date:

NOTES: \* If the thesis is CONFIDENTIAL or RESTRICTED, please attach with the letter from the organization with period and reasons for confidentiality or restriction

## ACKNOWLEDGEMENT

بِسْمِ اللَّهِ الرَّحْمَنِ الرَّحِيمِ

*In The Name of Allah The Most Gracious and The Most Merciful With The Selawat and Salam to Prophet Mohammad SAW.*

*Alhamdulillah and thankfulness to my almighty (Allah SW), who gives me the commitment and strength to finish this work. Uncountable thanks are also directed to my parents for their love and bless. They always provide me with strength, support, patience and encouragement to face the challenges with a fighter spirit. I will always grateful to them and for my brother and sisters for their continued moral support during my PhD. Their doa'a and blessing have allowed me to complete my thesis successfully.*

*I would like to express my gratitude and thanks to my supervisor Datuk. Prof. Dr. Kamarudin Hussin for his encouragements and supports during my PhD. journey. Also most sincere thanks to my co-supervisor Assoc. Prof. Dr. Khairul Nizar Ismail for his supervision and guidance during my thesis writing. I would like to thanks Mr. Mohd. Mustafa Al-Bakri Abdullah for many insightful discussion and helpful criticism. Without their help, I would not have been able to achieve what I have achieved.*

*I dedicated special thanks to all technicians and collages at school of Materials Engineering, University of Malaysia Perlis (UniMAP) and Center of Excellence Geopolymer & Green Technology (CEGeoTech) for their support and help during the practical work of this work, especially Mr. Azmi.*

*Last but not least, I am thankful to all my friends for the moments I shared with them. I pray to Allah for them to achieve nothing but success in this life and the next.*

**Omar A. Abdulkareem**  
**eng.omar83@yahoo.com**

## TABLE OF CONTENTS

	<b>PAGE</b>
<b>THESIS DECLARATION</b>	i
<b>ACKNOWLEDGEMENT</b>	ii
<b>TABLE OF CONTENTS</b>	iii
<b>LIST OF FIGURES</b>	xi
<b>LIST OF TABLES</b>	xvi
<b>LIST OF ABBREVIATIONS</b>	xviii
<b>LIST OF SYMBOLS</b>	xx
<b>ABSTRAK</b>	xxiii
<b>ABSTRACT</b>	xxiv
<b>CHAPTER 1 INTRODUCTION</b>	
1.1 Background	1
1.2 Problem Statement	5
1.3 Research Scope	7
1.4 Research Objectives	9
1.5 Contribution of Research	9
<b>CHAPTER 2 LITERTURE REVIEW</b>	
2.1 Introduction	11
2.2 Concrete	12
2.3 Types of Concrete	13
2.4 Structural Lightweight Aggregate Concrete (LWAC)	14
2.4.1 Historical Background of LWAC	15
	iii

2.4.2 Lightweight Aggregate (LWA)	17
2.5 Concrete and Environment	19
2.6 Introduction of Geopolymers	21
2.7 Constituents of Geopolymers	23
2.7.1 Source Materials	23
2.7.1.1 Fly Ash (FA)	25
2.7.2 Alkaline Activator	28
2.8 The Mechanism of the Geopolymerization Reaction	29
2.9 Fly Ash (FA) Geopolymer	32
2.9.1 Factors Influencing the FA Geopolymer Synthesis	33
2.9.1.1 The FA Origin and Composition	33
2.9.1.2 Types and Composition of the Alkaline Activator	36
2.9.1.3 Curing Temperatures	39
2.9.1.4 Curing Duration	41
2.9.2 Structure of FA Geopolymers	43
2.9.3 Microstructure of FA Geopolymers	45
2.9.4 Thermo-Physical Characteristics of FA Geopolymer	47
2.10 The Use of Geopolymers in Production of the LWAGC	54
2.11 Summary of Chapter	62
 <b>CHAPTER 3 RESEARCH METHODOLOGY</b>	
3.1 Introduction	63

3.2 Raw Materials	63
3.2.1 Fly Ash (FA)	65
3.2.1.1 The Chemical Composition	65
3.2.1.2 Particle size distribution	65
3.2.1.3 Microstructure	65
3.2.1.4 Phase Composition	66
3.2.2 Alkaline activator solution	66
3.2.2.1 Sodium Hydroxide Solution (NaOH)	66
3.2.2.2 Sodium Silicate Liquid ( $\text{Na}_2\text{SiO}_3$ )	67
3.2.3 Fine Aggregate (sand)	68
3.2.4 Lightweight Aggregate (LWA)	72
3.2.4.1 Density and Water Absorption of the LWA	73
3.2.4.2 Particle Size Distribution	74
3.3 Designing of the Lightweight Aggregate Geopolymer Concrete (LWAGC)	75
3.4 Actual Design of Lightweight Aggregate Geopolymer Concrete (LWAGC)	79
3.4.1 Optimum NaOH Solution Molarity	80
3.4.2 Optimum Mass Ratio of $\text{Na}_2\text{SiO}_3/\text{NaOH}$	81
3.4.2.1 Procedure of Optimizing the Mass Ratio of $\text{Na}_2\text{SiO}_3/\text{NaOH}$	81
3.4.3 Optimum Curing Temperatures	82
3.4.3.1 Procedure of Optimizing the Curing Temperatures	83
3.4.4 Optimum Curing Periods	83
3.4.4.1 Procedure of Optimum Curing Periods	84

3.5 First Trail Mixing of the LWAGC	84
3.5.1 Alkaline Activator Preparation	86
3.5.2 Preparation of the Aggregates (fine/LWA)	86
3.5.3 Mixing and Slump Measurement	87
3.6 Final Mix Design of the LWAGC	88
3.7 Synthesizing of the Lightweight Aggregate Geopolymer Concrete (LWAGC)	89
3.7.1 Mixing and Molding of LWAGC	89
3.7.2 Curing and Aging Conditions	89
3.8 Synthesizing of the Geopolymer Pastes and Mortar	90
3.9 Preparation of FA Geopolymer Pastes and LWAGCs with Different Activator/FA Mass Mixing Ratios	91
3.10 Synthesizing of LWAGCs with Different LWA Particle size and Grading	92
3.10.1 Synthesizing Procedure of LWAGCs with Different LWA Particle Size and Grading	93
3.11 Studies on the Thermal Behavior of the Geopolymeric Materials	94
3.11.1 Study on the Effect of Elevated Temperatures on the Compressive Strength of the Geopolymer Paste, Mortar and LWAGC	94
3.11.1.1 Procedure of Exposing to Elevated Temperatures	95
3.11.2 Study on the Residual Strength of the LWAGC after Heating at Temperature Range of (100 °C to 800 °C)	95
3.11.2.1 Test Procedure	95

3.11.3 Study on the Effect of the LWA Particle Size and Grading on the Thermal Behavior of the LWAGCs after Exposure to Elevated Temperature of 800 °C	96
3.11.3.1 Test Procedure	96
3.12 Analysis Methods of the Geopolymeric Materials Properties	96
3.12.1 Analysis methods of the Geopolymeric Materials Physical Properties	96
3.12.1.1 Slump Test	97
3.12.1.2 Density and Water Absorption Measurements	97
3.12.1.3 Total Porosity Content Measurement	98
3.12.2 Mechanical Compressive Strength Evolution	99
3.12.3 Microstructure Properties	100
3.12.4 Thermogravimetric Analysis	100
3.12.5 Dilatometry Measurements	101
3.12.6 Phase Composition Investigation	103
3.13 Test Program of the Research Methodology	103

## **CHAPTER 4 RESULTS AND DISCUSSIONS**

4.1 Introduction	105
4.2 Evaluations of the Mechanical and Physical Properties of FA Geopolymer Materials at Room Temperature	105
4.2.1 Analysis of the Raw Materials	106
4.2.1.1 Analysis of the FA	106

4.2.1.1.1	The Chemical Composition of the FA (XRF Analysis)	106
4.2.1.1.2	Particle Size Distribution of the FA	107
4.2.1.1.3	Microstructure of the FA (SEM Analysis)	109
4.2.1.1.4	The Phase Composition of the FA (XRD Analysis)	110
4.2.1.2	Analysis of Sand	110
4.2.1.2.1	Density and Water Absorption of the Sand	111
4.2.1.2.2	Particle Size Analysis	111
4.2.1.3	Analysis of LWA	112
4.2.1.3.1	Density and Water Absorption Analysis	112
4.2.1.3.2	Particle Size Distribution	113
4.2.2	Actual Design of the LWAGC	114
4.2.2.1	Optimum $\text{Na}_2\text{SiO}_3/\text{NaOH}$ Mass Ratio	115
4.2.2.2	Optimum Curing Temperature	117
4.2.2.3	Optimum Curing Period	119
4.2.3	Physical and Mechanical Properties of FA Geopolymer Paste, Mortar and LWAGC at 28 Days of Age	120
4.2.4	LWAGC Compressive Strength Developing Versus Aging Times	124
4.2.5	Effect of Activator/FA Mass Ratio on the Workability and Compressive Strength of the FA Geopolymer Paste and LWAGC	125
4.2.6	Effects of LWA Particle Size and Grading on the Physical and Mechanical Properties of LWAGC	128

4.2.6.1 Effect of LWA Particle Size and Grading on the Workability of the Fresh LWAGC Mixtures	129
4.2.6.2 Effects of LWA Particle Size and Grading on the Density and Mechanical Strength Properties of Hardened LWAGCs	131
4.2.6.3 Effects of LWA Particle Size and Grading on the Water Absorption and Total Porosity Characteristics of Hardened LWAGCs	135
4.3 FA Geopolymer Materials Thermo-Mechanical and Macro/Microstructure Evolution	138
4.3.1 Effect of Elevated Temperatures on the Thermal Behavior of the FA Geopolymer paste, Mortar and LWAGC	138
4.3.1.1 Thermo-Physical Properties of the Geopolymer Paste	141
4.3.1.2 Physical Observation of the Exposed FA Geopolymer Paste, Mortar and LWAGC to the Elevated Temperatures	146
4.3.1.3 Microstructural Analysis of the Exposed FA Geopolymer Paste and LWAGC to the Elevated Temperatures	151
4.3.1.3.1 Microstructural Analysis of the Exposed FA Geopolymer Paste to the Elevated Temperatures	151
4.3.1.3.2 Microstructural Analysis of the Exposed LWAGC to the Elevated Temperatures	160
4.3.1.4.3 Thermal expansion behavior of the LWA	162
4.3.2 Effect of Elevated Temperatures of 100 °C to 800 °C on the Residual Strength of LWAGC	164

4.3.3 Effect of LWA Particle Size and Grading on Residual Compressive Strength of the LWAGC	166
4.4 Summary of Results and Discussion	172
4.5 Guide of LWAGC Mix Design	172
<b>CHAPTER 5 CONCLUSION AND FUTURE WORK</b>	
5.1 Conclusions	174
5.2 Future Work	179
<b>REFERENCES</b>	181
<b>APPENDIX A LIST OF PUBLICATION AND EXHIBITION</b>	194

© This item is protected by original copyright

## LIST OF FIGURES

NO.		PAGE
1.1	Expanded clay LWA	3
2.1	Babylon, Iraq build by Sumerians in the 3 <sup>th</sup> millennium B.C. (Chandra & Berntsson,2002)	16
2.2	Hagia Sofia, in Istanbul, Turkey built in 4 <sup>th</sup> century A. D	16
2.3	Great Roman amphitheatre, Colosseum, built between 70 and 82 A.D	17
2.4	LWA spectrum (Chandra & Berntsson, 2002)	19
2.5	Poly (sialates) structures according to Davidovits (2005)	23
2.6	SEM micrograph of the FA (Bakharev, 2006)	27
2.7	Effect of FA source on the compressive strength development of FA geopolymers (Zhang et al. 2011)	35
2.8	Effect of different NaOH solution molarity on the strength of FA geopolymers (Abdullah, et al. 2011b)	37
2.9	Influence of curing temperature on strength development (Hardjito et al. 2002) A-1= mixing time 5 minutes, A-2= mixing time 4 minutes, A-3= mixing time 3 minutes, A-4= mixing time 2 minutes.	40
2.10	Influence of curing periods on the compressive strength of the FA geopolymers (Hardjito & Rangan, 2005)	42
2.11	XRD patterns of the base materials and the MK geopolymers (Barbosa et al. 2000)	44
2.12	XRD patterns of alkali activated FA mortars (Fernandez-Jimenez & Palomo, 2005)	44
2.13	High-resolution SEM micrograph of MK geopolymer (Hos et al. 2002)	45
2.14	Microstructure of the fly ash-based geopolymer (Palomo et al. 1999b)	46
2.15	Comparison in heat resistance between the FA geopolymer paste	

	and OPC cement (Kong & Sanjayan 2010)	49
2.16	TGA and dilatometric curves of FA geopolymers (Kong & Sanjayan, 2008)	50
2.17	Dilatometric data of FA geopolymers of different liquid/solid ratios Provis et al. 2009)	51
2.18	Effect of sample size on the FA geopolymer paste thermal behavior (Kong & Sanjayan, 2010)	52
2.19	Effect of aggregate size on the FA geopolymer concrete thermal behavior (Kong & Sanjayan, 2010)	53
2.20	Thermal expansion of coarse aggregate and FA geopolymer paste (Kong & Sanjayan, 2010)	53
2.21	Compressive strength vs. time of age of aerated concretes with BFS sand, (Arellano-Aguilar et al. 2010)	57
2.22	28 days compressive strength ( $f'c$ ) of geopolymer mortar and LWAGC (Yang et al. 2010)	58
2.23	Compressive strength ( $f'c$ ) of the geopolymers vs. OD-density (Yang et al. 2010)	58
2.24	Strength and density of foamed geopolymers vs. NaOH concentration (Zhang et al. 2011)	60
2.25	Compressive strength vs. curing type Abdullah et al. (2012)	61
3.1	Flowchart summarized the research methodology of this study	64
3.2	Sodium hydroxide (NaOH) powder	67
3.3	Liquid sodium silicate $Na_2SiO_3$	68
3.4	Sieve analysis test instrument	70
3.5	LWA used in the manufacturing of the LWAGC of this study	73
3.6	Slump test instrument used to test the fresh concrete slump	87
3.7	Batch 2 LWA of 8-16 mm	92
3.8	Geopolymer paste cylinder used in the preparing the dilatometry test specimens	102
4.1	Particle size distribution of the FA	108
4.2	SEM micrograph of the source material (FA)	109
4.3	XRD diffraction pattern of the FA	110
4.4	Geopolymer paste specimens prepared with different	

	Na <sub>2</sub> SiO <sub>3</sub> /NaOH ratios	115
4.5	Effect of different Na <sub>2</sub> SiO <sub>3</sub> /NaOH mass ratios on the compressive strength development of the FA geopolymers paste	116
4.6	Geopolymer paste specimens cured at different temperatures ranged of 60-90 °C	117
4.7	Effect of different curing temperatures on the compressive strength development of the FA geopolymers paste	118
4.8	Strength development of the geopolymers paste at different curing periods	119
4.9	Resultant FA geopolymer paste specimens (100×100×100 mm)	120
4.10	Resulted FA geopolymer mortar specimens (100×100×100 mm)	121
4.11	Resultant LWAGCs specimens(100×100×100 mm)	121
4.12	Microscopy image for the adopted LWA	123
4.13	Compressive strength development of the LWAGC versus aging times	124
4.14	Effects of Activator/FA ratio on the compressive strength of FA geopolymer paste at different aging times	127
4.15	LWAGCs of L4-8, L4-5 and L5-8 prepared from the graded LWA batch 1 of 4-8 mm	132
4.16	LWAGCs of L8-16, L8-12 and L12-16 prepared from the graded LWA batch 2 of 8-16 mm	133
4.17	Compressive strength data of the LWAGCs prepared with different LWA sizes and grading	134
4.18	Relationship between the water absorption and OD-density of the resultant LWAGCs	137
4.19	Relationship between total porosity and OD-density of the resultant LWAGCs	137
4.20	Initial strength data of the unexposed geopolymers and the residual strength of geopolymers after exposed to the elevated temperatures 400 °C, 600 °C and 800 °C	139
4.21	TGA curve of the unexposed FA geopolymer paste	142
4.22	DTG curve of the unexposed FA geopolymer	143
4.23	DTA curve of the FA geopolymer	144

4.24	Thermal expansion of the unexposed geopolymer paste	145
4.25	Photographs of the unexposed and exposed FA geopolymer pastes to elevated temperatures of 400 °C, 600 °C and 800 °C	147
4.26	Photographs of the unexposed and exposed FA geopolymer mortars to elevated temperatures of 400 °C, 600 °C and 800 °C	148
4.27	Photographs of the unexposed and exposed LWAGCs to elevated temperatures of 400 °C, 600 °C and 800 °C	150
4.28	SEM micrographs of unexposed and exposed FA geopolymer paste to elevated temperatures 400 °C, 600 °C and 800 °C	152
4.29	EDS analysis of the unexposed geopolymeric paste gel of Figure 4.28	153
4.30	EDS analysis of the exposed geopolymer paste to 400 °C of Figure 4.28	153
4.31	EDS analysis of geopolymeric gel zone (001) of the exposed geopolymer paste to 600 °C of Figure 4.28	154
4.32	EDS spot analysis of the crystal particles zone (002) of the exposed geopolymer paste to 600 °C of Figure 4.28	155
4.33	EDS analysis of the exposed geopolymer paste to 800 °C of Figure 4.28	156
4.34	XRD diffraction patterns of the unexposed and exposed geopolymer paste to 400 °C	158
4.35	XRD diffraction patterns of the unexposed and exposed geopolymer paste to 600 °C	158
4.36	XRD diffraction patterns of the unexposed and exposed geopolymer paste to 800 °C	160
4.37	SEM micrographs of unexposed and exposed LWAGCs to elevated temperatures of 400, 600 and 800 °C	162
4.38	Thermal expansion of LAW	163
4.39	High magnification SEM micrograph for the ITZ of the LWAGC exposed to 800 °C	164
4.40	Residual compressive strength of the LWAGCs after exposing to elevated temperatures of 100 °C to 800 °C	165

4.41	LWAGCs of L4-8, L4-5 and L5-8 prepared from the graded LWA batch 1 of 4-8 mm after exposed to 800 °C	167
4.42	LWAGCs of L8-16, L8-12 and L12-16 prepared from the graded LWA batch 2 of 8-16 mm after exposed to 800 °C	168
4.43	Residual compressive strength of the L4-5, L4-8, L5-8, L8-12, L8-16 and L12-16 after exposure to elevated temperature of 800 °C	169
4.44	Strength loss of the L4-5, L4-8, L5-8, L8-12, L8-16 and L12-16 after exposure to elevated temperature of 800 °C	170

© This item is protected by original copyright

## LIST OF TABLES

NO.		PAGE
2.1	Dramatic difference of FA geopolymers (van Jaarsveld et al. 1998; Swanepoel & Strydom 2002)	34
2.2	Compositions of FA and the reactive SiO <sub>2</sub> content, Mass% (Zhang et al. 2011)	35
2.3	Effect of Na <sub>2</sub> SiO <sub>3</sub> /NaOH ratio on the strength of FA geopolymers (Hardjito & Rangan, 2005)	38
2.4	Some of past studies on the effect curing temperature of FA geopolymers	40
2.5	Some of past studies on the effect curing durations of FA geopolymers	42
2.6	Residual mechanical strength of the exposed geopolymeric lightweight composite to elevated temperatures (Zuda et al. 2010)	56
2.7	Properties of FA foamed lightweight geopolymer concrete (Abdullah et al. (2012)	62
3.1	Trial batch proportioning of the LWAGCs	79
3.2	Mix proportioning of the geopolymer paste of different Na <sub>2</sub> SiO <sub>3</sub> /NaOH ratios	82
3.3	Mix design of the geopolymer paste cured at temperatures of 60-90 °C	83
3.4	Final trial mix design of the LWAGCs	85
3.5	Final mix proportioning of the LWAGCs	88
3.6	Mix proportion of the geopolymer paste and mortar (kg/m <sup>3</sup> )	90
3.7	Mix proportion of the LWAGCs prepared at different Activator/FA ratios	91
3.8	Mix proportioning of the paste specimens prepared at different Activator/FA ratios (g)	92
3.9	Test program of the current research	104
4.1	XRF analysis data of FA composition	107
4.2	Results of FA particle size analysis and operation conditions	108

4.3	Sieve analysis results for the sand	112
4.4	Physical properties of LWA	113
4.5	Sieve analysis for the LWA	114
4.6	Physical and mechanical Properties of the resultant geopolymers	122
4.7	Effect of the Activator/FA mass ratios on the properties of LWAGC	126
4.8	Sieve analysis of batch 2 LWA	128
4.9	Slump values of fresh LWAGC prepared at different LWAs size and grading	130
4.10	Water absorption and total porosity of the resulted LWAGCs	136
4.11	Strength loss of the geopolymers after exposure to elevated temperatures	140
4.12	Recommended mix design for LWAGC	173

© This item is protected by original copyright

## LIST OF ABBREVIATIONS

OPC	Ordinary Portland Cement
LWC	Lightweight Concrete
LWA	Lightweight Aggregate
LWAGC	Lightweight Aggregate Geopolymer Concrete
LWAC	Lightweight Aggregate Concrete
GHS	Green House Gasses
FA	Fly Ash
GGBS	ground granulated blast-furnace slag
AA	Alkali-Activated
MK	Metakaolinite
NWC	Normal Weight Concrete
LECA	Lightweight Expanded Clay Aggregate
ACI	American Concrete Institute
HWC	Heavy Weight Concrete
ASTM	American Standard of Testing Materials
LOI	Loss On Ignition
ACAA	American Coal Ash Association
SMA	Stone Mastic Asphalts
XRD	X-ray Diffraction
Class F	Low-calcium Fly ash
Class C	High-calcium Fly ash
RT	Room Temperature
SEM	Scanning Electron Microscopy
TGA	Thermogravimetric Analysis
AFLA	Alkali-activated FA Artificial LWA
EPS	Expanded Polystyrene Beads
OD	Oven- Dry
BFS	Blast Furnace Slag
HPA	High Performance Ash
RHBA	Rice Husk-Bark Ash

POC	Palm Oil Clinker
XRF	X-ray Fluorescence
SSD	Saturation Surface Dry
FM	Fineness Modulus
AD	Air-Dry Condition
BS	British Standard
UTM	Universal Testing Machine
EN	European Standard
EDS	Energy Dispersive Spectrometry
BSE	Backscattered Electron
DTG	Thermogravimetric Analysis
DTA	Differential Thermal Analysis
IMR	Individual Mass Retained
CPR	Cumulative Percent Retained
CPP	Calculated Percent Passing
ITZ	Interface Transition Zone
CTE	Coefficient of Thermal Expansion
PS	Poly-sialate
PSS	Poly-sialate siloxo
PSDS	Poly-sialate-disiloxo

## LIST OF SYMBOLS

Si	Silicon
Fe	Iron
Ti	Titanium
Al	Aluminum
O	Oxygen
Na	Sodium
K	Potassium
Ca	Calcium
Mg	Magnesium
M <sup>+</sup>	Alkali Ion
CO <sub>2</sub>	Carbon Dioxide
CaO	Calcium Oxide
H <sub>2</sub> O	Water
Na <sub>2</sub> O	Sodium Oxide
Al <sub>2</sub> O <sub>3</sub>	Aluminum Oxide
SiO <sub>2</sub>	Silicon Dioxide
Fe <sub>2</sub> O <sub>3</sub>	Iron Oxide
NaOH	Sodium Hydroxide
KOH	Potassium Hydroxide
%	Weight Percent
m	Meter
M	Molar
MPa	Mega Pascal
θ	Theta
cP	Centipoise
g	Gram
°C	Degree Celsius
mm	Millimeter
KN	Kilo Newton

kV	Kilo Volt
Å	Angstrom
Mam	Milliampere
µm	Micrometer
kg/m <sup>3</sup>	Kilogram Per Cubic Meter
Psi	Pascal
Ib	Pound
ft	Foot
yd	Yard
W <sub>s</sub>	SSD Weight
W <sub>d</sub>	OD Weight
W <sub>i</sub>	Immersed Weight
W <sub>SSW</sub>	Weight of Saturated Specimen in Water
ε	Thermal Strain
α	Coefficient of Thermal Expansion
Δl	Length Change
l <sub>o</sub>	Initial Length of the Specimens
ΔT	Temperature Difference
Q	Quartz
M	Mullite
H	Hematite
Ca(OH) <sub>2</sub>	Calcium Hydroxide
C-S-H	Calcium Silicate Hydrate
Ma	Magnetite
W	Wollatonite
A	Aegirine
C	Calcium Iron Silicate
He	Hercynite

T	Tridymite
#	Sodium Silicate
N	Nepheline
S	Sodium Aluminum Silicate
$f_c$	Residual Compressive Strength
$t$	Exposure Temperature
$f'_c$	Compressive Strength

© This item is protected by original copyright

## Kajian Kelakuan Mekanikal dan Terma Konkrit Geopolimer Agregat Ringan (LWAGC) Menggunakan Abu Terbang

### ABSTRAK

Geopolimer adalah sebahagian daripada sains polimer, kimia dan teknologi yang membentuk salah satu bidang utama sains bahan dalam menghasilkan bahan baru hijau yang boleh dijadikan alternatif bahan simen kepada Portland simen biasa (OPC) kerana sifatnya yang mesra alam. Kajian tentang struktur konkrit agregat ringan telah ditemui di dalam kajian sedia ada. Tesis ini membentangkan prosedur proses sintesis daripada konkrit geopolimer agregat Ringan (LWAGC) berdasarkan American Concrete Institute (ACI) Piawaian Jawatankuasa 211(ACI 211,2). LWAGC telah disediakan dengan menggunakan pengaktif alkali daripada Abu Terbang (FA) yang mengandungi natrium silikat ( $\text{Na}_2\text{SiO}_3$ ) dan larutan natrium hidroksida (NaOH). Pengikat geopolimer ini telah digunakan untuk mengikat campuran agregat semulajadi dan agregat ringan tanah liat berkembang (LECA). Ciri-ciri fizikal, mekanikal, mikrostruktur dan terma yang dihasilkan LWAGC sebelum dan selepas terdedah kepada suhu tinggi diantara 100 - 800 °C telah dikaji dengan terperinci melalui kajian ini. Keputusan fizikal dan mekanikal LWAGC yang tidak terdedah kepada suhu pemanasan 100° C hingga 800 °C menunjukkan ia menepati Piawaian ACI 211,2 untuk mereka bentuk LWAGC struktur berasaskan teknologi pengeopolimeran. Campuran LWAGC yang segar telah mencatatkan nilai penurunan iaitu 95 mm, manakala LWAGC keras memiliki kekuatan mampatan sebanyak 18.86 MPa dengan isipadu 1438.70 kg/m<sup>3</sup>, pada hari ke 28. Ini membenarkan ia diklasifikasikan sebagai LWAGC struktur yang boleh digunakan sebagai bahan binaan. LWAGC yang tidak terdedah juga menunjukkan kekuatan mampatan meningkat secara berterusan apabila penuaan dibuat sehingga 1 tahun. Kajian nisbah optimum Activator/FA digunakan diantara 0.3-0.7 menunjukkan bahawa nisbah Activator/FA yang dicadangkan oleh Piawaian ACI 211,2 iaitu 0.59 adalah kandungan pengaktif paling optimum. Ini adalah kerana ia menyediakan keboleherjaan yang dikehendaki dan mempunyai kekuatan mampatan yang paling tinggi berbanding dengan nisbah ujian lain. Keputusan mekanikal, fizikal dan mikrostruktur menunjukkan agregat (pasir/pasir + LWA) meningkatkan ketahanan api mortar geopolimer FA dan LWAGC. Kekuatan LWAGC meningkat selepas terdedah kepada suhu diantara 100 °C sehingga 300° C. Bahan-bahan ini adalah sangat sesuai untuk aplikasi pada suhu sehingga 300 °C.

## Study on Mechanical and Thermal Behavior of the Lightweight Aggregate Geopolymer Concrete (LWAGC) Using Fly Ash

### ABSTRACT

Geopolymers are part of polymer science, chemistry and technology that forms one of the major areas of materials science as well as in producing of new green materials that can alternative cementitious material to ordinary Portland cement (OPC) due to their brilliant environmentally-friendly benefits. Structural lightweight aggregate concrete LWAC has been found in the available literature. This thesis presents the synthesis process procedures of a structural lightweight aggregate geopolymer concrete (LWAGC) system based on the American Concrete Institute (ACI) committee 211-standard (ACI 211.2). The LWAGC was prepared by alkali activation of a Fly Ash (FA) consist of sodium silicate ( $\text{Na}_2\text{SiO}_3$ ) and sodium hydroxide solution ( $\text{NaOH}$ ). The geopolymer paste binder was used to bind a mixture of natural aggregates and lightweight expanded clay aggregate (LECA). The physical, mechanical, microstructural and thermal properties of the prepared LWAGC before and after being exposed to elevated temperatures ranged of 100-800 °C were extensively investigated through this work. The physical and mechanical results of the unexposed LWAGC to heating temperatures of 100 °C to 800 °C showed that it comply the ACI 211.2 standard for designing a structural LWAGC based on the geopolymerization technology. The fresh LWAGC mixture was recorded a slump value of 95 mm, while the hardened LWAGC possessed a compressive strength and volume of 18.86 MPa and 1438.70  $\text{kg/m}^3$ , respectively at 28 days. These classify it as a structural LWAGC which can be used as a construction material. The unexposed LWAGCs were also showed a continuous strength gaining versus aging times up to 1 year. The optimizing of Activator/FA mass ratio used in the LWAGC preparation has been also investigated at a range of 0.3-0.7, which revealed that the Activator/FA mass ratio proposed by the ACI 211.2 standard of 0.59 was the optimum activator content as it provide the desired workability and the highest compressive strength than other tested ratios. The microstructural and physical analysis showed that, the thermal properties of LWAGC improved significantly after been exposed to elevated temperature of 400 °C, 600 °C and 800 °C. The mechanical, physical and microstructural results showed the aggregates (sand/sand + LWA) significantly improved the fire resistance of FA geopolymer mortar and LWAGC. The strength of the LWAGC increased after exposed to 100 °C to 300 °C. These materials are excellent for the applications up to 300 °C.

# CHAPTER 1

## INTRODUCTION

### 1.1 Background

The developing of lightweight building materials has good mechanical properties become a constant request. It is known that the lightweight materials can reduce the deadweight of structure, provide better thermal insulation for buildings and cost less to transport or erect when pre-fabricated structural components are made in factory (Wu & Sun, 2007). According to Chandra & Berntsson (2002) there are three types of lightweight concretes (LWCs) used for different applications as lightweight building materials, which are:

1. The *non-load bearing concrete* which used in heat insulation purposes, prepared by introducing large voids within the concrete mass and is known as aerated, foamed or gas concrete.
2. Low-density concrete formed by omitting the fine aggregate causing a large number of interstitial voids and is known as *no-fines concrete*. Generally, coarse aggregate of normal density is used, but lightweight aggregate (LWA) gives considerably reduced weight and better heat-insulation properties.
3. The *Lightweight aggregate concrete* (LWAC) with monolithic structure in which the coarse lightweight aggregates is used instead of normal weight aggregate. The normal weight fine aggregate is mostly used in the preparation of LWAC which is therefore also called the sand lightweight concrete.

The LWAC has its obvious advantages of high strength to weight ratio, good tensile strength, low coefficient of thermal expansion, and superior heat and sound insulation characteristics due to air voids in LWA (Mouli & Khelafi, 2008). The utilized LWA in preparation of the LWAC could be from natural origin like pumice, scoria, volcanic cinders, tuff, and diatomite or artificial LWA produced by heating like expanded clay, shale, slate, diatomaceous shale, expanded perlite, obsidian, and vermiculite (Hu et al. 2009). Also, the industrial cinders and blast-furnace slag that has been specially cooled can be used as LWA (Arellano-Aguilar et al. 2010). Furthermore, the LWAC can be used as a structural concrete which is similar to the normal weight concrete (NWC) except it has low density. According to the American Concrete institute committee 213R (ACI 213R-87), the structural LWAC has a 28 days compressive strength in excess of 17 MPa (2500 psi) and a 28 days air dried unit weight not exceeding 1850 kg/m<sup>3</sup> (115 lb/ft<sup>3</sup>). The structural LWACs are commonly used in the construction of buildings, bridge deck pavements, and in more limited role, for entire bridge superstructures (Swamy & Lambert, 1981; Swamy & Lambert, 1983; Swamy & Jiang, 1993). The LWA used for production the structural LWAC known as the structural LWA which are meeting the requirements of the American Society for Testing and Materials committee 330 (ASTM C 330) include:

1. Rotary kiln expanded clays (Figure 1.1), shales, and slates.
2. Sintering grate expanded shales and slates.
3. Pelletized or extruded fly ash.
4. Expanded slags.



Figure 1.1: Expanded clay LWA.

Furthermore, other structural LWAs can also be produced by processing other materials like the naturally occurring pumice and scoria. The structural LWAs have densities significantly lower than normal-weight aggregates, ranging from  $560 \text{ kg/m}^3$  to  $1120 \text{ kg/m}^3$  (35 pcf to 70 pcf), compared to  $1200 \text{ kg/m}^3$  to  $1760 \text{ kg/m}^3$  (75 pcf to 110 pcf) for normal-weight aggregates (Mehta & Monteiro, 2006).

On the other hand, the concrete usage around the world is second only to water (Malhotra, 2002). The Ordinary Portland cement (OPC) is conventionally used as the primary binder to produce concrete. However, the environmental issues associated with the production of the OPC are well known and can be addressed in terms of the carbon dioxide  $\text{CO}_2$  released during the manufacturing of the OPC. Hardjito & Rangan (2005) reported that the production of one tone of the OPC releases approximately one tone of  $\text{CO}_2$  to the atmosphere due to the calcination of the limestone (the raw material of the OPC) and combustion of fossil fuel. Accordingly, the amount of greenhouse gas (GHS) emitted from the worldwide production of OPC corresponds to 7% of the total GHS

emission released into the Earth's atmosphere (Malhotra, 2002). In addition, the extent of energy required to produce OPC is only next to steel and aluminum (Davidovits, 1988). Therefore, many researchers in the concrete industry have investigated diverse approaches of minimizing the use of OPC in the last two decades as a global efforts to reduce GHS emissions. These efforts can be summarized as, firstly, using additives by-product materials such as fly ash (FA) or ground granulated blast-furnace slag (GGBS), which are partially replaced the OPC to reduce its amount used in the making of concrete.

Secondly, develop novel materials that capable of replacing the traditional OPC. Many studies have been carried out since the 1960s on the development of GGBS-or-FA-based alkali-activated (AA) mortar and concrete. Correspondingly, as early as the 1980s, Davidovits rediscovered after intensive research a new family of mineral polymers, which they called *alkali-activated aluminosilicate geopolymers* or simply *geopolymers*. The name was chosen because of the similarities with organic condensation polymers regarding to their hydrothermal synthesized conditions (Davidovits, 1982; Davidovits & Sawyer, 1985). Geopolymers are defining as members of the family of inorganic polymers, their chemical composition is similar to the natural zeolitic materials, but their microstructure is amorphous (Davidovits, 1982). Davidovits (1988, 1994) revealed that the geopolymer material can be prepared by the alkali activation of a source material which is rich in silicon (Si) and aluminum (Al) of geological origin or by-product materials by alkaline activator liquid like sodium or potassium hydroxide (NaOH, KOH) mixed with sodium silicate ( $n\text{SiO}_2\text{Na}_2\text{O}$ ) or potassium silicate ( $n\text{SiO}_2\text{K}_2\text{O}$ ). The resultant geopolymer material can be used as a binder instead of the OPC binder to bind different types of aggregates to produce geopolymer mortars and concretes. The geopolymer materials reported to be capable of

reducing the CO<sub>2</sub> emission by 80% to 90% comparing to the OPC (Davidovits, 1999). Other studies reported that the geopolymers have early strength, low permeability, excellent resistance to chemical attacks, good freezing thawing cycles and a tendency to immobilize the heavy metal ions in their structure (Hardjito & Rangan, 2005; Wallah & Rangan, 2006; Li et al., 2004; Gourly & Johnson, 2005).

The typical source materials used for making geopolymers are metakaolin (MK) or industrial by-products like Fly ash (FA), slag and rice husk ash (Duxson et al. 2007a; Detphan & Chindapasirt, 2009). However, geopolymer materials synthesized by treating by-products like FA will enhance the environmental and economic credentials of the end product (Rickard et al, 2012). Furthermore, the usage of the FA as a source material in preparing of the geopolymers will decrease the preparation cost as there is no calcination or further preparation processes required for the source material like the metakaolin which required pre-heating at 750 °C prior to usage. FA geopolymer cement and concrete have been investigated by many researchers who concluded that these materials are superior to the traditional OPC cement and concrete due to their higher mechanical and thermal properties (Hardjito & Rangan, 2005; Kong & Sanjayan, 2010) and better chemically attack resistance (Guo et al. 2010; Wallah et al. 2005; Song, et al. 2005).

## **1.2 Problem Statement**

As mentioned in section 1.1, the geopolymer materials have been recently presented as a pioneer technology of producing environmental-friendly and low cost cement-less materials that could replaces the traditional OPC. At the same time, the utilization of the geopolymerization technology in production of green lightweight aggregate geopolymer

concrete (LWAGC) has its obvious commercial advantages of integrating the energy saving with production of new green building materials possess excellent mechanical, thermal and chemical resistance properties. Nevertheless, paucity in the published studies and researches regarded to the utilization of the geopolymerization and LWAs in production of LWAGC has been reported in the available literature (Hu et al. 2009; Wu & Sun, 2007; Zuda et. al. 2010; Yang et. al. 2010, Ng & Foster, 2011; Nazari et al. 2012). The concretes of these researches were prepared by the usage of GGBS or a combination of FA and metakaolinite (MK) or all as source materials activated by different types of alkaline activators in order to preparing the geopolymer binder (geopolymer paste). Furthermore, the concretes reported in these researches were from the no-fines LWC types which therefore not considered as a structural LWAC (Chandra & Berntsson, 2002), except the LWAC reported by Yang et al. (2010). The details of these LWCs are presented in Chapter 2, section 2.10. Additionally, base on our knowledge there is no published work yet has been utilized the FA individually as a source material and normal weight sand as a fine aggregate in production of structural LWAGC, despite the high attention paid to the advantages of FA geopolymeric cement and NWC materials as mentioned in section 1.1. Moreover, the designing bases of the structural LWAGC are yet unrevealed by any published standard document.

From the above, part of the this work was therefore dedicated to study and investigate the designing and preparation procedures of a structural LWAGC prepared by the usage of FA as only source material of making geopolymer binder. Consequently, the designing and preparation procedures of structural LWAGC were then included the optimization of the all preparation parameters which control the geopolymerization and design processes that leads to produce LWAGC with desired slump and compressive strength values.

Moreover, the thermal performance of the structural LWAGC system at high temperature environments is unavailable in the literature especially when they exposed to variable elevated temperatures. The previous studies were carried out to investigate the thermal properties of the FA geopolymers paste and NWC have been reported low thermal shrinkage and good strength maintenance after exposed to high elevated temperatures (Bekharev, 2006; Kong & Sanjayan, 2008; Kong & Sanjayan, 2010; Richard et al. 2010). The FA geopolymers in these papers were directly heated from room temperatures up to elevated temperatures of 800 °C or further up to 1200 °C, without consider the significance changes in the geopolymer phase composition occurred at temperatures ranged from about 600 to 800 °C which are recently highlighted by Provis et al. (2009) and Rickard et al. (2012). Therefore, the second part of this work was dedicated to study and investigate the thermal performance and significance changes in the geopolymeric phase composition of exposed LWAGC to different elevated temperatures up to 800 °C. In addition, the effect of the LWAs inclusion on the thermal performance of the exposed LWAGC to elevated temperatures was also explored by comparing it with the thermal performance of the exposed FA geopolymer pastes and mortars to elevated temperatures.

### **1.3 Research Scope**

The main scope of this research is experimentally studying the designing and preparation procedures utilized in producing a low density (less than 1850 kg/m<sup>3</sup>) LWAGC based on the alkali-activation of FA as the only source material without any other additives materials. The alkaline activator used in the FA activation process is a mixture of liquid sodium silicate (Na<sub>2</sub>SiO<sub>3</sub>) and 12M sodium hydroxide (NaOH)

solution. The aggregate used in the LWAGC preparation was a mixture of aggregates consisting of lightweight expanded clay aggregate (LECA) and normal weight sand.

In addition, the designing process based on the American Concrete Institute (ACI) committee 211-standard (ACI 211.2) as there is no standardized documents yet deals with the geopolymers as a cementitious material. This standard is the only available online standardized document that described in details the designing and proportioning processes of a lightweight aggregate structural concrete for OPC system. This is followed by performs an actual design to the preparation parameters that the initial LWAGC mix proportioning (resulted from the ACI 211.2 standard) did not specify them. These preparation parameters affects significantly on the geopolymerization rate and the LWAGC final compressive strength. These parameters comprise the NaOH solution concentration, mass mixing ratio of  $\text{Na}_2\text{SiO}_3/\text{NaOH}$ , curing temperature, curing period. The actual design was performed on the geopolymer paste then the optimum parameters values were applied during the LWAGC preparation.

Another scope of this work is investigate and address the significance changes in the geopolymeric phase composition of the exposed LWAGC to elevated temperatures of 400 °C, 600 °C and 800 °C . This is achieved by comparing the thermal behavior of the exposed LWAGC to elevated temperatures (400 °C, 600 °C and 800 °C ) with other geopolymeric binders (FA geopolymer paste and mortar) mechanical, thermo-physical and microstructure characteristics. Moreover, the effect of elevated temperatures ranged from 100 °C to 800 °C on the residual strength of the prepared LWAGC is also statistically analyzed. Finally, the effect of variable LWAs size and grading on the mechanical and thermal properties of the LWAGC is also extensively studied.

## **1.4 Research Objectives**

1. Designing and preparation of a structural LWAGC possesses the requirements density and mechanical strength using FA as the only source material for making the geopolymer binder without any additives materials.
2. To investigate the mechanical strength and physical properties of the prepared LWAGC at normal temperature and comparing these properties with its constituents of FA geopolymer paste and mortar materials.
3. To investigate the thermal behavior and gradual changes in the geopolymeric phase composition of the LWAGC and its constituents (FA paste and mortar) after exposed to elevated temperatures of 400 °C, 600 °C and 800 °C. In addition, evaluating the fire resistance of the LWAGC after exposed to elevated temperatures ranged from 100-800 °C.
4. To investigate the effect of the different aggregate particle size and grading LWA on the compressive strength and physical properties of the concrete at normal and elevated temperature of 800 °C.

## **1.5 Contribution of Research**

The contribution of the current research can be summarized as:

- i. Designing and preparation of a new green structural LWAC can be used in construction applications as a structural concrete with excellent mechanical strength, low-density as well as totally environmentally-friendly properties.
- i. Investigating the thermal durability and behavior of the LWAGC at high temperature environment up to 800 °C by mechanical, thermo-physical and

microstructural experimental studies. However, this investigation conducted to the LWAC prepared by the geopolymerization technology is not available in the literature.

© This item is protected by original copyright

## CHAPTER 2

### LITERATURE REVIEW

#### 2.1 Introduction

This chapter presents a background on the concrete manufacturing technology, its types and some of the famous concrete buildings in past and modern history. This chapter is also presents a background of the lightweight aggregate concrete (LWC), its historical usage, advantages as well as a description of its types and application. The environmental issues attendant to the utilization of the Ordinary Portland Cement (OPC) in the concrete technology as well as the recent suggestions of reducing the OPC quantities that involved in the making of concrete are also addressed in Chapter 2. One of these suggestions was developing new supplementary materials that could partially or totally replacing the OPC, and the geopolymer material is one theses materials. Therefore, the geopolymers, in particularly, the fly ash (FA) based geopolymer is the backbone of this chapter. The FA based geopolymer advantages, types, macro/microstructure, methods of production and factors that significantly influenced their properties are also discussed. Finally, this chapter reports the past researches that involved in usage of the geopolymerization technology in the production of lightweight geopolymeric concrete in all of its types and the significant results of these reports.

## 2.2 Concrete

Concrete is a composite construction material made primarily with aggregate, OPC, and water. The word *concrete* comes from the Latin word "concretus" which is meaning compact or condensed (Mehta & Monteiro, 2006). The concrete technology was known by the ancient Romans and was widely utilized in making of large structural buildings like the Colosseum. However, after the Romans Empire passed, the use of concrete became scarce until the technology was re-pioneered in the mid-18th century. Nowadays, it is estimated that there are nearly 3 tons of concrete produced each year for every human on the planet, which making the concrete the most used man-made product in the world (Chandra & Berntsson, 2002). The concrete is widely used for making architectural structures, foundations, brick/block walls, pavements, bridges/overpasses, motorways/roads, runaways, parking structures, dams, pools/reservoirs, pipes, footings for gates, fences and poles and even boats. The famous concrete structures include the Burj Khalifa (world's tallest building), Hoover Dam, the Panama Canal, the Roman Pantheon.

Mehta & Monteiro, (2006) reported the reasons behind the widely usage of the concrete in the construction as firstly, the concrete possesses excellent resistance to water unlike the wood and ordinary steel. The ability of concrete to withstand the action of water without serious deterioration makes it an ideal material for building structures to control, store and transport water. The second reason of the widespread use of concrete is ease with which structural concrete elements can be formed into a variety of shapes and sizes. Finally, the third reason is the low cost and availability of the concrete's raw materials.

## 2.3 Types of Concrete

Generally, it is not possible here to list all concrete types due to numerous modified concretes and different methods of classification which are depended to the concrete properties and application. Although, most commonly concrete classification methods are based on the compressive strength and unit weight of the hardened concrete. Accordingly, concrete can be classified based on its compressive strength value in a method known as strength grading (Mehta & Monteiro, 2006). The strength grading of the concrete is prevalent in Europe and many other countries in which the concrete can be divided into three general categories based on compressive strength as:

- *Low-strength concrete*: less than 20 MPa.
- *Moderate-strength concrete*: 20 to 40 MPa.
- *High-strength concrete*: more than 40 MPa.

Moreover, the concrete can be also classified based on the unit weight into three broad categories (Mehta & Monteiro, 2006). The concrete containing natural sand and gravel or crashed-rock aggregates, generally weighting about  $2400 \text{ kg/m}^3$ , is called *normal-weight concrete* (NWC), which it is the most commonly used concrete for structural purposes. When the concrete used for radiation shielding applications, the concrete is produced by using high-density aggregate and the resulted concrete is called the *Heavy-Weight Concrete* (HWC) which is usually having a unit weight more than  $3200 \text{ kg/m}^3$ .

Furthermore, when higher strength-to-weight ratio is desire, it is possible to reduce the bulk density of the concrete by using natural or artificial aggregates with lower

density. The term *lightweight concrete* (LWC) is used for the concrete that weighs less than  $1800 \text{ kg/m}^3$ . As described earlier in Chapter 1, the LWC can be classified into three types which are: the *non-load concrete*, *no-fines concrete* and *lightweight aggregate concrete* (LWAC) which is used as a structural material since the Sumerians days. Nowadays, the LWAC are well-desired in the constructions as with the usage of lighter concrete the framework supports less pressure than would be in the case with ordinary concrete and also the total weight of materials to be handled is reduced with a consequent increase in productivity (Mouli & Khelafi, 2008). As a result, the reduction in dead-weight of the construction by the use of LWAC could result in decreasing the cross sections of columns, beams, plates and foundations with resultant reduction in the construction costs.

#### **2.4 Structural Lightweight Aggregate Concrete (LWAC)**

The structural lightweight aggregate concrete (LWAC) is a structural concrete in every respect, except that the concrete is made with a cellular LWA so that its density is almost two-third of the density of concrete made with NWA. As mentioned in Chapter 1, the required 28 days compressive strength for the structural LWAC is more than 17 MPa, with a unit weight (density) at 28 days not more than  $1850 \text{ kg/m}^3$  (ACI 213R-87). The LWAC may prepared by utilization of LWA fine and coarse or a combination of LWA and normal-weight aggregate. However, due to the requirement of good workability for the LWAC, a combination of normal-weight sand as a fine aggregate and coarse LWA with maximum size of 19 mm are usually used preparation of LWAC (Mehta & Monteiro, 2006).

### 2.4.1 Historical Background of LWAC

LWAC is not a new innovation in the concrete technology, it has actually been known since the ancient times (Chandra & Berntsson, 2002). Therefore, it is possible to find many examples for the usage of the LWAC which were made by using of natural aggregate of volcanic origin such as pumice, scoria, etc. The Sumerians used the LWAC in building of Babylon in the 3<sup>th</sup> millennium B.C as illustrates in Figure 2.1.

The Greeks and the Romans used pumice in building construction. One of these magnificent ancient structures is the Hagia Sofia, in Istanbul, Turkey which built in 4<sup>th</sup> century A.D shown in Figure 2.2. Also the Roman temple, Pantheon which was erected in the years 118 to 128 A.D, and the great Roman amphitheatre, Colosseum, built between 70 and 82 A.D shown in Figure 2.3. In addition to building constructions, the Romans used natural lightweight aggregates and hollow clay vases for their “Opus Caementitium”, in order to reduce the structure weight. These famous ancient buildings and many others are signifies the advantages of the LWACs which were known by the ancient civilization.

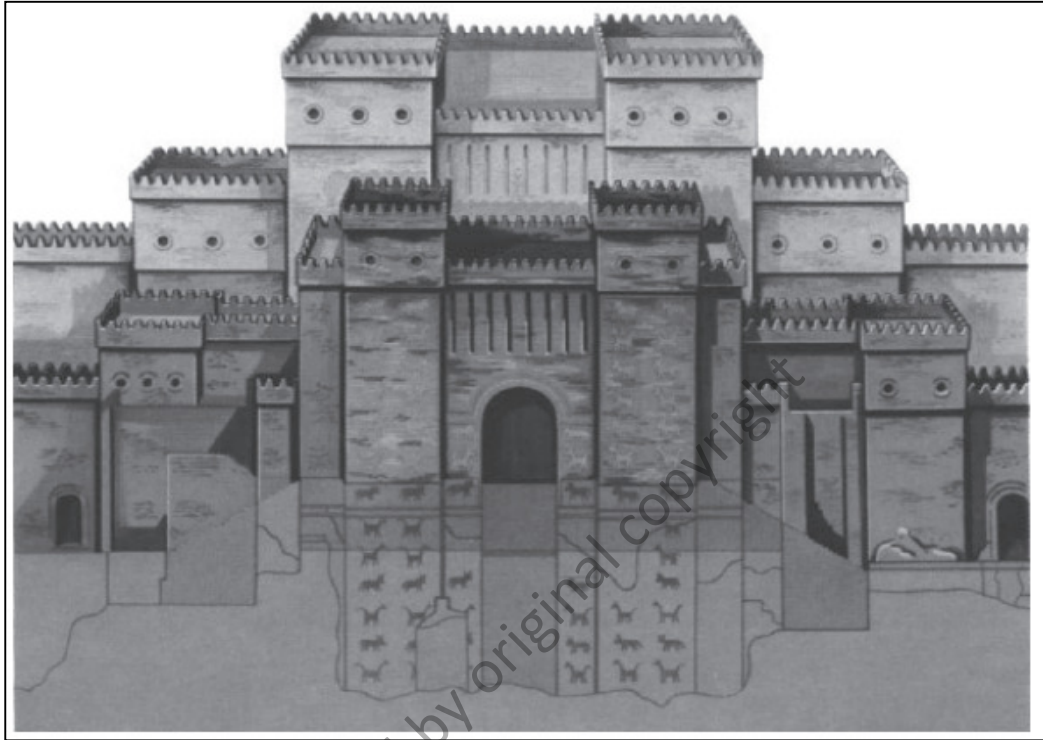


Figure 2.1: Babylon, Iraq build by Sumerians in the 3<sup>th</sup> millennium B.C. (Chandra & Berntsson, 2002).



Figure 2.2: Hagia Sofia, in Istanbul, Turkey built in 4<sup>th</sup> century A. D.



Figure 2.3: Great Roman amphitheatre, Colosseum, built between 70 and 82 A.D.

#### 2.4.2 Lightweight Aggregate (LWA)

According to Mehta & Monteiro, (2006) the aggregates that weight less than  $1120 \text{ kg/m}^3$  are generally considered lightweight, and find application in the production of various types of LWACs. The light weight of the aggregate is due to the cellular or highly porous microstructure. The LWAs can be classified into two main categories which are the natural LWA, and the synthesized LWA. The major resources of the natural LWA are the volcano material (Chandra & Berntsson, 2002). For the volcano original LWA, the volcanic rocks are crushed to the desired particle size and the resulted LWA is usually the pumice, scoria or tuff depending on the original volcanic rock (Mehta & Monteiro, 2006).

Moreover, the synthesized LWAs are manufactured by thermal treatment of a variety of materials. These materials can be divided into three groups:

- Natural materials, like perlite, vermiculite clays, shale, slate.
- Industrial products, such as glass.
- Industrial by-products, such as fly ash (FA), blast-furnaces slag, and bed ash.

Actually, there is a whole spectrum of LWAs weighting from  $80 \text{ kg/m}^3$  to  $900 \text{ kg/m}^3$ , as shown in Figure 2.4 (Chandra & Berntsson, 2002). The high porous LWA at the lighter end of the spectrum are generally weak and therefore utilized for making nonstructural insulating concrete. While at the other end of the spectrum the LWA are relatively less porous and if the pore structure is consist of uniformly distributed fine pores, the aggregate are strong enough to be used in the producing of structural concretes (Mehta & Monteiro, 2006).

© This item is protected by original copyright

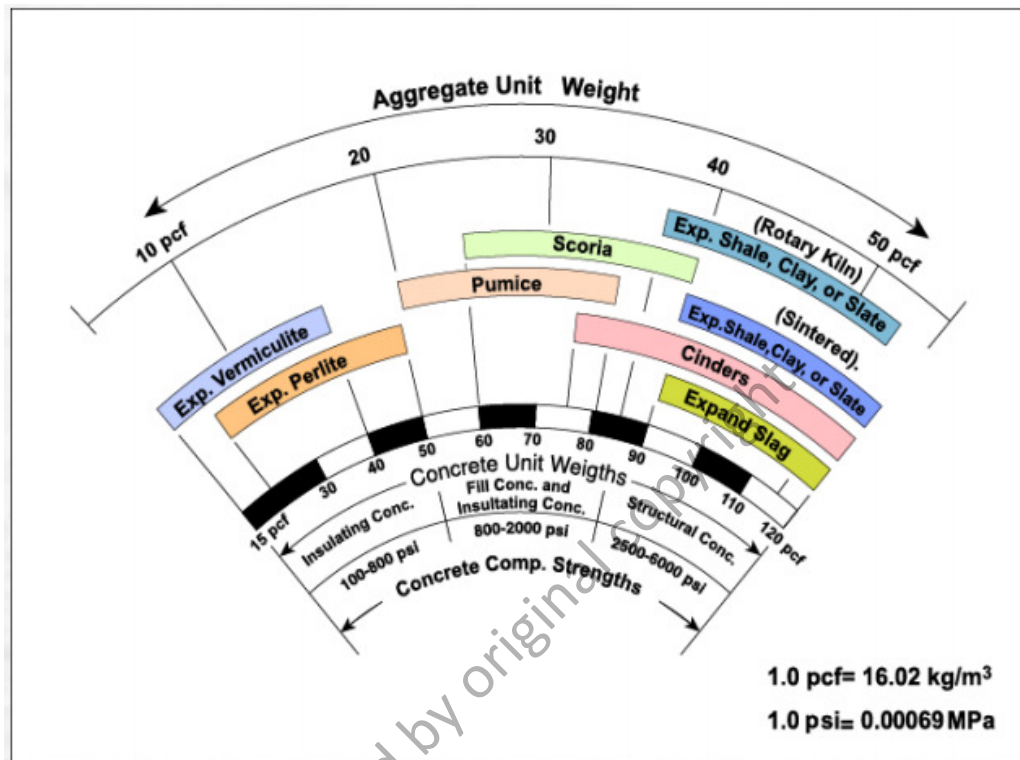


Figure 2.4: LWA spectrum (Chandra & Berntsson, 2002).

## 2.5 Concrete and Environment

As mentioned in section 2.2, the demand of the concrete is significantly increasing with increasing the human being population and the needs of new infrastructures. This demand have made the concrete consuming just second only to the water. The OPC is the conventional primary binder used in the concrete production. MacCaffrey (2002) reported that the global production of the OPC is increasing about 3 % annually. Basically, the production process of the OPC involving the calcination of the OPC's raw material which is the limestone that composed mainly from calcium carbonate ( $\text{CaCO}_3$ ) at high temperature of  $1450\text{ }^\circ\text{C}$  in a kiln as indicated in the following formula (Mehta & Monteiro, 2006):



Thus, the amount of the liberated carbon dioxide (CO<sub>2</sub>) from the calcination process as well as from the fuel combustion (which is usually fossil fuel) is estimated to be as one tone of each resulted one tone of OPC (Hardjito & Rangan, 2005). In year 2000, the amount of CO<sub>2</sub> resulted from the worldwide production of the OPC is estimated to be of 1.35 billion tones contributed about 7 % of the total greenhouse gasses (GHS) emission released into the earth's atmosphere (Malhotra, 2002). These GHS significantly contributes the global warming and climate change that the Earth experience recently. In addition, the extent of energy required in the OPC production is only next to steel and aluminum production (Davidovits, 1988). Furthermore, it has been reported that the durability of ordinary OPC concrete especially those built in corrosive environments, start to deteriorate after 20 to 30 years, even though they have been designed for more than 50 years of service life (Mehta & Burrows, 2001).

The concrete industry has recognized these issues; therefore, extensive efforts were progressed in the last three decades to minimize the use of OPC in the concrete in order to reduce the GHS emissions. In brief, these efforts were included the usage of additives by-product materials like FA or GGBS which were partially replaced the OPC and reduced its amount in the concrete. In addition, other efforts were specialized in developing of novel materials able to replacing the traditionally OPC.

As early as 1980s professor Joseph Davidovits proposed a controversial theory that some of the Egyptian pyramids were not build by mining limestone blocks and transformed them into their place, but were cast in their place and allowed to set, creating an artificial zeolitic rocks. This theory which gained acceptance culminated in a book "*The Pyramids An Enigma Solved*" written together with Magie Morris and

published in 1988. Intensive research initiated by Davidovits and co-workers to prove this theory has resulted in the rediscovery of a new family of mineral polymers called *alkali-activated aluminosilicate geopolymer* or simply *geopolymer*. The geopolymer material which can be synthesized by relatively simple alkali activation of a raw material rich in silicon (Si) and aluminum (Al) whether it from geological origin or by-product, can be used as a binder instead of the OPC binder in making geopolymer mortars and concrete (Davidovits, 1991). The geopolymer materials are able to reduce the CO<sub>2</sub> emission dramatically compared to the OPC, as well as having superior mechanical, chemical, and thermal properties than the OPC (Hardjito & Rangan, 2005; Wallah & Rangan, 2006; Li et al. 2004; Duxson et al. 2007a; Gourly & Johnson, 2005; Arellano-Aguilar et al. 2010; Wu & Sun, 2007; Kong & Sanjayan, 2010; Rickard et al. 2012).

## 2.6 Introduction of Geopolymers

Davidovits (1979) described a new family of materials named geopolymer whose matrix is based on a poly (sialate) Si-O-Al-O framework structure with alternating SiO<sub>4</sub> and AlO<sub>4</sub> tetrahedra joined together in three dimensions by sharing all oxygen atoms. The replacement of Al<sup>+3</sup> ( four-fold coordination) of Si<sup>+4</sup> causes a negative charge, which needs alkalis to balance, like ( Na<sup>+</sup>, K<sup>+</sup>, Ca<sup>2+</sup> or Mg<sup>2+</sup>). Davidovits (1988) suggested the geopolymeric empirical formula as:



where, M is the alkaline element or cation such as potassium, sodium or calcium;





Accordingly, several minerals and industrial by-product materials have been reported in the literature in the past decade like metakaolinite (MK) or calcined Kaolin (Davidovits 1999; Palomo et al. 1999; Barbosa et al. 2000; Teixeira-Pinto et al. 2002; Duxson et al. 2007b; Hu et al. 2009), FA (Swanepoel & Strydom, 2002; Bakharev, 2006; Kong & Sanjayan, 2008, 2010; Rickard et al. 2010; Provis, et al. 2009; Rickard et al. 2012), natural Al-Si minerals (Xu & van Deventer, 2000), combination of calcined mineral and non-calcined material (Xu & van Deventer, 2002), combination of FA and MK (Swanepoel & Strydom, 2002; van Jaarsveld et al. 2003; Wu & Sun, 2005; Zuhua et al. 2009; Arellano-Aguilar et al. 2010), and combination of ground granulated blast furnace slag (GGBS) and MK (Cheng & Chiu 2003) have been studied as source materials.

MK is preferred by the niche geopolymer product developers due to its high rate of dissolution in the reactant solution, easier control on the Si/Al ratio and its white color (Gourley 2003). However, geopolymer materials synthesized by treating the by-products like FA will enhance the environmental and economic of credentials of the end product (Rickard et al. 2012). In addition, it was stated that the calcined source materials, such as FA, slag, MK demonstrated a higher final compressive strength when compared to those made using non-calcined materials, for instance kaolinite clay, mine tailings, and naturally occurring materials (Barbosa et. al., 2000). However, Xu & van Deventer (2002) found that the using of a combination of calcined (e.g. FA) and non-calcined material (e.g. kaolinite or kaolin clay and albite) resulted in significant improvement in compressive strength and reduction in reaction time.

For the FA geopolymers, the type of the FA source which is depended on its calcium oxide (CaO) content (more discussion on FA source classification is presented in section 2.7.1.1) has also significant affect on the geopolymerization reaction. Gourley (2003) reported that the Low-calcium (Class F) FA is preferred as a source material than

high-calcium (Class C) FA as the presence of calcium in high amount may interfere with the polymerization process and alter the microstructure. This statement was argued later by Ng & Foster (2010) who found that the (Class C) FA favorite the geopolymerization reaction and produced higher strength, especially when the use of (Class C) FA is reported to lead to fast setting geopolymer as well as an increase in rate of strength development (van Jaarsveld et al. 2003; Xu & van Deventer, 2002). In accordance, van Jaarsveld, et al. (2003) found that the FA with higher amount of CaO produced higher compressive strength, due to the formation of calcium-aluminate-hydrate and other calcium compounds, especially in the early ages. The other characteristics that influenced the suitability of the FA to be source material for geopolymers are the particle size, amorphous content, as well as morphology and the origin of FA (Hardjito & Rangan 2005).

Natural Al-Si minerals have shown the potential to be the source materials for geopolymerization, although quantitative prediction on the suitability of the specific mineral as the source material is still not available, due to the complexity of the reaction mechanisms involved (Xu & van Deventer 2000). Among the by-product materials, only FA and slag have been proved to be potential source materials for making geopolymers. FA is considered to be advantageous due to high reactivity that comes from its finer particle size than slag. Moreover, FA is more desirable than slag for geopolymer feedstock material.

#### **2.7.1.1 Fly Ash (FA)**

The American Concrete Institute Committee 116R (ACI Committee 232, 2004), defining the Fly ash (FA) as *'the finely divided that results from the combustion of*

*ground or powdered coal and that is transported by flue gasses from the combustion zone to the particle removal system*'. FA is removed from the combustion gases by the dust collection system, either mechanically or by using electrostatic precipitators, before they are discharged to the atmosphere. FA particles are typically spherical, finer than Portland cement and lime, ranging in diameter from less than 1  $\mu\text{m}$  to no more than 150  $\mu\text{m}$  (Hardjito & Rangan, 2005). Figure 2.6 shows the SEM micrograph of FA reported by Bakharev (2006).

The types and relative amounts of incombustible matter in the coal determined the chemical composition of FA. The chemical composition of the FA is mostly composed of the oxides of silicon ( $\text{SiO}_2$ ), aluminum ( $\text{Al}_2\text{O}_3$ ), iron ( $\text{Fe}_2\text{O}_3$ ), and calcium ( $\text{CaO}$ ), whereas magnesium, potassium, sodium, titanium, and sulphur are also present in a lesser amount. The major influence on the FA chemical composition comes from the type of original coal. The combustion of sub-bituminous coal contains more calcium and less iron than FA from bituminous coal (Hardjito & Rangan, 2005). Furthermore, the physical and chemical characteristics depend on the combustion methods, coal source and particle shape. The chemical compositions of various FAs show a wide range, indicating that there is a wide variation in coal used in power plants all over the world (Malhotra & Ramezani pour, 1994).

FA that results from burning sub-bituminous coals is referred as ASTM (Class C) FA or high-calcium FA, as it typically contains more than 10 percent  $\text{CaO}$ , while FA from the bituminous and anthracite coals is referred as ASTM (Class F) FA or low-calcium FA (ASTM C618-08a). The color of FA can be tan to dark grey, depending upon the chemical and mineral constituents (Malhotra & Ramezani pour, 1994; ACAA, 2004). Aside from the chemical composition, the other characteristics of FA that generally considered are loss on ignition (LOI), fineness of FA mostly depend on the operating

conditions of coal crushers and grinding process of the coal itself. Finer gradation generally results in a more reactive ash and contains less carbon.

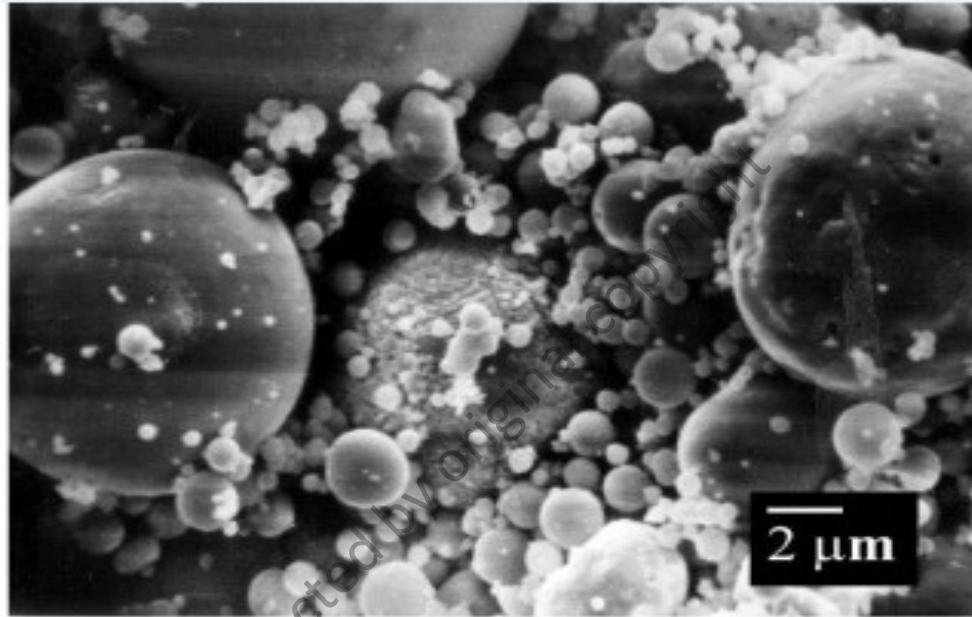


Figure 2.6: SEM micrograph of the FA (Bakharev, 2006).

Worldwide, the estimated annual production of coal ash in 1998 was more than 390 million tons mainly produced in China and India, and only about 14 % of this FA was utilized, while the rest was disposed in landfills (Malhotra, 1999). In 2010, the annually increasing in FA production worldwide was estimated to be about 780 million tons (Malhotra, 2002). The utilization of FA especially in concrete production, has significant environmental benefits via improved concrete durability, reduced use of energy, diminished greenhouse gas production, reduced amount of FA that must be disposed in landfills, and saving of the other natural resources and materials ( ACAA 2004).

The typical FA produced from the Malaysian power stations is light to mid-grey in color, similar to the color of the cement powder. In Malaysia, the production of the FA

is generally comes from the power stations (electrical generated power plants) which most of them using coal as source of power. Reshi (2011) estimated that the production of FA in Malaysia is over 2 million tons annually, and it is expected to double in 2013 as the demand of power is growing rapidly. The application of the Malaysian FA till now is limited in the Stone Mastic Asphalts (SMA) as a filler/modifier. Even though, the usage of the FA in the SMA industry is not popular enough (Reshi, 2011). Thus, the disposed of the local produced FA in landfills is expected to be a serious problem in Malaysia in the nearest future due to abounded production.

### **2.7.2 Alkaline Activator**

Generally, the using of alkaline activator in the preparation of the geopolymers is a constant demand regardless the type of the source material. This is due to the nature of geopolymerization reaction which is based in the first place on the dissolution of the source materials which are mostly consisting from acidic compounds like  $\text{SiO}_2$ ,  $\text{Al}_2\text{O}_3$  and  $\text{Fe}_2\text{O}_3$  and then required a high alkali environment in order to dissolve. Therefore, the usage of water is insufficient and does not consider as a reactor in the geopolymerization reaction.

The most common alkaline activator used in geopolymerization of different source materials is a liquid combination of sodium hydroxide (NaOH) or potassium hydroxide (KOH) and sodium silicate ( $\text{Na}_2\text{SiO}_3$ ) or potassium ( $\text{K}_2\text{SiO}_3$ ) silicate (Davidovits, 1999; Xu & van Deventer, 2002; Bakharev, 2005; Duxson et al. 2006; Kong & Sanjayang, 2008, 2010; Rukzon et al. 2009; Zhang et al. 2011; Nazari, 2012; Rickard et al. 2012). The use of single alkaline activator has been also reported (Teixeira-Pinto et al. 2002; Provis, et al. 2009; Zuda et al. 2010; Hanjistuwan et al. 2011; Rashad & Zeedan, 2011).

Furthermore, the usage of single powdered activator (powder  $\text{Na}_2\text{SiO}_3$ ) has been reported by Yang et al. (2010).

Palomo et al. (1999b) concluded that the type of alkaline activator liquid plays an important role in the polymerization process, and the reactions occur at a high rate when the alkaline activator liquid contains soluble silicate, either sodium or potassium silicate, compared to the use of only alkaline hydroxide. That statement is also shared by Criado et al. (2005). Furthermore, Xu & van Deventer, (2000) confirmed that the addition of sodium silicate solution to the sodium hydroxide enhanced the reaction between the source material and the solution. Although, after a study of the geopolymerization of sixteen natural Al-Si minerals, they found that the NaOH solution caused a higher extent of dissolution of minerals than the KOH solution.

## **2.8 The Mechanism of the Geopolymerization Reaction**

Basically, the exact reaction mechanism which explains the setting and the hardening of geopolymers is not yet quite understood, although it is thought to be depended on the prime material as well as on the alkaline activator type. According to Glukhovsky et al. (1981), the mechanism of alkali-activation is composed of conjoined reactions of destruction-condensation, that include the destruction of the prime material into low stable structural units, their interaction with coagulation structures and creation of condensation structures. The first steps consisting of breakdown of covalent bounds of Si-O-Si and Al-O-Si, which happened when the pH of the alkali solution rises, so those groups are transformed to a colloid phase. Then an accumulation of the destroyed products occurs, which interacts among them to form a coagulated structure, leading in a third phase to the generation of a condensed structure.

Alvarez-Ayuso et al. (2008) reported that the geopolymerization reaction occurs in the alkaline solutions with aluminosilicate oxides and silicates (either solid or liquid) as reactants. In addition, the mechanism involving the dissolution of the aluminum and silicon species from the surface of the source material as well as the surface hydration of undisclosed particles. Afterward, the polymerization of active surface groups and soluble species take place to form a gel, generating subsequently a hardened structure.

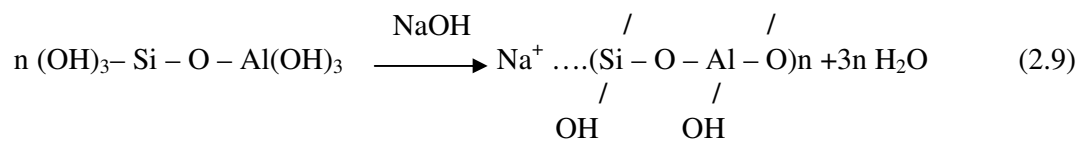
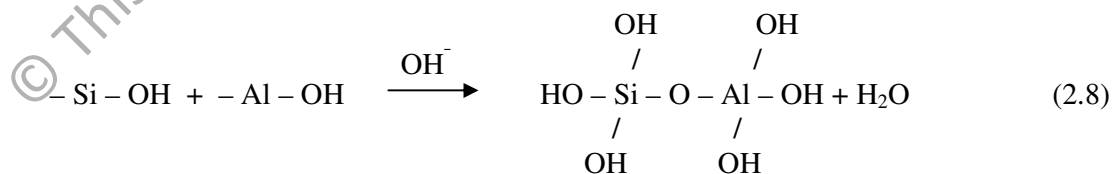
Thakur & Ghosh, (2009) reported a description for the geopolymerization of FA geopolymers, as the main reaction product in the alkali-activated FA is an alkaline silico-aluminate gel and the  $\text{OH}^-$  ions acts as a reaction catalyst during the activation process, while the alkaline metal ( $\text{Na}^+$ ) acts as a structure-forming element. The structure of the pre-zeolite gel chains Si and Al tetrahedral randomly distributed along the polymeric chains that are cross-linked so as to provide cavities of sufficient size to accommodate the charge balancing hydrated sodium ions (Xu & Deventer, 2000). Furthermore, the development of the compressive strength of the hardened FA geopolymers is attributed to the resulted aluminosilicate gel phase in the geopolymer matrices.

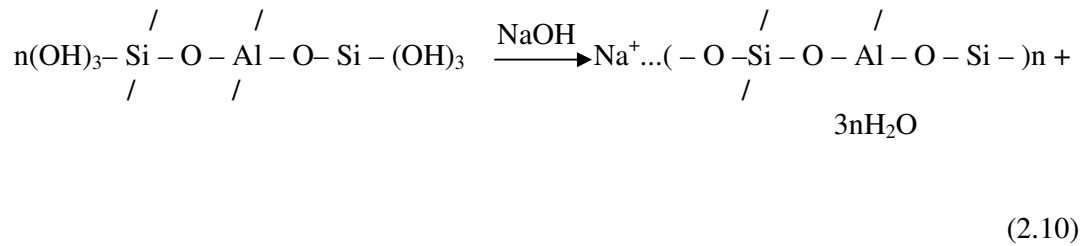
Moreover, Zuhua et al. (2009) reported that the role of the water content in the geopolymerization process, as the reaction occurred approximately into two periods: the dissolution-hydrolysis period and the hydrolysis-polycondensation period. These two steps probably occur simultaneously once the solid material mixed with the alkaline activator (Wang et al. 2003). Zuhua et al. (2009) proposed that the exact separation of these two steps is hard and the partition here is only from the point of view of thermodynamics, the period (I) including the dissolution of the  $\text{SiO}_2$  and  $\text{Al}_2\text{O}_3$  species and hydrolyses it, as indicated in the equations (2.5) to (2.7). It can be seen that the

water and the  $(\text{OH}^-)$  is the reactant in this period, if the concentration of the  $(\text{OH}^-)$  is high enough; more water will accelerate the dissolution and hydrolysis period



On the other hand, the water plays as product in the period (II), as indicated in equations (2.8) to (2.10). Therefore, when the water content is too much, it will hinder the geopolymerization kinetically (Zuhua et al. 2009).





## 2.9 Fly Ash (FA) Geopolymer

FA geopolymer materials are generally synthesized by the alkali-activation (using an alkaline activator of those mentioned in section 2.7.2) of a dry FA source, usually at room temperature with different mixture proportions, depending on the alkaline liquid characteristics and the application of the resultant geopolymer. The FA geopolymer mortar or NWC are synthesized by the incorporation of the aggregate (fine/fine +coarse NWA) into the advanced prepared FA geopolymer paste and the mixing process of all ingredients are similar to the one used in synthesizing of the OPC mortar and concrete.

The utilization of FA in the developing of geopolymeric materials for construction purposes has been and continues to be the subject of many research studies. The FA geopolymer materials have high mechanical properties, low density, less water absorption, negligible shrinkage and significant chemical and fire resistance characteristics (Thakur & Ghosh, 2009). Due to these properties, FA geopolymer materials are viewed as an alternative to the OPC, especially when their ability of reducing the CO<sub>2</sub> emissions by 80% compared to OPC have been already confirmed (Kong & Sanjayan, 2008). In addition, the FA geopolymerization has been observed to provide probably the greatest opportunities of commercial utilization due to the plentiful worldwide raw material supply derived from coal-fired electrical generation. For the FA geopolymer concrete, recent works have reported their ability to achieve a compressive

strength of higher than 60 MPa after thermally curing (Kovalchuk et al. 2007; Duxson et al. 2005), excellent durability to most aggressive acids (Fernandez-Jimenez et al. 2007), and resist sulfate attacks better than the OPC mortars in reinforcement steel bounding (Wallah et al. 2005; Song et al. 2005; Fernandez-Jimenez et al. 2006).

### **2.9.1 Factors Influencing the FA Geopolymer Synthesis**

In general, there are several factors have been identified as important parameters affecting the mechanical, physical, microstructural and thermal properties of the FA geopolymer materials, these parameters are: FA origin and composition, types and composition of the alkaline activator, curing temperature and curing duration.

#### **2.9.1.1 The FA Origin and Composition**

As the FA is a by-product from coal-fired power stations, it differs from one station to another because each station uses different source of coal and the processing procedure may not be the same. Thus, the FA properties such as its chemical composition (primarily the glassy phase), thermal history and calcium content as well as the lost on ignition (LOI) significantly affect the final properties of the resultant geopolymer matrix (Jiang & Roy, 1992; van Jaarsveld, et al. 2003; Jahanian & Rostami, 2001). For example, comparing results of two published papers the first hold by van Jaarsveld et al. (1998) and the second hold by Swanepoel & Strydom (2002) to demonstrate the complexity encountered in identifying the main influencing factors from FA on geopolymers synthesizing. In both papers, the FA geopolymer paste prepared using FA of the same name “SASOL”, but from two different power stations

with similar mix design. All samples were 50 mm paste cubic and initially cured in an oven at 50 °C for 24 hours. Although the sample size and curing conditions are same for these two cases, the strength difference of 36 MPa was extremely big. The difference from the raw material composition has been calculated and given in the column of ‘difference’ in Table 2.1.

Table 2.1: Dramatic difference of FA geopolymers (van Jaarsveld et al. 1998; Swanepoel & Strydom 2002).

Research Group	Group 1	Group 2	Differences (%)
SiO <sub>2</sub>	50.1	46.3	0.78*
Al <sub>2</sub> O <sub>3</sub>	28.3	21.3	3.35*
FA (%) CaO	8.2	4.3	2.09*
Fe <sub>2</sub> O <sub>3</sub>	4.0	9.8	-3.60*
LOI	4.1	10.9	-4.20*
Mix (%) FA	57	60	--
Kaolinite	15	10	5.0
Na <sub>2</sub> O. SiO <sub>2</sub>	3.5	5	1.5
H <sub>2</sub> O	20	20	0.0
NaOH	4	5	1.0
28 days strength (MPa)	43	7	36

\*They were calculated with the percentage of FA in each mix.

Moreover, recently Zhang et al. (2011) reported the effect FA source on the compressive strength of the FA geopolymers prepared with five different FA sources cured at two different curing temperatures. According to the authors, the FA has higher

CaO content produced the highest compressive strength regardless the effect of curing temperature as shown in Figure 2.7 and Table 2.2.

Table 2.2: Compositions of FA and the reactive SiO<sub>2</sub> content, Mass% (Zhang et al. 2011).

FA	SiO <sub>2</sub>	Al <sub>2</sub> O <sub>3</sub>	CaO	Fe <sub>2</sub> O <sub>3</sub>	K <sub>2</sub> O	LOI <sup>#</sup>	SiO <sub>2</sub> <sup>*</sup>
<b>Source</b>							
MP	72.1	22.1	0.2	1.2	1.8	0.9	57.3
WR	62.9	26.5	0.3	1.6	3.0	3.2	48.1
GS	47.5	27.4	4.3	14.3	0.5	0.2	40.4
MM	56.3	33.5	2.6	3.0	0.6	0.5	40.0
CL	54.7	32.1	1.1	7.5	0.2	0.9	35.5

\*Reactive SiO<sub>2</sub>, <sup>#</sup>Loss of ignition

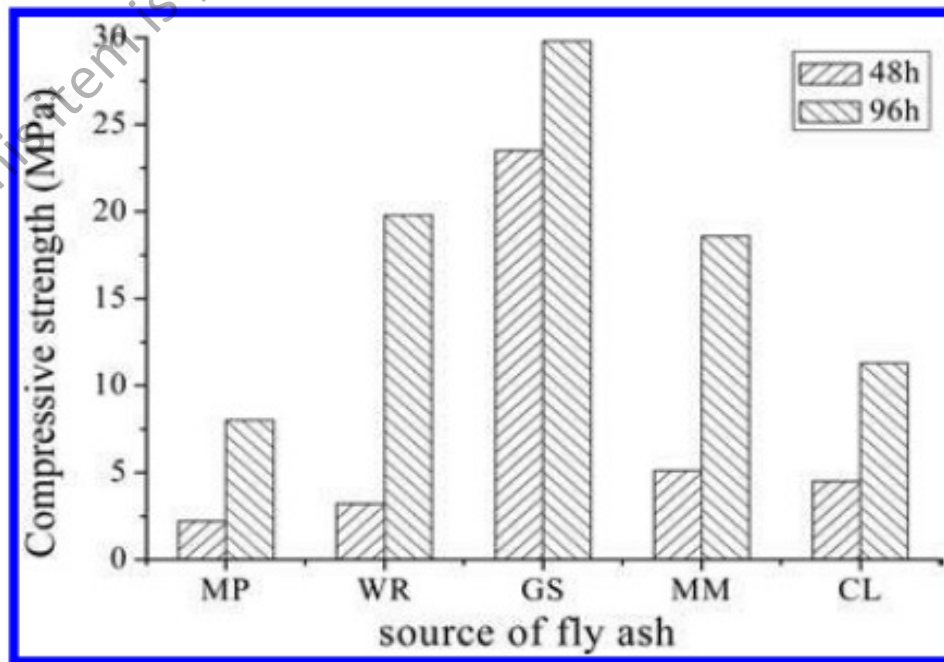


Figure 2.7: Effect of FA source on the compressive strength development of FA geopolymers (Zhang et al. 2011).

### 2.9.1.2 Types and Composition of the Alkaline Activator

As mentioned in section 2.7.2 that the most used alkaline activator in the geopolymerization technology is an alkaline mixture consisting of NaOH or KOH solution and sodium or potassium silicate ( $\text{Na}_2\text{SiO}_3$  or  $\text{K}_2\text{SiO}_3$ ). However, the usage of an alkaline activator of sodium base is more preferable over an activator of potassium base, due to economic aspects (Hardjito & Rangan, 2005). Accordingly, the concentration of the alkaline activator constituents, in particular, the NaOH solution as well as the mixing ratio of the  $\text{Na}_2\text{SiO}_3$  and NaOH solution have significant effects on the FA geopolymerization reaction and, therefore, on the resultant geopolymer mechanical and physical properties. The effects of the alkaline activator (mixture of  $\text{Na}_2\text{SiO}_3 + \text{NaOH}$  solution) characteristics on the FA geopolymerization as reported in the literature are:

- i. *NaOH Solution Concentration:* In the literature, it was reported the usage of different molarities of NaOH solution in the activation of different source materials to prepare various geopolymeric materials. However, for the FA geopolymers, Katz (1998) reported a low compressive strength of 6 MPa at age of 7 days when a FA source was activated with NaOH solution of 4 M. Puertas et al. (2000) encountered similar difficulties, when the adopted FA was activated by 10 M NaOH solution; the resulted geopolymer achieved only 6 MPa at age of 28 days. Furthermore, Abdullah et al. (2011a, 2011b, 2012) have been investigated the optimal NaOH solution molarity that resultant in optimum strength for the FA geopolymer prepared with similar FA source used throughout this study at range of 6-16 M. According to the authors, the

utilization of 12 M NaOH solution produced the highest compressive strength for the FA geopolymers at different aging periods as shown in Figure 2.8. In addition, the usage of 12 M NaOH solution has been reported by many other authors (Wan et al. 2006; Alvarez-Ayuso et al. 2008; Ng & Foster, 2010). Thus, it was decided to use the NaOH solution at concentration of 12 M in the preparation of the all geopolymers in this work as will further discussed in Chapter 3.

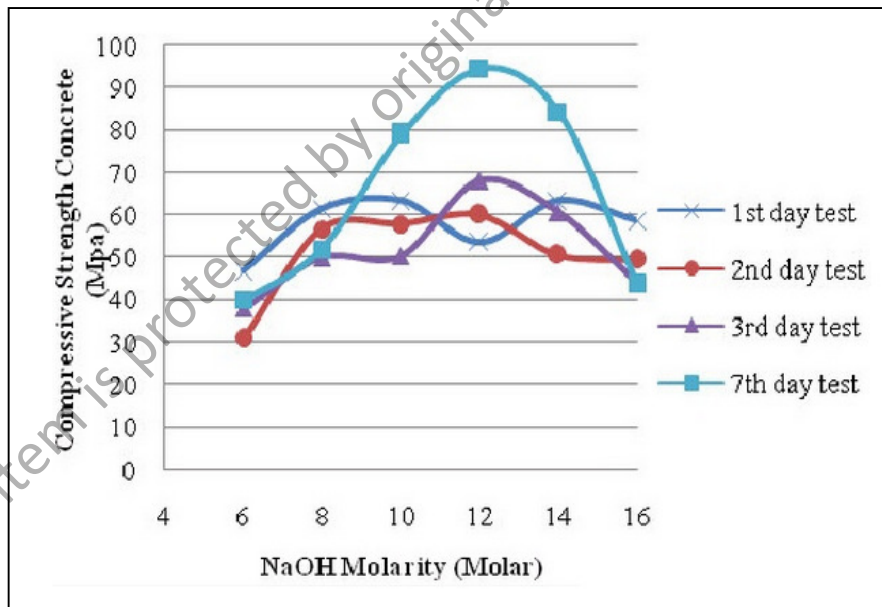


Figure 2.8: Effect of different NaOH solution molarity on the strength of FA geopolymers (Abdullah, et al. 2011b).

ii. *Mass Ratio of  $Na_2SiO_3/NaOH$* : In general, there are few researches have been reported the effect of  $Na_2SiO_3/NaOH$  ratio on the geopolymerization reaction of the geopolymers synthesized by an activation of a source material with alkaline activator consisting of  $Na_2SiO_3$  and NaOH solution. For the FA geopolymers, Pinto, (2004) reported that the  $Na_2SiO_3/NaOH$  ratio significantly influences the

compressive strength of the geopolymers prepared by the activation of FA source of (Class F). Similarly, Hardjito & Rangan, (2005) reported a limited study on the effect of the  $\text{Na}_2\text{SiO}_3/\text{NaOH}$  mass mixing ratio of 0.4 and 2.5 on the compressive strength of FA (Class F) geopolymer concrete. According to their study, the compressive strength of the geopolymer concrete increased as the  $\text{Na}_2\text{SiO}_3/\text{NaOH}$  ratio increased to 2.5 for two different concentrations of NaOH solution (8 M and 14 M) as listed in Table 2.3.

Table 2.3: Effect of  $\text{Na}_2\text{SiO}_3/\text{NaOH}$  ratio on the strength of FA geopolymers. (Hardjito & Rangan, 2005).

Mixture	NaOH (M)	$\text{Na}_2\text{SiO}_3/\text{NaOH}$ mass ratio	Compressive strength (MPa)
1	8	0.4	17
2	8	2.5	57
3	14	0.4	48
4	14	2.5	67

Moreover, for the FA geopolymers prepared with FA of (Class C) type, Chindapasirt et al. (2007) reported the effect of  $\text{Na}_2\text{SiO}_3/\text{NaOH}$  ratio in details using ratios range of 0.67 to 3.0. According to their results, the optimum compressive strength of the resulted FA geopolymer concrete was in the range of (0.67-1.00), with respect to the fact that these results were for NaOH solution concentrations of 10, 15 and 20 M. However, Chindapasirt et al. (2009) used Activator/FA mass mixing ratio of 1.5 in preparation of geopolymers based on the alkaline activation of FA (Class C) and bottom ash. Thus, it is observed that the usage of an optimum  $\text{Na}_2\text{SiO}_3/\text{NaOH}$  mass mixing ratio is strongly depended the

type and composition of the adopted FA source. Therefore, in the literature, there is no exact statement clearly specifies the optimum  $\text{Na}_2\text{SiO}_3/\text{NaOH}$  ratio mass that produced the optimum (higher) compressive strength for the resultant FA geopolymers. In other words, the optimum  $\text{Na}_2\text{SiO}_3/\text{NaOH}$  mass ratio leads to the highest compressive strength for a FA geopolymer synthesized by the activation of an individual FA source can be obtained by only performing an experimental investigation.

### 2.9.1.3 Curing Temperatures

The curing of the geopolymer materials at a temperature higher than the ambient is a constant trend in order to accelerate the geopolymerization reaction and reducing the setting time (Bakharev, 2005). In previous studies, the most curing temperatures used to cure the FA geopolymers were in the range of 20 °C to 120 °C (Hardjito et al. 2002; Sindhunata et al. 2004; Bakharev, 2005; Kong & Sanjayan, 2010; Rashad & Zeedan 2011; Rickard et al. 2012). Hardjito et al. (2002) studied the effect of curing temperature of 30, 60 and 91 °C, on the compressive strength as shown in Figure 2.9, which clearly illustrates the essential benefit of evaluated the curing temperature, and the best curing temperature of 60 °C.

Table 2.4 is listed some of past studies performed to evaluate the effect as well as obtain the optimum curing temperatures of the FA geopolymers. It can be observed that the optimum curing temperature that given the highest compressive strength for the FA geopolymer is in the range of 60 °C to 90 °C. Anyway, the exact optimum curing temperature for FA geopolymers is not specifically appointed, and in order to achieve it, an experimental investigation is needed as the optimum curing temperature is depended

on the FA source, type of alkaline activator as well as the used curing period (Alvarez-Ayuso et al. 2008).

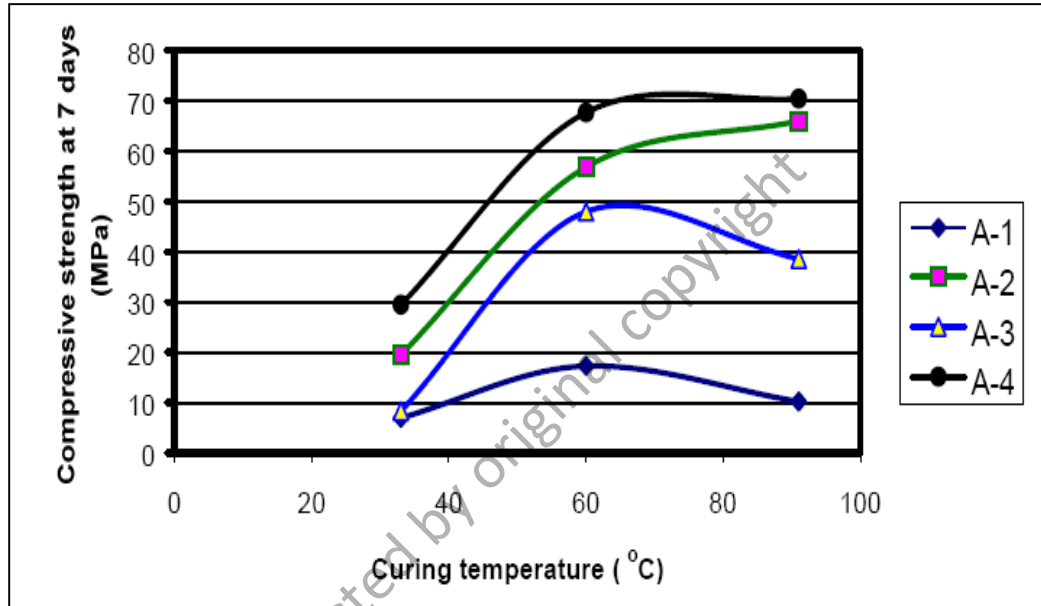


Figure 2.9: Influence of curing temperature on strength development. (Hardjito et al. 2002). A-1= mixing time 5 minutes, A-2= mixing time 4 minutes, A-3= mixing time 3 minutes, A-4= mixing time 2 minutes.

Table 2.4: Some of past studies on the effect curing temperature of FA geopolymers.

No.	Range (°C)	Optimum (°C)	Reference
1	30, 60, 91	60	Hardjito et al. (2002)
2	30, 75	75	Sindhunata et al. (2004)
3	75, 90	90	Bakhariv (2005)
4	45, 65, 85	85	Fernandez-Jimenez & Palomo, (2002)
5	22, 80	80	Wu & Sun, (2007)
6	20, 75	75	Arellano-Aguilar, et al. (2010)
7	40 to 120	85	Thakue & Ghosh, (2009)

#### 2.9.1.4 Curing Duration

As there are different proposed optimal curing temperatures in the literature, there are many suggestions for the optimum curing period that varied from one study to another. Past studies investigated the FA geopolymers curing period at range of curing periods of 6 hours to 96 hours (Hardjito & Rangan, 2005; Sindhunata et al. 2004; Bakhariv, 2005; Wu & Sun, 2007; Thakur & Ghosh, 2009; Alvarez-Ayuso et al. 2008; Chindapasirt et al. 2007). Furthermore, Table 2.5 is showing some of the past research results that investigated the effect of curing periods on the FA geopolymer properties. It observed that the curing period of 24 hours is the most reported optimal curing duration which gave the FA geopolymers the highest compressive strength. In accordance, van Jaarsveld et al. (2002) reported that the prolonged curing beyond 24 hours has a negative effect on the microstructure of the geopolymer matrix resulting in low compressive strength. However, other authors reported that the 48 hours resulted in the highest compressive strength (Wu & Sun, 2007; Thakur & Ghosh, 2009). Even, Hardjito & Rangan, (2005) adopted the 24 hours as the optimum curing period, the results of their study showed that the FA geopolymers were continuously gained strength when they cured at curing periods beyond the 24 hours. As a fact, however, they adopted the 24 hours as an optimum curing period due to economical aspects as the heating the geopolymers for a period more than 1 day would increase the cost of FA geopolymers production as well as the strength gaining rate at longer curing time than 24 hours was actually little as Figure 2.10 represented. Thus, the exact curing period that produced the highest compressive strength for the FA geopolymers is not yet reported in the literature, which therefore needs to be experimentally achieving similar to the optimum  $\text{Na}_2\text{SiO}_3/\text{NaOH}$  mass ratio and curing temperature.

Table 2.5: Some of past studies on the effect curing durations of FA geopolymers

No	Range (hour)	Optimum (hour)	Reference
1	6 - 96	24	Hardjito & Rangan,(2005)
2	12,24,48, 72	24	Sindhunata et al. (2004)
3	6,24	24	Bakhariy (2005)
4	12,24, 48	24	Fernandez-Jimenez &Palomo, (2002)
5	6, 24, 48	48	Wu & Sun, (2007)
6	24-96	24	Chindaprasirt et al. (2007)
7	6-72	48	Thakur & Ghosh, (2009)

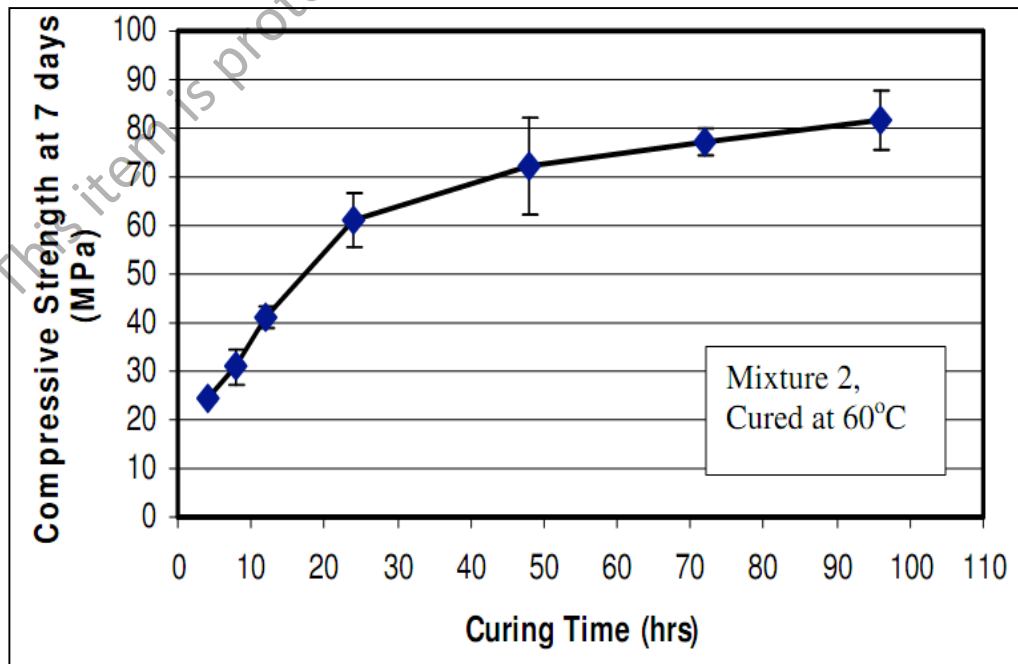


Figure 2.10: Influence of curing periods on the compressive strength of the FA geopolymers (Hardjito & Rangan, 2005).

## 2.9.2 Structure of FA Geopolymers

In general, the inorganic aluminosilicate polymers or geopolymers that results from the dissolution and polycondensation of various alkali-aluminosilicate are essentially X-ray amorphous materials (Davidovits, 1991). Barbosa et al. (2000) studied X-ray diffraction (XRD) patterns of the source materials (kaolinite +MK) and MK geopolymers of different molar oxide ratios of  $\text{SiO}_2/\text{Al}_2\text{O}_3$ ,  $\text{Na}_2\text{O}/\text{SiO}_2$ , and  $\text{H}_2\text{O}/\text{Na}_2\text{O}$  as indicated in Figure 2.11. The kaolinite (Figure 2.11a) shows a typical diffraction pattern of a well-ordered mineral. The quartz impurity (asterisked) remains as a sharp diffraction line after dehydroxylation at  $750^\circ\text{C}$  (Figure 2.11b) and polymerization of geopolymers with different oxide molar ratios cured at room temperature (RT) and at  $65^\circ\text{C}$  (Figure 2.11C to 2.11G). It can be seen that the XRD patterns of all MK geopolymers shows a similar amorphous character independent of curing treatment, with a halo peak at about  $27$  to  $29^\circ 2\theta$ . These data also suggest that the structure of all the MK geopolymers is similar to those of feldspatic glasses, consisting of randomly developed Al-Si polyhedral with a lack of periodically repeating atomic units (Barbosa et al, 2000).

For the FA geopolymers, Figure 2.12 shows the XRD patterns of the original FA as well as the FA geopolymers as reported by Fernandez-Jimenez & Palomo, (2005), shows that the crystalline phases originally existing in the FA (quartz, mullite etc,) have not been apparently altered by the activation reaction. Similar finding were reported by other authors (Bakhariv, 2005; Thakur & Ghosh, 2009; Rashad & Zeedan 2011; Alvarez-Ayuso et al. 2008; Jo et al. 2007; Rickard et al. 2012), confirming that the typical FA geopolymer structure characteristics are amorphous with the existing of some crystalline phases of FA itself.

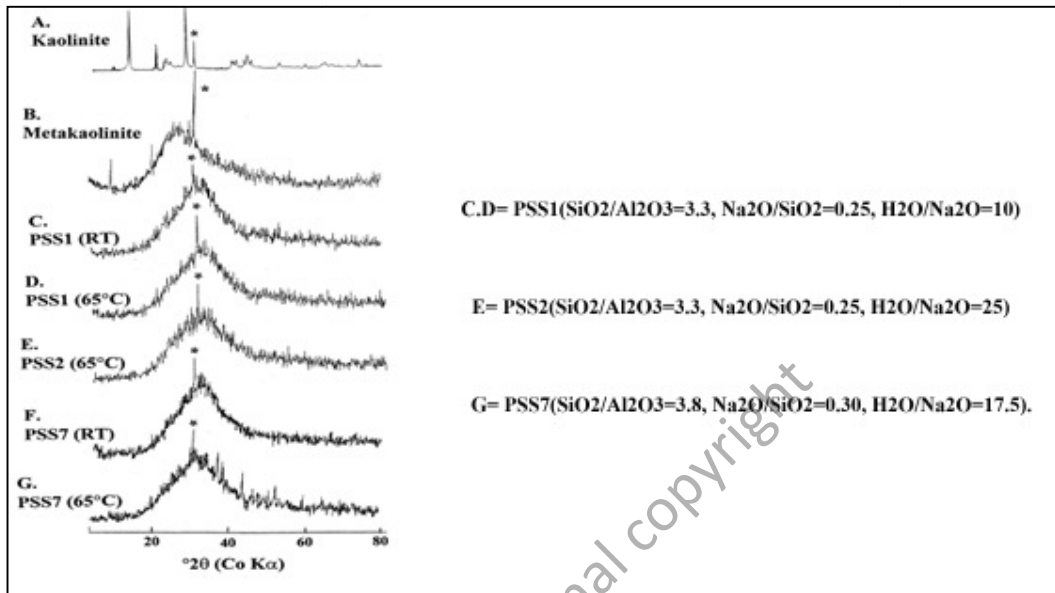


Figure 2.11: XRD patterns of the base materials and the MK geopolymers (Barbosa et al 2000).

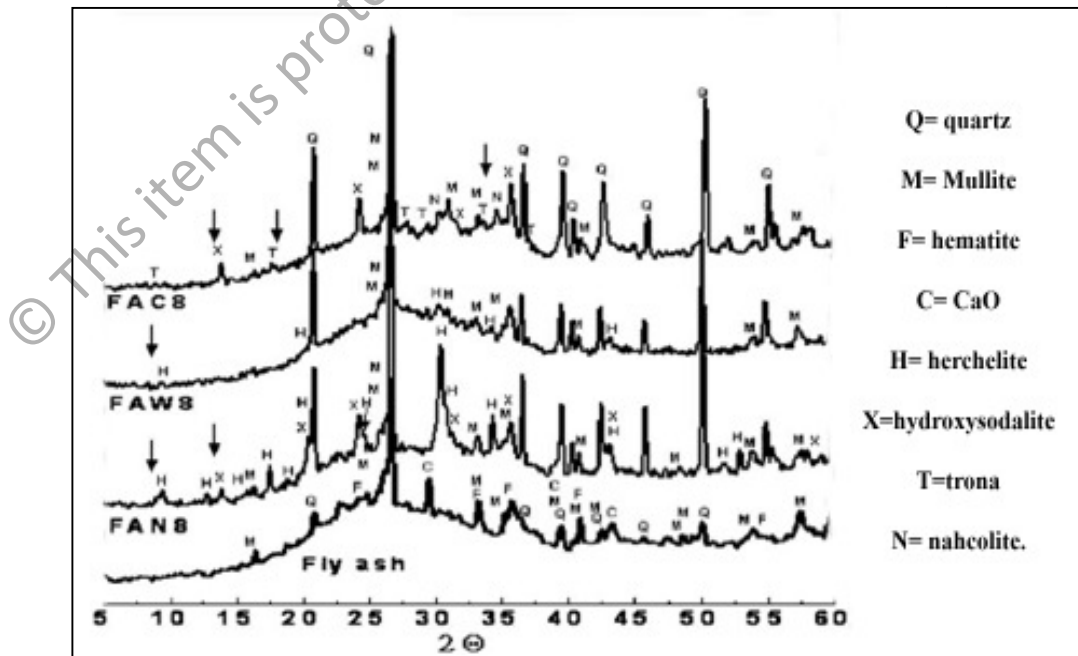


Figure 2.12: XRD patterns of alkali activated FA mortars (Fernandez-Jimenez & Palomo, 2005).

### 2.9.3 Microstructure of FA Geopolymers

Hos et al. (2002) systematically analyzed the microstructure of MK geopolymer by using scanning electron microscopy (SEM) and observed the nonporous microstructure of their materials. According to the authors, the microstructure is a result of extensive dissolution of aluminosilicate species that occurs before polycondensation commences and consolidates the shapes of the specimen through a chaotic three-dimensional network of polysodium aluminosilicate (Figure 2.13).

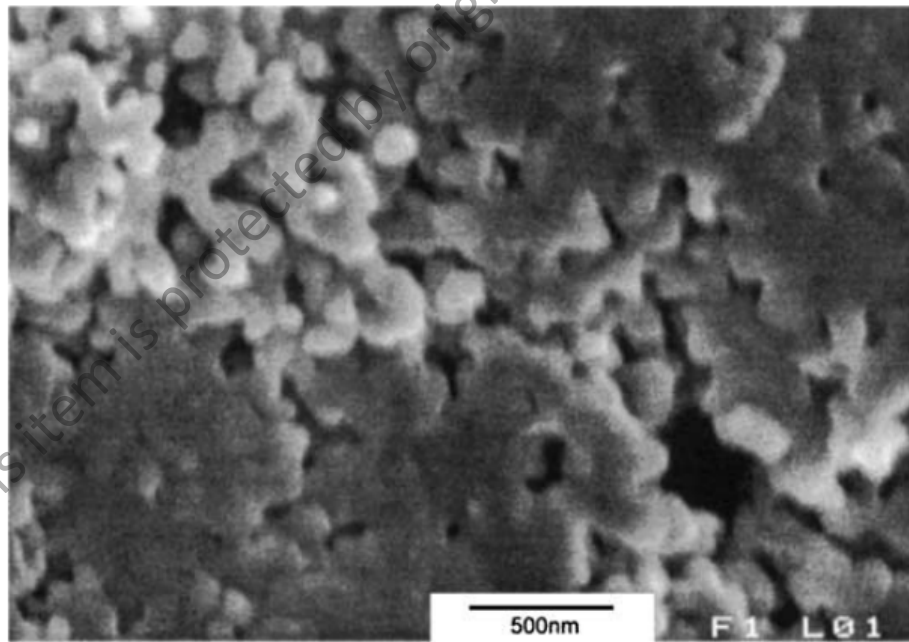


Figure 2.13: High-resolution SEM micrograph of MK geopolymer (Hos et al. 2002)

For the FA geopolymers, the past studies investigated the microstructure of these geopolymers reported that the FA geopolymeric material consisted mainly from a dense, porous and semi-homogenous aluminosilicate gel matrix, which resulted from the geopolymerization process (Palomo et al. 1999b; Thakur & Ghosh, 2009; Rashad & Zeedan, 2011; Alvarez-Ayuso et al. 2008).

Palomo et al. (1999b) reported that the FA geopolymer material is very porous and the microspheres (originating from FA grains) are surrounded by a crust of reaction product as shown in Figure 2.14. According to these authors, the adherence of crust to the sphere does not appear to be very strong and the bond between grains is produced through the necks of reaction product as indicated in Figure 2.14a. In addition, the crack development is evident in the middle of the matrix and is likely to have been initiated from the pore (Figure 2.14b).

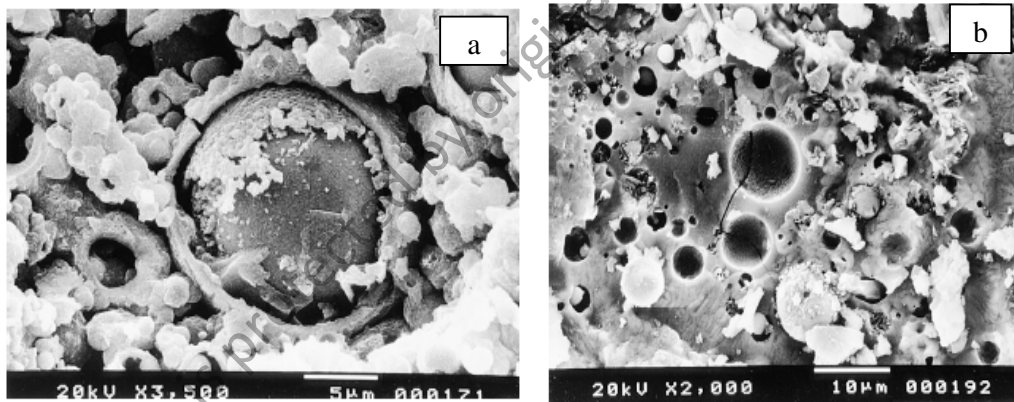


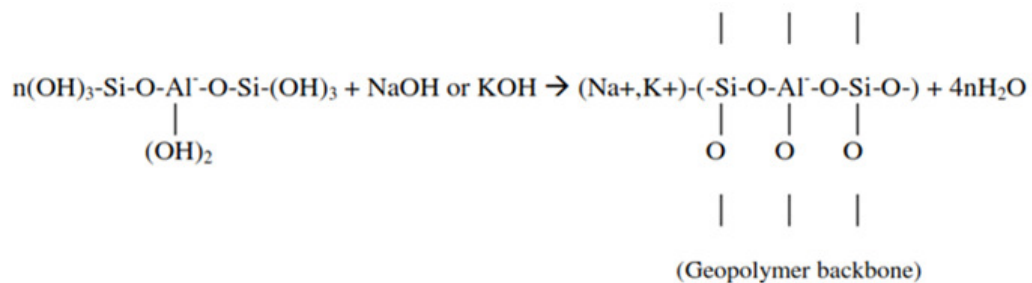
Figure 2.14: Microstructure of the fly ash-based geopolymer (Palomo et al. 1999b)

Furthermore, it was found that the microstructure of the FA geopolymers, in particular, the quality of the aluminosilicate matrix and the content of the unreacted FA microspheres significantly affected by the type and the concentration of the alkaline activator (Xie & Xi, 2001; Alvarez-Ayuso et al. 2008). Thakur & Ghosh, (2009) reported that increasing the alkaline activator concentration increases the quality and the dense of the geopolymeric gel matrix by decreasing the unreacted FA microspheres which indicating the formation of more aluminosilicate gel. High quality and the dense of the geopolymeric gel matrix comes for the high dissolution of the FA in high alkali concentration environment resulted in high compressive strength for the hardened FA

geopolymer (Thakur & Ghosh, 2009; Porvis et al. 2009; Rickard et al. 2012). Furthermore, it was reported that the microstructure of the FA geopolymers contains a portion of crystals like-structures distributed in the gel matrix which is composed mainly form sodium silicate hydrate and small amount of aluminum and iron (Xie & Xi, 2001). In addition, recent studies reported that the high concentration activators produce high compressive strength for the FA geopolymers are also producing high content of unreacted silicate which may causing structural failure at high temperatures (700 °C to 800 °C) due to sintering and densification process (Porvis et al. 2009; Rickard et al. 2012). This will discussed further in the thermo-physical characteristics of the FA geopolymers section (2.9.4).

#### 2.9.4 Thermo-Physical Characteristics of FA Geopolymer

The hardened geopolymer material contains three types of water that will escape during heating of a geopolymer at temperatures above 100 °C (Davidovits, 2008). These water types are: the physically bonded water or free water, the chemically bounded water and the hydroxyl groups OH. Physically bonded water is the water generated during the geopolymerization reaction as a part of the resultant products according to Equation 2.11 (van Jaarsveld et al., 1997; Davidovits, 1999).



(2.11)

The chemically bounded water existing in the geopolymer gel and also known as 'zeolitic water', whereas, the hydroxyl groups OH presence at the surface and edges of each geopolymeric micelle. Each type of this mentioned water evaporates at a specific range of temperatures when the geopolymeric material is heated at temperatures above 20 °C. The physically bonded water evaporates in the range of temperature of 20 °C to 100 °C. Further heating for the geopolymer paste to temperatures above 100 °C, the chemically bonded water and the hydroxyl groups OH evaporate from the structure due to the dehydration and dehydroxylation processes at high temperatures. The chemically bonded water evaporates at range of 100 °C to 300 °C, and finally the dehydroxylation of OH groups evaporates at temperature above 300 °C (Davidovits, 2008; Duxson et al., 2007a). The evaporation of water from the geopolymer structure is associated with mass loss that could cause the formation of cracks due to the thermal shrinkage, which will be discussed later on in this section.

Davidovits, (1984, 1994) and Barbosa & MacKenzie, (2003a, b,) have been reported that the geopolymer materials possess excellent heat resistant up to 1200 °C and 1400 °C due to their inorganic framework. While, Cheng & Chin, (2003) regarded the good heat resistant of geopolymers to their ceramic like-properties.

Kong et al. (2007) compared the thermal resistance of FA and MK geopolymers and found that the FA geopolymers porous structure decrease the thermal damaging during heating above 100 °C, whereas the MK geopolymers do not. Also, Kong & Sanjayan, (2010) have been compared the thermal resistance of the FA geopolymer with equivalent OPC paste and found that the FA geopolymer materials have superior thermal resistance over the OPC as shown in Figure 2.15. In accordance, similar finding was reported by Rashad & Zeedan, (2011) showed the high thermal resistance of the FA geopolymers compare with the OPC cement. Other studies have been found that the FA

geopolymer possessed low shrinkage and excellent compressive strength retention after exposing to high temperatures (Dombrowski & Buchwald, 2007; Bakharev, 2006; Rickard et al. 2011; Temuujin et al. 2010; Kong & Sanjayan 2008, 2010).

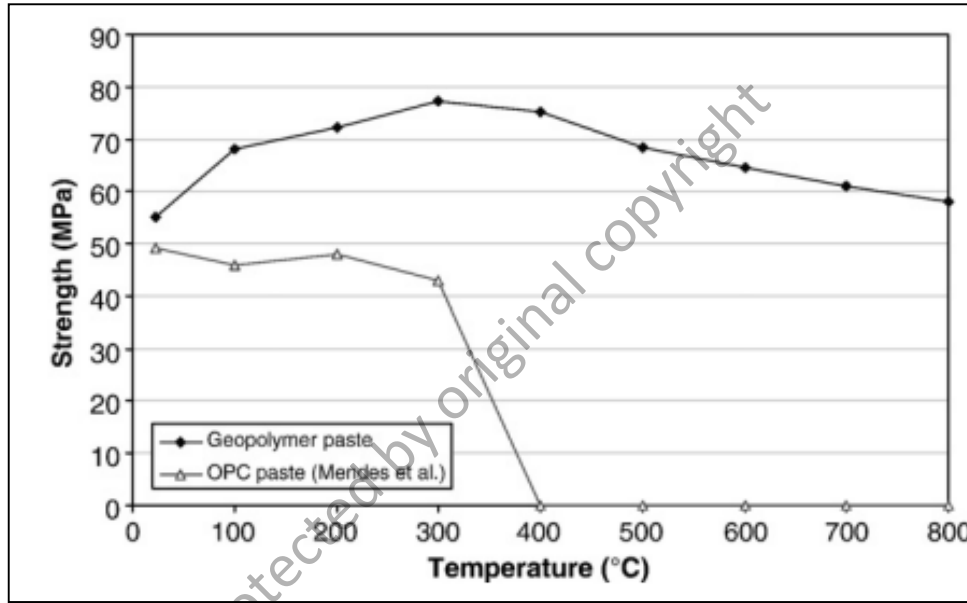


Figure 2.15: Comparison in heat resistance between the FA geopolymer paste and OPC cement (Kong & Sanjayan 2010).

Actually, the heating of a hardened geopolymer at temperatures above the 100 °C resulting in a transformation of the geopolymeric structural water that resulted from the geopolymerization reaction as shown in equations 2.10 and 2.11, into a water vapor (Davidovits, 2008). As the heating temperature increases, the liberation rate of the vapor increases, which resulted in thermal shrinkage due to the mass loss in term of water vapor, which can be detected by thermogravimetric analysis (TGA) and dilatometric analysis similar to the one reported by Kong & Sanjayan, (2008) shown in Figure 2.16. However, when the geopolymeric material has high density and less permeability, the dispersion of the water vapor would induce the thermal stresses, which enhanced with increase the heating temperatures, resulted in intensive thermal cracks. This

phenomenon is called the vapor effect (Hu et al. 2010). The thermal shrinkage and thermal stress are responsible for the strength deterioration when the FA geopolymer heated at high temperatures (Kong & Sanjayan, 2008, 2010).

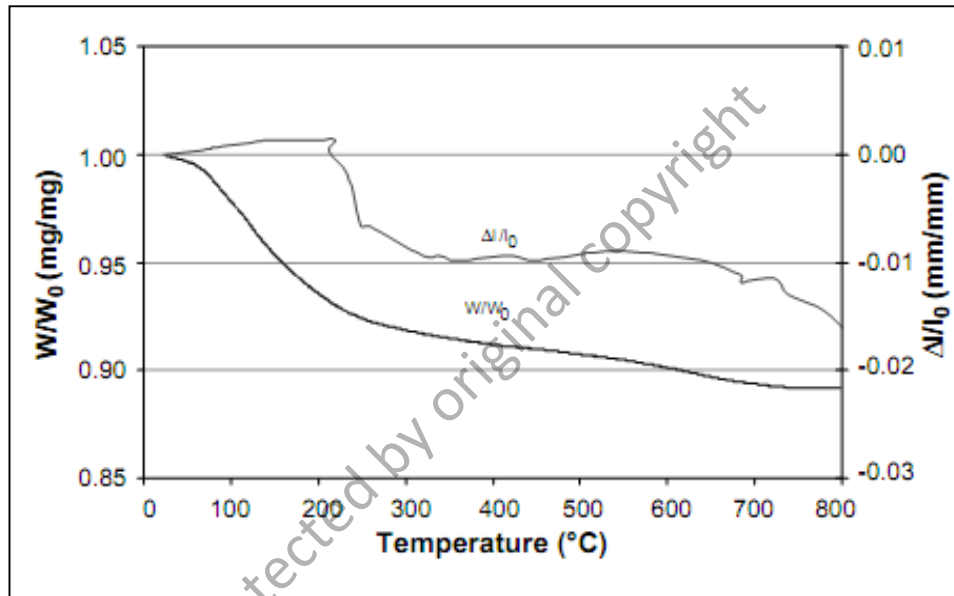


Figure 2.16: TGA and dilatometric curves of FA geopolymers (Kong & Sanjayan, 2008)

Nevertheless, when the heating temperature exceeds 700 °C, the damage of the water vapor becomes not only the cause behind the strength deterioration for the heated FA geopolymer. Recently, Provis et al. (2009) and Rickard et al. (2012) have been reported that a portion of the activating solution remained unreacted or partially reacted during the formation of the geopolymer remaining in hardened sample. The content of this residual species (high silicate content) is increasing with increase the liquid/solid mass ratio. During heating of the FA geopolymer at temperature of 700 °C to 800 °C, the residual silicate experience extremely densification and sintering processes due to the swelling of the high silicate secondary phases (Rickard et al. 2012). The densification of the residual silicate phase can be detected by the dilatometric analysis as illustrated in

Figure 2.17 (Provis et al. 2009). Similar findings have been also reported for the MK geopolymers (Rahier et al. 1996; Subaer & van Riessen, 2007).

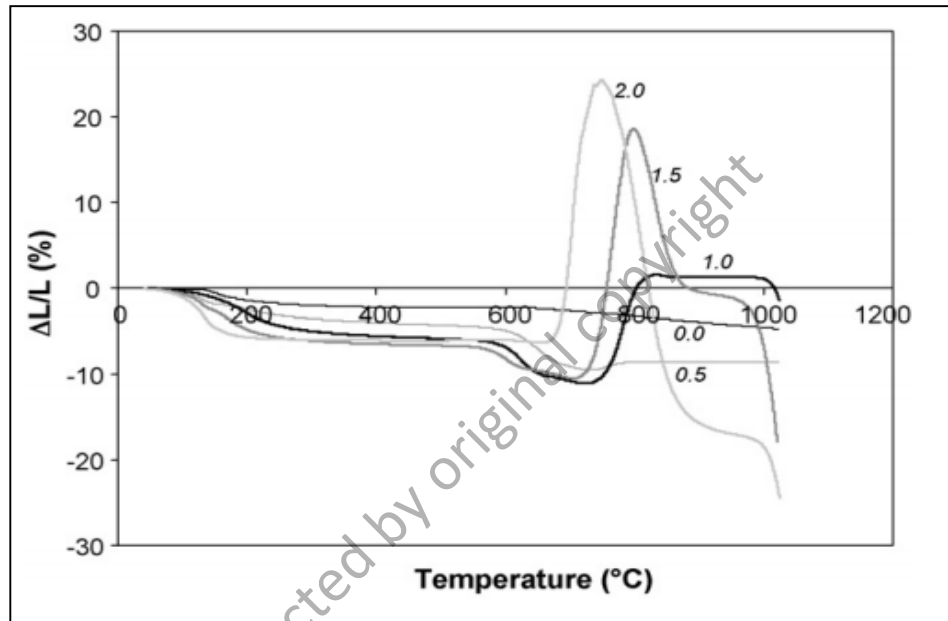


Figure 2.17: Dilatometric data of FA geopolymers of different liquid/solid ratios (Provis et al. 2009).

Moreover, Kong & Sanjayan, (2010) reported that the thermal resistance of the FA geopolymer paste is significantly affected by the sample size. According to their research, as the sample size decreases, the residual strength of the exposed geopolymers to elevated temperature of 800 °C is increased, as demonstrated in Figure 2.18.

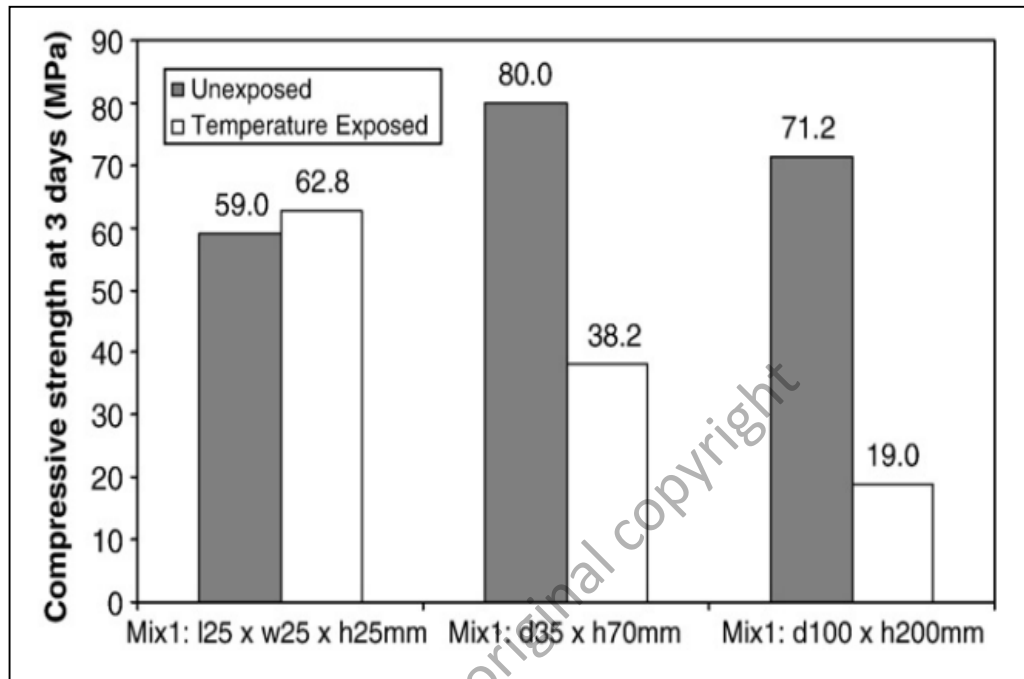


Figure 2.18: Effect of sample size on the FA geopolymer paste thermal behavior (Kong & Sanjayan, 2010).

Additionally, Kong & Sanjayan, (2010) also studied the thermal behavior of FA geopolymer concrete and they concluded that the coarse aggregate size have a major affect on the thermal performance of the FA geopolymer concrete as illustrated in Figure 2.19. In addition, they reported that the differences in the thermal expansion between the geopolymer paste matrix and the aggregate shown in Figure 2.20 were dominated over the thermal shrinkage and led to the strength deterioration of the FA geopolymer concrete after exposed to high elevated temperature of 800 °C.

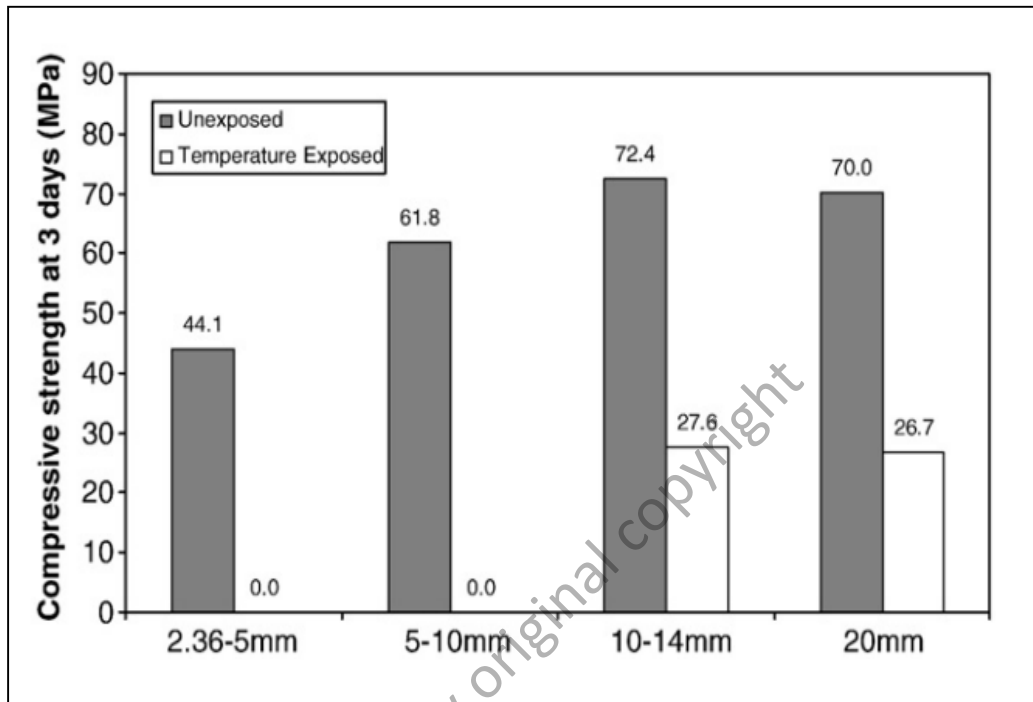


Figure 2.19: Effect of aggregate size on the FA geopolymer concrete thermal behavior (Kong & Sanjayan, 2010).

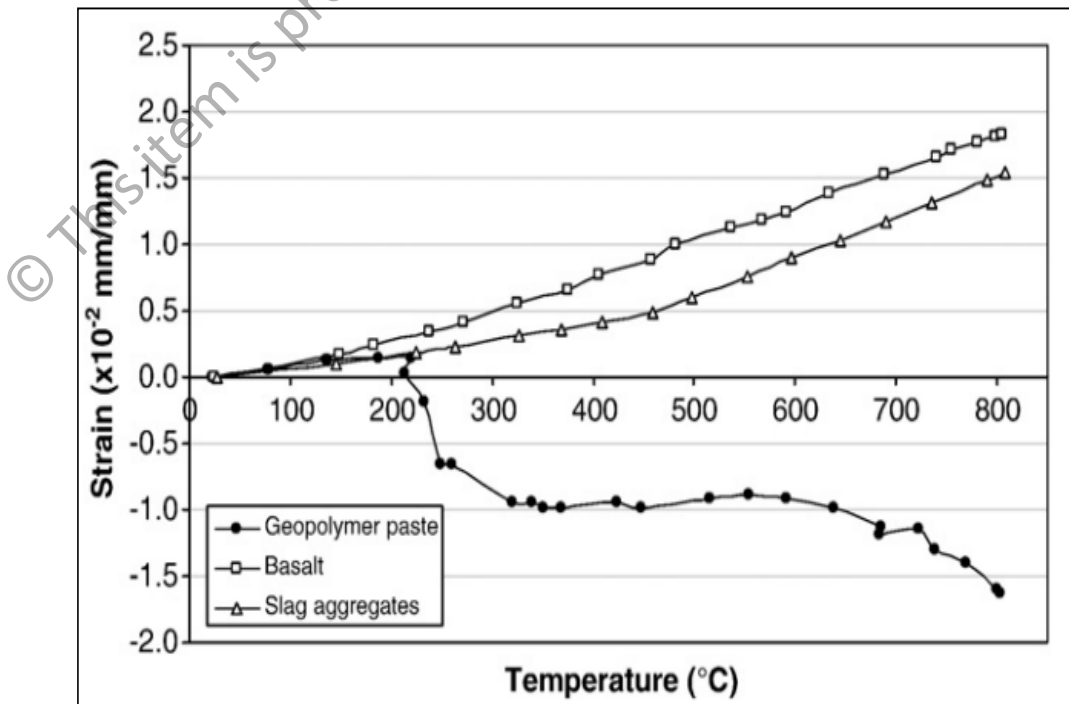


Figure 2.20: Thermal expansion of coarse aggregate and FA geopolymer paste (Kong & Sanjayan, 2010).

## 2.10 The Use of Geopolymers in Production of the LWAGC

Despite of the increase attention to the advantages of geopolymer materials, there are significantly few published studies and researches regarded to utilization of these novel technology in production of lightweight geopolymer concrete (LWAGC). The following published studies are represents the only available researches that dealt with using of the geopolymerization in the production of lightweight concretes.

The first attempt was carried out by Jo et al. (2007) who used the geopolymerization of a FA by liquid alkaline activator in production of geopolymeric LWAs or what they named it the alkali-activated FA artificial LWA (AFLA). These AFLAs were used in production of OPC-based LWAC.

While, Wu & Sun, (2007) reported a no-fine LWAGC based on the activation of source material combination of FA and MK by liquid mixture of  $\text{Na}_2\text{SiO}_3$  and NaOH solution. In their study, two types of LWAs, namely, Cenospheres and Expanded Polystyrene Beads (EPS) were used as LWAs in production of no-fine LWAGC. The optimum EPS concrete possessed a compressive strength of 22.6 MPa and an Oven-dry (OD) density of  $1010 \text{ kg/m}^3$  at 28 days, while the optimum Cenospheres concrete produced a compressive strength of about 12.8 MPa and an OD-density of  $1020 \text{ kg/m}^3$  at the same aging period.

Furthermore, Hu et. al., (2009) studied the fire-resistance of lightweight geopolymer mortars prepared by the activation of MK with alkaline activator of soluble  $\text{Na}_2\text{SiO}_3$  and NaOH solution after exposed to elevated temperature of  $950 \text{ }^\circ\text{C}$ . According to this study, the lightweight geopolymer mortars were prepared by using crushed shale haydite sand possessed a maximum aggregate size of 4.75 mm, as a lightweight fine aggregate, mixed at three different geopolymer/haydite mass ratios. The results showed

that the highest geopolymer/haydite mass ratio led to lowest strength loss, also as the particle size of haydite decreased, the strength loss rate decrease as well. For instance, the lightweight geopolymer mortars prepared with haydite sand possessed a grain size of 2.36-4.75 mm, experienced a strength loss of 63 % after exposed to elevated temperature, while the mortar prepared with haydite sand of 1.18-2.36 mm experienced a strength loss of 59 %.

Zuda et al. (2010) investigated the thermal performance of no-fine lightweight aggregate alkaline activated composite prepared by the alkali-activation of a fine ground slag as a source material using liquid  $\text{Na}_2\text{SiO}_3$ . The geopolymer composite (concrete) was prepared by the incorporation of a combination of two LWAs, namely, expanded vermiculite and electrical porcelain. The thermal performance of the resulted concrete was investigated at range of elevated temperatures of 200 to 1200 °C. According to their results, the compressive strength of the heated geopolymer composite was decreased sharply up to 800 °C, followed by a compressive strength regain after heating the concrete at 1000 and 1200 °C as shown in Table 2.6. In addition, Zuda et al. (2010) reported a microstructure and the porosity investigation of geopolymeric composites after exposure to elevated temperatures.

Arellano-Aguilar et al. (2010) reported a lightweight geopolymeric aerated concrete prepared with alkali-activation of a source material consisting of MK or MK + FA (at different MK/FA mass mixing ratios) by liquid  $\text{Na}_2\text{SiO}_3$ . In their study, two types of the aerated lightweight geopolymeric concretes were achieved, one by using aerated agent ( $\text{Al}_2\text{O}_3$  powder) that generated air bubbles in the structure with no LWAs, and the other prepared by the addition of a fine blast furnace slag (BFS) sand of particle size smaller than 4.75 mm as a fine LWA to the aerated agent. Hence, this study reported two techniques of making aerated lightweight geopolymeric concretes of using an aerated

agent once, and addition fine LWA to the agent to prepare a LWA-aerated concretes. In addition, this study reported mechanical, thermal and microstructural investigations of the lightweight geopolymeric aerated concretes possessed relatively low densities of 1200, 800 and 600 kg/m<sup>3</sup>. Based on the study results, the compressive strength of the LWA-aerated concretes were increased with increasing their densities, also the concrete strength significantly increased by the introducing of the FA to the geopolymerization reaction as shown in Figure 2.21. Furthermore, the thermal properties of the resulted aerated concrete (no LWA) investigations reported a reduction in the thermal conductivity of the concrete with decreasing its density. While the microstructure study results of the LWA-aerated concrete revealed that there is a dense and strong interfacial zone between the BFS sand grains and the geopolymeric matrix due to the BFS participation in the reaction (Arellano-Aguilar et al. 2010).

Table 2.6: Residual Mechanical strength of the exposed geopolymeric lightweight composite to elevated temperatures (Zuda et al. 2010)

<b>Elevated Temp. (°C)</b>	<b>Residual compressive strength (MPa)</b>
200	21.2
400	18.4
600	14.2
800	7.9
1000	10.1
1200	29.2

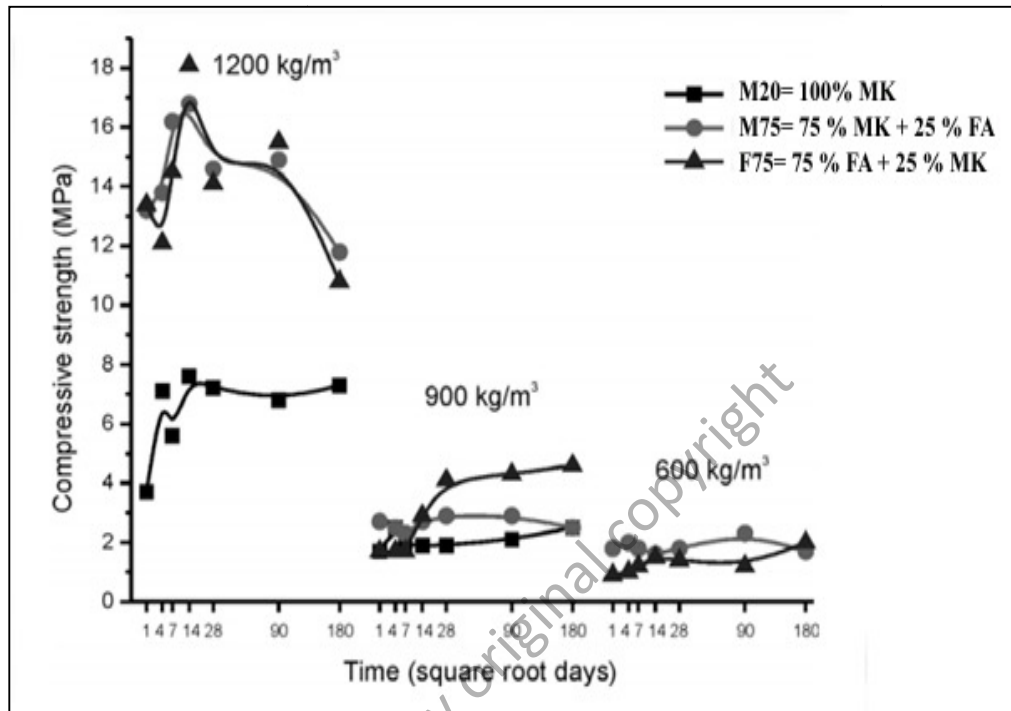


Figure 2.21: Compressive strength vs. time of age of aerated concretes with BFS sand, (Arellano-Aguilar et al. 2010).

Moreover, Yang et al. (2010) reported the usage of fine/coarse lightweight expanded clay aggregates (LECA) and normal-weight sand in preparation of lightweight alkaline activated geopolymeric mortars and concretes, based on the alkali-activation of ground granulated blast-furnace slag (GGBS) with powder sodium silicate and water. In practice, the geopolymeric lightweight mortars were prepared using water/binder ratios of 0.4, 0.5 and 0.6, while the LWAGCs were prepared at water/binder ratio of 0.5. Furthermore, the replacing of normal-weight sand by the fine LWA was investigated and evaluated in term of the geopolymers resultant compressive strength. According the study results, the compressive strength of the resulted geopolymer mortars and LWAGC was decreased continuously with increasing the replacing level due to decreasing of the OD-density of the resultant geopolymers, as shown in Figures 2.22 and 2.23.

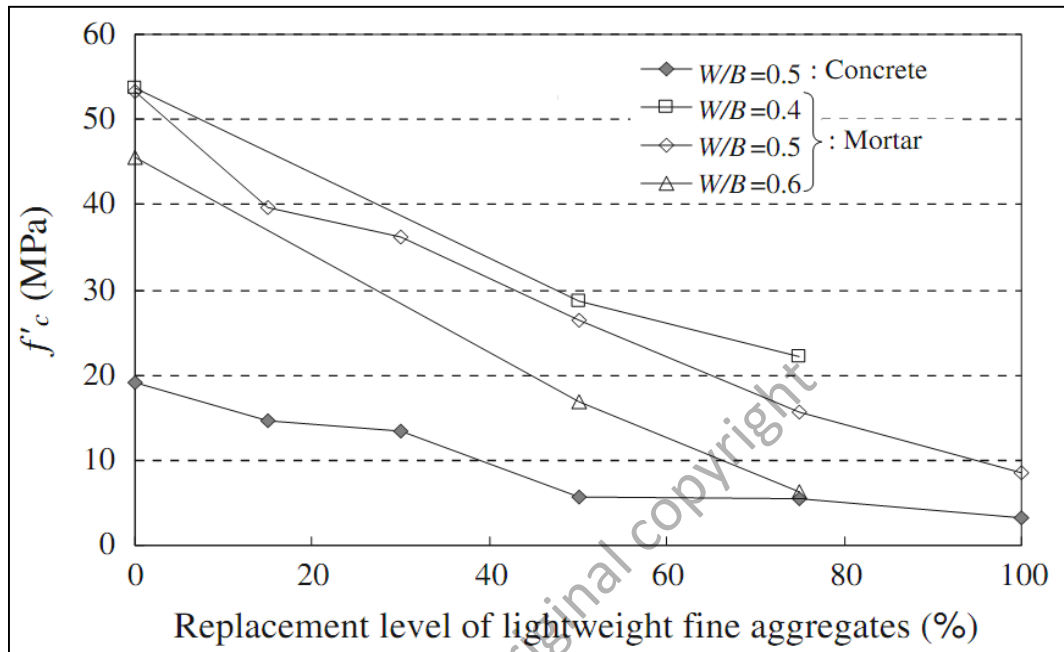


Figure 2.22: 28 days compressive strength ( $f'_c$ ) of geopolymer mortar and LWAGC (Yang et al. 2010).

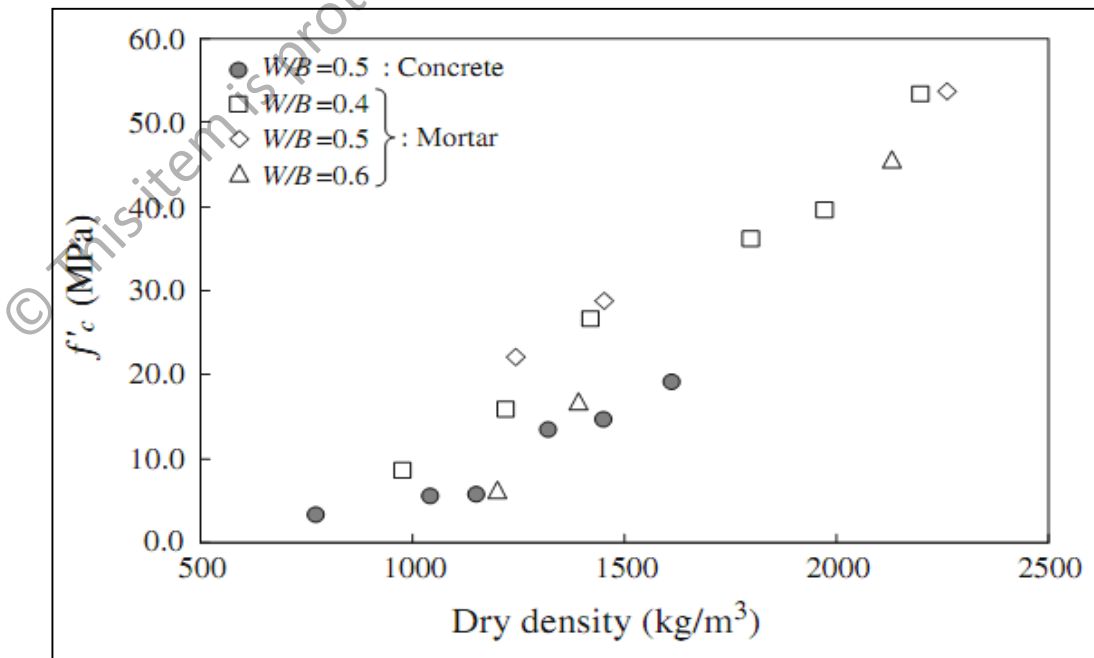


Figure 2.23: Compressive strength ( $f'_c$ ) of the geopolymers vs. OD-density (Yang et al. 2010).

In addition, the results showed a range of bulk density for geopolymer mortars and LWAGC of  $775 \text{ kg/m}^3$  to  $1615 \text{ kg/m}^3$  and a compressive strength range of 3.3 MPa to 19.1 MPa at age of 28 days. Furthermore, Yang et al. (2010) reported the applicability of using the mathematical equations used for the theoretical calculations of some mechanical properties of the structural OPC lightweight concrete in measuring the same properties for the geopolymeric based LWAC. Finally, this work is considered the first and the only available published study reports the preparation of a structural geopolymeric lightweight concrete, as it reports the preparation of a LWAGC consisting of coarse LWA, fine-normal weight sand and geopolymeric binder.

Ng & Foster, (2010) studied the shear strength of a lightweight fiber reinforced geopolymer concrete beam, manufactured by the geopolymerization of high performance ash “HPA” which is a combination consisting of FA+ slag + kaolite by alkaline activator mixture of 12 M NaOH and  $\text{Na}_2\text{SiO}_3$ . The concrete beam was prepared by the usage of fine lightweight ceramic microsphere fillers has trade name of E-spheres<sup>®</sup> SLG of 150-400  $\mu\text{m}$  in particle size used as fillers in the concrete with two types of steel fibers. According to the study results, the fiber reinforced geopolymeric lightweight beams were more ductile, and at failure, it is exhibited substantially higher deformation capacities than the plain concrete.

Zhang et al. (2011) used a foaming agent in preparation of foamed lightweight geopolymeric concrete by the activation of different FA sources with alkaline activator mixture of NaOH solution (8 and 14 M) and  $\text{Na}_2\text{SiO}_3$ . Actually, this study was more focused on the effect of FA sources and curing conditions on the strength development of the FA geopolymer paste. However, the authors reported that the resulted foamed lightweight geopolymeric concrete possessed low strength comparing with geopolymer pastes, and the curing at high temperature (90 °C) caused the formation of visible

relatively wide macrocracks on the foamed concrete. In addition, it was reported that the using of NaOH solution of 10M resulted in good compressive strength of 8.9 MPa even it density was only 1.0 g/cm<sup>3</sup> as shown in Figure 2.24 .

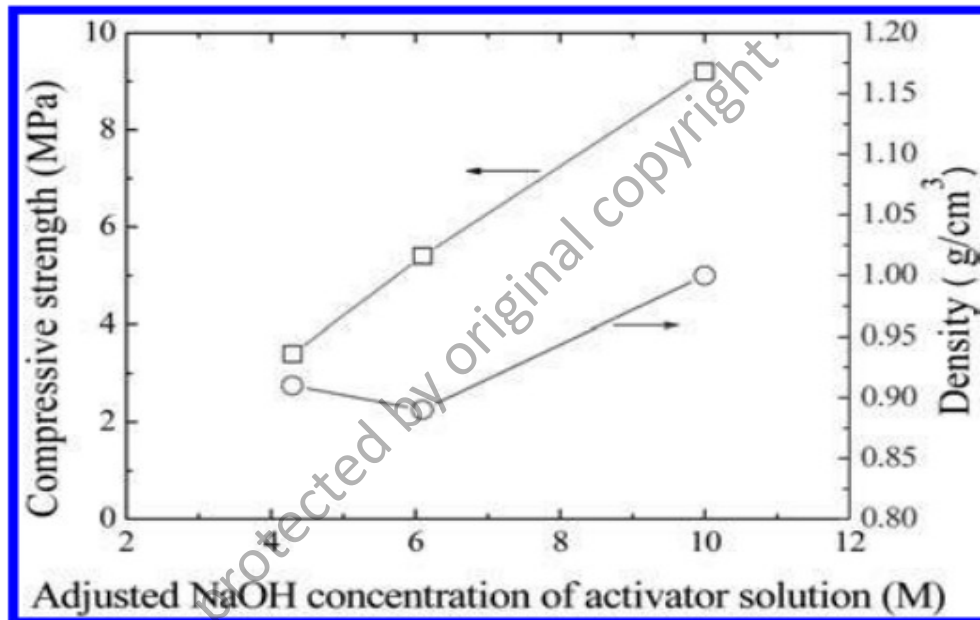


Figure 2.24: Strength and density of foamed geopolymers vs. NaOH concentration (Zhang et al. 2011).

Whereas, Abdullah et al. (2012) reported a foamed FA geopolymer lightweight concrete prepared by the alkaline activation of a (Class C) FA source by alkaline activator mixture of NaOH solution (12 M) and Na<sub>2</sub>SiO<sub>3</sub>. The authors reported the effect of two curing conditions of 60 °C for 24 hours and room temperature on the strength development and other physical properties of the foamed concrete as shown in Figure 2.25 and Table 2.7. It can be seen that thermal curing at 60 °C resulted in highest compressive strengths of the foamed FA geopolymer lightweight concrete at early ages of 1 and 7 days than the concrete cured at room temperature. While, at age of 28 days the foamed FA geopolymer lightweight concretes cured at 60 °C and at room

temperature developed approximately the same compressive strength. Furthermore, the foamed FA geopolymer lightweight concrete cured at room temperature possessed highest porosity content that the concrete cured at room temperature as shown in Table 2.7.

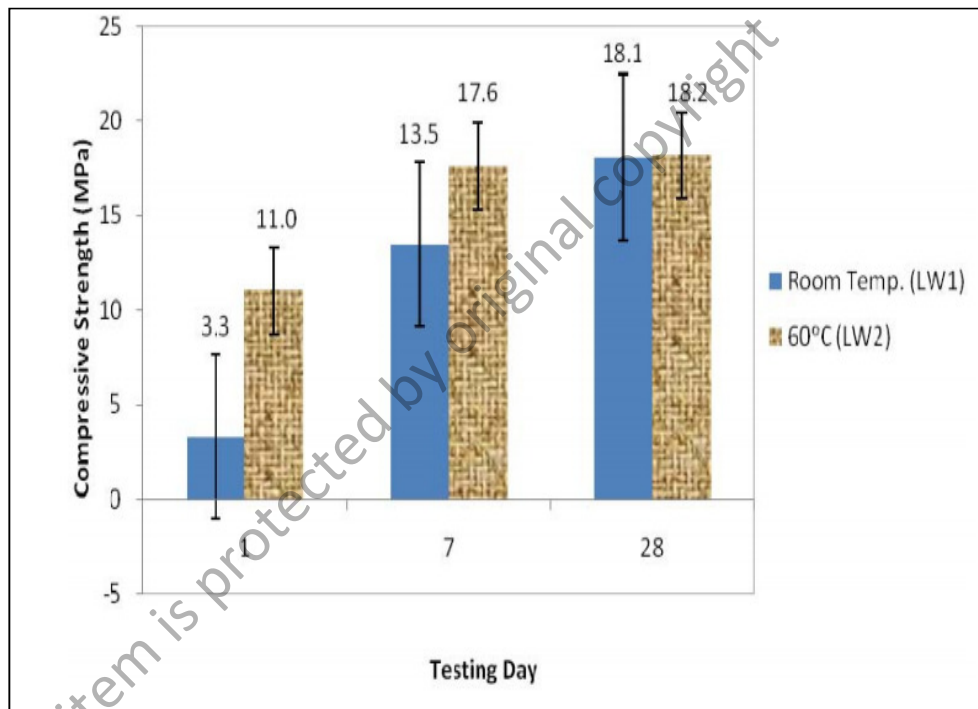


Figure 2.25: Compressive strength vs. curing type Abdullah et al. (2012).

Finally, Nazari et al. (2012) reported LWAGC manufactured by the alkali- activation of a source material consisting of ashes combination of FA and rice husk-bark ash (RHBA) by alkaline activator mixture of NaOH solution (12 M) and  $\text{Na}_2\text{SiO}_3$ . Palm oil clinker (POC) of particle size less than 7 mm and 7-18 mm were used as fine and coarse LWA in the preparation of the LWAGC of this study at three volume fractions of 30, 50 and 70 %. This study does not provide any mechanical performance as it is dedicated to study the water absorption of resultant concrete.

Table 2.7: Properties of FA foamed lightweight geopolymer concrete (Abdullah et al. (2012).

Properties	Room Temperature	60 °C for 24 hour
Compressive strength at 1 days	3.3 (MPa)	11.0 (MPa)
Compressive strength at 7 days	13.5 (MPa)	17.6 (MPa)
Compressive strength at 28 days	18.1( MPa)	18.2 (MPa)
Porosity	15.29(%)	6.78(%)
Water absorption	2.35(%)	1.22(%)
Density	1650 (kg/m <sup>3</sup> )	1667 (kg/m <sup>3</sup> )

## 2.11 Summary of Chapter

Chapter 2 presented the fly ash (FA) geopolymer materials as the ideal alternative cementitious material to the OPC as well as the latest reported microstructural, mechanical and thermo-physical properties of these geopolymers existed in the published literature. In addition, the essential advantages of using the lightweight concrete (LWC), in particularly, the structural lightweight aggregate concrete (LWAC) in the constructions has been also addressed in this chapter. However, the rare reports and researches regarded to usage of the geopolymerization technology in production of different types of LWCs mentioned in section 2.10 demonstrated the limited knowledge and understanding about the physical, mechanical and thermal properties of LWCs based on the geopolymer materials. Therefore, more efforts are necessary to carry on to investigate the suitability of the geopolymer materials, especially the FA geopolymers in producing of lightweight aggregate geopolymer concrete LWAGC as well as their designing bases before they can be suggested as construction building materials.

## CHAPTER 3

### RESEARCH METHODOLOGY

#### 3.1 Introduction

This chapter is related to describe the details of the practical experiments carried out through this research which involves the designing and preparing of different geopolymeric materials as well as illustrate the conducted studies and tests aimed to evaluate their mechanical, physical, microstructural and thermal durability properties. Furthermore, the current chapter reports the detail descriptions and analysis of the raw materials and the pre-preparation methods that applied to some of them prior to involve into the practical processes of making the geopolymer materials of this work. This chapter includes the method of designing the lightweight aggregate geopolymer concrete (LWAGC) as well as the optimization process of the LWAGC preparation parameters, which is known as the actual design of the concrete. Accordingly, the research methodology Chapter presents the experimental procedures that assisted to achieve the research objectives addressed earlier in chapter 1. Figure 3.1 represents the flow chart of the research methodology.

#### 3.2 Raw Materials

The origin and the analysis methods of the raw materials used in the preparation of the lightweight geopolymer concrete (LWAGC), geopolymer paste and mortar are presented in this section.

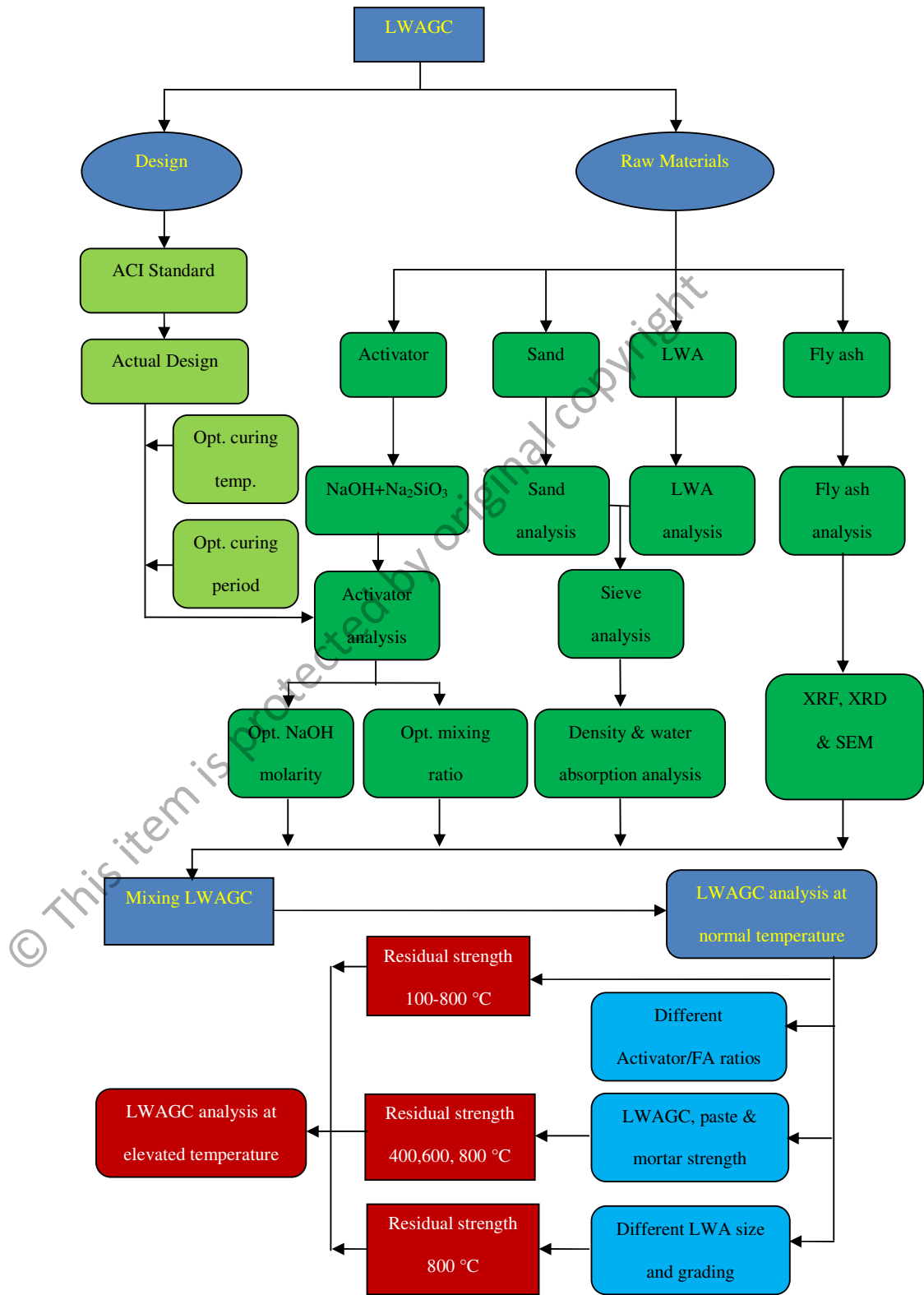


Figure 3.1: Flow chart summarized the research methodology of this study.

### **3.2.1 Fly Ash (FA)**

In this work, the fly ash (FA) was sourced from the Manjung Power Station, Lumut, Perak, Malaysia. The FA is a fine dry powder has sharp gray color with no appearance of other contaminates materials. The FA was stored in a shade at ambient temperature and covered by a thin plastic layer to seal it from the ambient humidity and to maintain the powder clean. The FA was analyzed before the utilization in the mixing.

#### **3.2.1.1 The Chemical Composition**

The chemical composition of the FA was determined by X-ray fluorescence (XRF), using (XRF-Qualitax, Italy), in School of Materials Engineering, University of Malaysia Perlis (UniMAP). The results of the XRF test are listed in Chapter 4, Table 4.1.

#### **3.2.1.2 Particle Size Distribution**

The particle size of the FA was measured by Malvern Instruments Mastersizer MS2000, in school of Materials Engineering, University of Malaysia Perlis (UniMAP).

Figure 4.1 and Table 4.2 of Chapter 4 are represented the results of the particle size of the FA.

#### **3.2.1.3 Microstructure**

The microstructure of the FA was examined by scanning electron microscopy (SEM) using SEM JSM-6460 LA Jeol, Japan, in School of Materials Engineering, University

of Malaysia Perlis (UniMAP). The test was carried out using secondary as well as backscattered electron detectors. Figure 4.2 shown in Chapter 4 is demonstrated the resulted microstructure characteristics of the FA.

#### **3.2.1.4 Phase Composition**

The phase analysis and the crystallinity content of the FA was tested by the X-ray diffraction (XRD) using XRD-6000, X-ray Diffractometer Shimadzu, Japan, at the School of Materials Engineering, University of Malaysia Perlis (UniMAP). The test was performed at operating conditions of 40 kV and 30 Ma, Cu-K $\alpha$  wavelengths: 1.54060 and 1.54439 Å. In collecting data sets, the  $2\theta$  step size was 0.02°, the collecting time step was 1.2 second, and the  $2\theta$  range between 10 to 80°. Figure 4.3 in Chapter 4 is showing the resulted XRD pattern.

#### **3.2.2 Alkaline Activator Solution**

The alkaline activator used in the preparation of the geopolymer materials of this study was a mixture of the sodium hydroxide (NaOH) solution and liquid sodium silicate (Na<sub>2</sub>SiO<sub>3</sub>).

##### **3.2.2.1 Sodium Hydroxide Solution (NaOH)**

The sodium hydroxide solids was in powder form of Formosoda-P sodium hydroxide powder supplied by Ercros Pty Ltd, Spain, with purity of 99 %, shown in Figure 3.2,

was used in the preparation of the alkaline activator utilized in the synthesizing of the geopolymeric materials of this work.



Figure 3.2: Sodium hydroxide (NaOH) powder

### 3.2.2.2 Sodium Silicate Liquid ( $\text{Na}_2\text{SiO}_3$ )

The liquid  $\text{Na}_2\text{SiO}_3$  used in the preparation of the alkaline activator in this work was a technical grade sodium silicate liquid supplied by South Pacific Chemicals Industries Sdn. Bhd. (SPCI), Malaysia. The chemical compositions of the  $\text{Na}_2\text{SiO}_3$  were  $\text{SiO}_2=30.1\%$ ,  $\text{Na}_2\text{O}=9.4\%$ ,  $\text{H}_2\text{O}=60.5\%$ , with modulus ratio ( $M_S$ ) equal to 2 (where  $M_S = \text{SiO}_2/\text{Na}_2\text{O}$ ), and specific gravity at  $20\text{ }^\circ\text{C}=1.4\text{ gm/cc}$  with viscosity at  $20\text{ }^\circ\text{C}$  of  $0.4\text{ cP}$ . Figure 3.3 shows the used  $\text{Na}_2\text{SiO}_3$  in the current study.



Figure 3.3: Liquid sodium silicate  $\text{Na}_2\text{SiO}_3$

### 3.2.3 Fine Aggregate (Sand)

The fine aggregate used in the manufacturing of the LWAGC and the geopolymer mortar was locally available river sand. Two of tests were conducted to obtain the important physical properties of the sand before using it in the making of the geopolymeric materials. These physical properties are the specific gravity, water absorption and the particle size distribution. The specific gravity and the water absorption were measured according to ASTM (C128-01); while the particle size distribution test was performed according to ASTM (C136-06).

The specific gravity and the water absorption test were performed by measuring 2 kg of sand sample from a pre-dried at  $110\text{ }^\circ\text{C}$  bulk sand. The sand sample was left to cool in air, and then it was immersed in water for 24 hours. After that, to obtain the saturated surface dry condition (SSD) of the sand sample, it was drained from the water and

spread on flat surface exposed to a gentle current of warm air for about 5 minutes. The sample was then stirred frequently until obtain a free-flowing condition. After that, a portion of the sand sample was placed in a mold and damped. The resulted surface moisture was removed by a piece of cloth. Next, 500 g of the sand at SSD condition was placed in a glass calibrated flask, and the water is added to fill it to its maximum calibrated mark. The total mass of the flask, sample (sand) and water was determined. Later, the sand was then carefully washed from the flask into a pan which then placed in an oven at 110 °C for 24 hours. Afterward, the mass of the oven dry (OD) condition was determined. Finally, the mass of the flask filled with water (with no aggregate) to it maximum calibrated mark was determined. The specific gravity and water absorption of the sand was calculated by using the following Equations:

$$\text{Bulk specific gravity (sand)} = A/(S+B-C) \quad (3.1)$$

$$\text{Water absorption (\%)} = [(S-A)/A] \times 100 \quad (3.2)$$

where, A =mass of the OD (g);

S = mass of the SSD (g);

B = mass of the flask filled with water (g);

C = the mass of flask with sample and water to the calibration or filling mark (g).

The test results presented in Chapter 4 section 4.2.1.2.1 revealed that the sand has a specific gravity of 2.5 and water absorption of 2.2 %. Moreover, the particle size analysis of the sand was measured using the standard sieving analysis unit shown in Figure 3.4 at the school of Environment Engineering, University of Malaysia Perlis

(UniMAP), according to ASTM (C136-06), with maximum sieve size of 4.75 mm, for a sand test sample of 400 g.



Figure 3.4: Sieve analysis test instrument.

The sand particle size test results are calculated after obtained the individual mass retained (IMR), which is represented the mass of the sand that each sieve retained during testing in grams. In addition, both the cumulative percent retained (CPR) and

calculated percent passing (CPP) are analytical values that calculated for each sieve mass retained in order to calculate the fineness modulus (FM) of the sand using the following equations (ASTM C136-06):

$$IPR \% = IMR/W_s \times 100 \quad (3.3)$$

$$CMR = IMR + \text{Sum of the IMRs above it} \quad (3.4)$$

$$CPR \% = CMR/W_s \times 100 \quad (3.5)$$

$$CPP \% = 100 - CPR \times 100 \quad (3.6)$$

$$FM = \sum (CCP \%) / 100 \quad (3.7)$$

Where,  $W_s$  is the weight of the sand sample = 400g.

The results of this test is presented in Chapter 4 section 4.2.1.2.2 Table 4.3 illustrating that the sand has a maximum particle size of 2.38 mm and the calculated fineness modulus (FM) = 2.83. Furthermore, this analyzing method was also used in the analyzing the LWA sand particle size analysis distribution as mentioned later in section 3.2.4.2.

### 3.2.4 Lightweight Aggregate (LWA)

The LWA used in the preparation of the lightweight aggregate geopolymer concrete (LWAGC) of this research was a commercial lightweight expanded clay aggregate (LECA), supplied by Hydroponics & Plant Care Pte Ltd, Singapore. Figure 3.5 is showing the LWA which illustrates that the exterior color of it is brown with a spongy cellular structure inside. According to the manufacturer, the LECAs are made by baking pure natural clay at 1200 °C for 3 hours in a rotary kilns in process called “pyroprocessing”, which causing an expansion to the material into a synthetic lightweight aggregate. The used clay in the preparation of the LECA is very fine-grained, moisture-retentive, naturally occurring material composed principally of silicates of alumina. The end product is a ceramic material, spherical in shape with closed surface having slightly rough porous texture, non-toxic, pH neutral, does not degrade and it is an autoclavable. Furthermore, the LECA is a chemically-inert material; therefore it does not react with alkaline media during mixing the LWAGC gradients.

The physical properties of the LWA were analyzed prior to the usage into the designing of the LWAGC, as the mix proportioning significantly depended on the LWA properties. These properties including:

- a. Density and water absorption of the LWA.
- b. Particle size distribution.



Figure 3.5: LWA used in the manufacturing of the LWAGC of this study.

#### 3.2.4.1 Density and Water Absorption of the LWA

The density and water absorption measurements of the LWA were performed according to ASTM (C127-01). The LWA test sample was prepared by measured 2 kg of the aggregate, placed in a known weight wire basket container. The top of container was sealed with plastic layer to prevent the LWA from buoying outside the container when immersed in water for 24 hours. Then, the container was moved from the water and the bulk aggregate was allowed to dry by placing it on a cloth piece for 3 minutes. After weighting the weight of the saturation surface dry (SSD), the aggregate sample within the container was suspended to a high sensitively balance by a wire while it completely submerged in water, and the apparent weight was recorded. Afterward, the sample container was put in a furnace and heated to 105 °C for 24 hours. Finally, after the heating period was over, the oven-dry (OD) weight was recorded.

The resulted weight values which are presented in Chapter 4 section 4.2.1.3.1 Table 4.4 were used to calculate the following physical properties of the LWA from the following equations:

$$\text{Relative density (specific gravity) in OD} = A / (B-C) \quad (3.8)$$

$$\text{Relative density (specific gravity) in SSD} = B / (B-C) \quad (3.9)$$

$$\text{Apparent relative density (Apparent specific gravity)} = A / (A-C) \quad (3.10)$$

$$\text{Density (OD) kg/m}^3 = 997.5 \times A / (B-C) \quad (3.11)$$

$$\text{Density (SSD) kg/m}^3 = 997.5 \times B / (B-C) \quad (3.12)$$

$$\text{Apparent Density} = 997.5 \times A / (A-C) \quad (3.13)$$

$$\text{Water absorption (\%)} = [(B-A)/A] \times 100 \quad (3.14)$$

where, A = mass of the OD (g);

B = mass of the SSD (g);

C = mass of the apparent (g).

### 3.2.4.2 Particle Size Distribution

. The test was performed using a set of standard sieves (Figure 3.4) possessed a maximum size of 9.5 mm and minimum size of 2.38 mm. Furthermore, the test results have been analyzed in similar method conducted to analyzing sand's particle size distribution test presented in Chapter 4, section 4.2.1.2.2. The sieve analysis result of

the LWA is listed in Chapter 4, Table 4.5 which showing that the LWA have a particle size of 4-8 mm.

### **3.3 Designing of the Lightweight Aggregate Geopolymer Concrete (LWAGC)**

The design of the LWAGC was based on a standard utilized of designing and proportioning of a lightweight OPC concrete proposed by the American Concrete Institute (ACI) committee 211-standard (ACI 211.2). This standard is the only available online standardized document that described in details the designing and proportioning processes of a lightweight aggregate structural concrete for OPC system. Furthermore, most of the published papers and reports that deals with designing of OPC-based LWACs, have been used and followed the recommendations of the ACI (211.2) in designing processes (Babu et al., 2006; Sancak et al., 2008). Accordingly, through the designing process of the lightweight aggregate geopolymer concrete (LWAGC); the term of the water/cement ratio used by the standard was modified to Activator/FA ratio, in order to fit the terms used in the geopolymerization technology. While, the rest of the designing concepts were followed as described by the standard. The LWAGC was designed by the weight method (specific gravity pycnometer) which is applicable to the sand-lightweight concrete systems. The LWAGC was designed according to specific characteristics which are:

- I. A compressive strength higher than 17 MPa at 28 days, in order to meet the minimum required compressive strength of a structural LWAC as reported by American Concrete Institute ACI (ACI 213R-87).

- II. Unit weight less than  $1850 \text{ kg/m}^3$  at 28 days, in order to meet the minimum required unit weight of the LWAC as reported by American Concrete Institute ACI (ACI 213R-87).
- III. Fly ash as the solid source material of making the paste binder with 0% OPC or any other additives.

Moreover, the materials used in the designing of the LWAGC are:

- I. Fly ash of section (3.2.1)
- II. Alkaline activator consisting of a mixture of  $\text{Na}_2\text{SiO}_3$  and NaOH solution of section (3.2.2).
- III. LWA of 4-8 mm particle size of section (3.2.3).
- IV. River sand with maximum size of 2.35 mm and fineness modulus of 2.8 of section (3.2.4).

Accordingly, the LWAGC designed and proportioning method involves the following steps as the ACI (211.2) is presented:

- I. **Choice of the slump value:** The recommended slump value for a structural lightweight aggregate structural concrete is in the range of 75-100 mm or 3-4 inch as recommended by Table (3.2.2.1) of ACI (211.2) standard.
- II. **Estimating of the maximum nominal size of the LWA:** The nominal maximum size of the adopted LWA, which is defines as one sieve size larger than the first sieve to retain more than 10 percent of the material by weight (Roberts et al., 1996). Though, according to sieve analysis data of the LWA

presented in Chapter 4, Table 4.4, the nominal maximum size of the LWA is 9.5 mm.

**III. Estimating of alkaline activator liquid content:** The alkaline activator content is estimating according to the chosen slump and nominal size of LWA values. Therefore, according to Table (3.2.2.2) of the ACI (211.2), the alkaline activator content should be 340 lb/yd<sup>3</sup> or 201.72 kg/m<sup>3</sup>.

**IV. Selection of Activator/FA ratio:** Estimating of the Activator/FA ratio is depending on the targeted compressive strength value at age of 28 days, which is targeted previously of higher than 17 MPa. Thus, an Activator/FA ratio of 0.59 was selected according to Table (3.2.2.3a) of the ACI (211.2).

$$\begin{aligned}\therefore \text{The FA content} &= \text{Alkaline activator content (201.72)} \times 0.59 \\ &= 341.89 \text{ kg/m}^3.\end{aligned}$$

**V. Estimating the volume of the LWA:** The selection oven-dry (OD) volume of LWA is depending on the sand fineness modulus and nominal maximum size of the LWA. The OD volume of LWA per unit volume of the concrete then should be 0.54 as recommended by Table (3.2.2.4) of ACI (211.2). As the OD-density of the LWA = 897.57 kg/m<sup>3</sup> (Table 4.3 presented in Chapter 4),

$$\begin{aligned}\therefore \text{The weight of the LWA} &= 0.54 \times 897.57 \\ &= 484 \text{ kg/m}^3.\end{aligned}$$

**VI. The weight of the concrete:** The estimation of the concrete weight is depended on the specific gravity factor of the LWA and the desired air content in the concrete which was chosen of 4%. The specific gravity factor of the LWA is 1.6, which calculated from the following Equation (ACI 211.2):

$$\text{Specific gravity factor}(S) = C/C-E \quad \text{Equation (3.9)}$$

where, C = weight of aggregate in air (kg);

E= weight of aggregate sample under water (kg).

Though, the concrete weight can be obtained from Table (3.2.2.5) of ACI (211.2)

standard and it should be 3210 lb/yd<sup>3</sup> or 1851 kg/m<sup>3</sup>.

**VII. Estimating the fine aggregate weight:** From the above known weights the sand content can be calculated as:

$$\begin{aligned} \text{weight sand} &= \text{weight concrete} - (\text{weight FA} + \text{weight Activator} + \text{weight LWA}) \\ &= 823.39 \text{ kg/m}^3 \end{aligned}$$

**VIII. Estimating the extra water content:** extra water was added to constrain the water content absorbed by aggregates (sand + LWA) during mixing, in particularly, the LWAs absorption; since they have high water absorption property. The extra water content was equivalent to the quantity of the water absorption of each aggregate type. The measured water absorption of the LWA was 17.2 %, while the sand has water absorption of 2.2 % as the test results presented in Chapter 4, sections 4.2.2.1 and 4.2.3.2 are showing. Then, the extra water is calculating as :

$$\begin{aligned} \text{extra water content} &= \text{weight of LWA} \times 17.2 \% + \text{weight of sand} \times 2.2 \% \\ &= 101.36 \text{ kg/m}^3. \end{aligned}$$

Though, the first trail batch of the LWAGC is known and it is given in Table 3.1. Nevertheless, the optimum curing conditions as well as the optimum alkaline activator constituent mixing and concentration were unknown yet. In other words, the LWAGC is

need for actual design before mix the first trail batch. Therefore, further experimentally investigations were conducting in order to achieve the best curing conditions and alkaline activator preparation method prior to mix the LWAGC constituents. This investigation is called the actual design of a concrete and it is presented in section 3.4.

Table 3.1: Trial batch proportioning of the LWAGCs

Constituents	(kg/m <sup>3</sup> )
FA	341.89
Alkaline activator	201.72
Activator/FA	0.59
LWA	484.00
Sand	823.39
Extra H <sub>2</sub> O	101.36

### 3.4 Actual Design of Lightweight Aggregate Geopolymer Concrete (LWAGC)

The actual design of a concrete is typically performed to obtain the optimum preparation parameters like optimum water/cement ratio, fine/coarse aggregate ratio and optimum curing conditions that gives the fresh concrete the best workability as well as the highest compressive strength to the hardened concrete. The actual design is usually perform to the cement paste samples and the obtained optimal preparation parameters are adopted during the manufacturing processes of the concrete.

For the LWAGC, the ACI (211.2) standard is able to specify some of the optimal preparation parameters like fine/coarse aggregate mass ratio, total aggregate/paste mass

ratio and the Activator/FA mass ratio as shown in section (3.3). However, the ACI (211.2) does not include all of the optimum preparation parameters which are significantly affecting the mechanical and physical properties of the resultant LWAGCs. Therefore, these parameters need to be experimentally investigated in order to get their optimum values, and applied these parameters during the preparation of the LWAGC. These parameters are:

- I. NaOH solution molarity
- II. Mass ratio of  $\text{Na}_2\text{SiO}_3/\text{NaOH}$
- III. Curing temperature
- IV. Curing period

Accordingly, more experiments were performed prior to mix the LWAGC ingredients in order to obtain the above listed parameters optimum values. Thus, the experimentally procedures of optimizing these parameters are presented below, while the results of these experiments are presented in Chapter 4, section 4.2.2.

#### **3.4.1 Optimum NaOH Solution Molarity**

As mentioned in Chapter 2, section 2.9.1.2, Abdullah et al., (2011a, 2011b, 2012) reported the optimum NaOH solution concentration that resulted in the highest compressive strength of the FA geopolymers prepared with the same FA source used in this work. According to these authors, the optimum NaOH solution concentration of 12 molar (M) produced the highest compressive strength for FA geopolymers at different aging periods. Thus, based on this statement, it was decided to use the NaOH solution at

concentration of 12 M in the preparation of the LWAGC without the need of further investigation.

### **3.4.2 Optimum Mass Ratio of Na<sub>2</sub>SiO<sub>3</sub>/NaOH**

It was mentioned in Chapter 2, section 2.9.1.2, that there is no statement precisely specifying the optimum Na<sub>2</sub>SiO<sub>3</sub>/NaOH mass mixing ratio results in maximum strength for the hardened geopolymer, which therefore, needs to be experimentally achieved with respect to the utilized range of this ratio mentioned in the literature.

#### **3.4.2.1 Procedure of Optimizing the Mass Ratio of Na<sub>2</sub>SiO<sub>3</sub>/NaOH**

The alkaline activator was made by mixing the advanced prepared NaOH solution of 12 M with the Na<sub>2</sub>SiO<sub>3</sub> at six Na<sub>2</sub>SiO<sub>3</sub>/NaOH mass mixing ratios ranged from 0.5 to 3.0. The mix proportioning of geopolymer pastes is listed in Table 3.2. The geopolymer paste specimens were synthesized by adding the alkaline activator gradually to the dry FA at the specified earlier Activator/FA ratio of 0.59. After 10 minutes of hand mixing, the fresh homogeneous geopolymers were poured into 50 × 50 × 50 mm plastic molds and vibrated on a vibration table for 2 minutes to remove the entrapped air bubbles. Later, the molds were wrapped using a thin plastic sheet to prevent water evaporation. Then, the geopolymer paste specimens were cured at furnace at 60 °C for 24 hours. After the end of curing, the molds were taken out from the furnace and left to cool at room temperature before demolding. The sealed molds were aged at targeted aging periods of 3, 7, and 28 days at ambient conditions. The compressive strength of the specimens was evaluated according to ASTM C (109/C 109 M), using the Shimadzu

Universal Testing Machine after the end of each aging period. A minimum of three specimens was tested to evaluate the compressive strength.

The results of this experiment presented in Chapter 4, section 4.2.2.1 shows that the  $\text{Na}_2\text{SiO}_3/\text{NaOH}$  mass ratio of 1.0 is the optimum ratio that produced the highest compressive strength at all tested ages.

Table 3.2: Mix proportioning of the geopolymer paste of different  $\text{Na}_2\text{SiO}_3/\text{NaOH}$  ratios.

Mix no.	FA(g)	$\text{Na}_2\text{SiO}_3/\text{NaOH}$	$\text{Na}_2\text{SiO}_3(\text{g})$	NaOH(g)
1	450.00	0.5	88.00	177.00
2	450.00	1.0	132.75	132.75
3	450.00	1.5	153.90	102.60
4	450.00	2.0	177.00	88.00
5	450.00	2.5	189.64	75.85
6	450.00	3.0	199.12	66.37

### 3.4.3 Optimum Curing Temperatures

It was mentioned in Chapter 2, section 2.9.1.3 about the significance of the curing temperatures on the geopolymerization process. In addition, it was reported that the suggested curing temperatures for the FA geopolymer is in the range of 60 °C to 90 °C, although, the exact optimum curing temperature is still unrevealed and needs to be practically achieving. Therefore, this experiment was performed to obtain the optimum curing temperature from the range of 60 °C to 90 °C, in order to use it in the curing of LWAGCs through this research.

### 3.4.3.1 Procedure of Optimizing the Curing Temperatures

The alkaline activator used in this experiment was prepared by mixing the 12 M NaOH with the  $\text{Na}_2\text{SiO}_3$  at the optimum  $\text{Na}_2\text{SiO}_3/\text{NaOH}$  mass ratio of 1.0 that achieved from the experiment mentioned in section 3.4.2. The mix proportioning of the geopolymers is illustrating in Table 3.3. In addition, the geopolymers preparation procedure was exactly similar to the one used in the previous experiment of section 3.4.2, except that the geopolymers after casting into  $50 \times 50 \times 50$  mm, molds were cured at different curing temperatures of 60, 70, 80 and 90 °C for 24 hours. The sealed geopolymers were aged at 3, 7 and 28 days prior to test their compressive strength.

The results of optimum curing temperatures presented in Chapter 4, section 4.2.2.2 reveals that the 70 °C is the optimum curing temperature that resultant in the highest compressive strength to the prepared geopolymers in all tested ages. Accordingly, the 70 °C is adopted as the curing temperature in the preparation of LWAGCs in this work.

Table 3.3: Mix design of the geopolymer paste cured at temperatures of 60 °C to 90 °C.

FA(g)	$\text{Na}_2\text{SiO}_3/\text{NaOH}$	$\text{Na}_2\text{SiO}_3(\text{g})$	NaOH(g)
450.00	1.0	132.75	132.75

### 3.4.4 Optimum Curing Periods

The last preparation parameter needs to be practically investigated in order to obtain its optimum value is the curing period. According to the literature (Chapter 2, section 2.9.1.4), the optimum curing duration was laid between 24 and 48 hours, despite that the 24 hours is more favorable curing period due to its economical advantages over the 48

hours (Harrdjito & Rangan, 2005). Nevertheless, there is no statement clarified that the curing period of 24 hours is the optimum curing period for all FA geopolymers. Therefore, it was decided to perform an experimentally investigation to obtain the optimum curing period with respect to economical aspects and the attempts to minimize the curing period that results in optimum compressive strength. Thus, curing periods ranged from 6 hours to 30 hours were tested in this experiment.

#### **3.4.4.1 Procedure of Optimum Curing Periods**

The geopolymer paste specimens were synthesized in similar method mentioned in section (3.4.2.1). The geopolymers in this experiment were cured at the optimum curing temperature of 70 °C obtained from the results of the optimum curing temperature experiment presented in Chapter 4, section 4.2.2.2, at curing periods of 6, 12, 18, 24 and 30 hours. The geopolymers preparation, aging times and condition procedures as well as the evaluation of the specimens compressive strength were similar to the that used in the obtaining the optimum  $\text{Na}_2\text{SiO}_3/\text{NaOH}$  ratio mentioned in section 3.4.2.1. The results of this experiment are shown in Chapter 4, section 4.2.2.3 specifying that the curing period of 24 hours resulted in the highest strength to the prepared geopolymers in all tested ages, therefore, it was used in the curing regime in the preparation of LWAGCs through this research.

### **3.5 First Trail Mixing of the LWAGC**

The first trail mixing of the LWAGC was performed after achieving and collecting all the optimum preparation parameters from the actual design results presented in

Chapter 4, section 4.2.2. The LWAGC gradients illustrated in Table 3.1 was modified after adding the optimum weights of the alkaline activator constituents which were calculated as:

The alkaline activator weight is  $201.73 \text{ kg/m}^3$  and the optimum mixing ratio of the  $\text{Na}_2\text{SiO}_3/\text{NaOH}$  of 1.0 as presented in Chapter 4, section 4.2.2.1.

$$\therefore \text{Weight of } \text{Na}_2\text{SiO}_3 = \text{NaOH} = 100.86 \text{ kg/m}^3.$$

Though, Table 3.4 shows the first trail mixing of the LWAGC. The LWAGC was synthesized by the activation of the FA with the advanced prepared alkaline activator to form the cement-like geopolymeric material (binder) which used to bind the aggregates (fine + LWA) and produce the geopolymer concrete.

Table 3.4: First trail mix design of the LWAGCs

Constituents	( $\text{kg/m}^3$ )
FA	341.89
$\text{Na}_2\text{SiO}_3$	100.86
NaOH	100.86
Activator/FA	0.59
LWA	484.00
Sand	823.39
Extra $\text{H}_2\text{O}$	101.36

### 3.5.1 Alkaline Activator Preparation

The alkaline activator was primary prepared by preparing the 12 M NaOH solution. The NaOH solution was prepared by dissolving a specific mass of the NaOH solid in distilled water. After that, the solution was poured in a standard 1 liter volumetric flask. Then, the volume of distilled water required to make 1 liter of NaOH solution in any desired concentration, which is marked on the flask itself, was added. The flask was left to cool down to room temperature as the reaction between the NaOH solid and the distilled water generated high heat. Afterward, the NaOH solution was mixed with the liquid  $\text{Na}_2\text{SiO}_3$  at mass mixing ratio of  $\text{Na}_2\text{SiO}_3/\text{NaOH}$  of 1.0.

### 3.5.2 Preparation of the aggregates (fine/LWA)

Prior to mix, the LWA and fine aggregate (sand) were pre-prepared in standard conditions of oven-dry condition (OD) and air-dry condition (AD), respectively, in order to maintain the water content in the mixture at a constant level. Hence, the absorbed moisture content by the aggregate especially by the LWAs which they have high moisture absorption property would not causing any negative effect on the fresh and hardened physical and mechanical properties. For the LWA, the aggregates were per-dried at furnace at 105 °C for 24 hours to remove any residual moisture. After the end of drying process, the LWAs were packed in plastic packs and sealed from ambient until the time of mixing. On the other hand, the sand was prepared in AD-condition as described by Yang et al., (2010). The sand was firstly washed with a tap water to removed any dirties, and drying in a shade for 24 hour prior to mix.

### 3.5.3 Mixing and Slump Measurement

The solid constituents of the LWAGC which are the FA and the aggregates (fine + LWA) were mixed in 5 liter capacity pan mixer, for 3 minutes. Then, the advanced prepared alkaline activator liquid and the extra water dosages were gradually added to the solid constituents. The wet mixing was continued for further 5 minutes until the mixture being homogenized. Afterward, the slumps of the fresh concretes were measured according to the BS (EN 12350-2), using the slump cone presented in Figure 3.6. The slump cone has dimensions of 300 mm height, 200 mm bottom and the cone top diameter of 100 mm. The slump test was carried out by filling the cone with the fresh mixture into three equal layers and tamping the mixture down 25 times for each layer. After that, the cone was removed and the slump measured by measuring the height of the tamped fresh mixture.



Figure 3.6: Slump test instrument used to test the fresh concrete slump.

### 3.6 Final Mix Design of the LWAGC

The first trial mixing of the LWAGC resulted in slump values range of 132-137 mm after six test attempts. These slump values, however, are much higher than the designed slump of 75-100 mm mentioned in section 3.3. Therefore, an adjustment to the mixture was needed by decrease the liquid content in the mixture with maintained the solid constituent quantities in order to achieve the desired slump value. However, it is believed that decreasing the liquid alkaline activator content in the mixture might leads to deteriorate the geopolymerization reaction rate and then the mechanical and as well as microstructural properties of the resulted LWAGCs. Accordingly, it was decided to decrease the extra added water to achieve the desired slump. Consequently, after many try and error attempts, decreasing of the extra water content from  $101.36 \text{ kg/m}^3$  to  $91.47 \text{ kg/m}^3$  resulted in slump value of 95 mm, which is applicable to the designed slump range. Hence, the new extra water content was added to the final mix design of the LWAGC, and then the mix proportioning of Table 3.4 is modified to the final mix design given in Table 3.5.

Table 3.5: Final mix proportioning of the LWAGCs.

<b>Constituents</b>	<b>(kg/m<sup>3</sup>)</b>
FA	341.89
Na <sub>2</sub> SiO <sub>3</sub>	100.86
NaOH	100.86
Activator/FA	0.59
LWA	484.00
Sand	823.39
Extra H <sub>2</sub> O	91.47

### **3.7 Synthesizing of the Lightweight Aggregate Geopolymer Concrete (LWAGC)**

The LWAGCs were synthesized after achieving the final mix proportioning illustrated in Table 3.5. The alkaline activator was prepared exactly similar to the one used in the first trial batch as well as the aggregates (sand+ LWA) pre-preparation methods presented in section (3.5. 2).

#### **3.7.1 Mixing and Molding of LWAGC**

The mixing procedure and the slump test were similar to that used in the first trial which was mentioned in section (3.5.3). The fresh mixture was dark in color (due to the dark color of the FA) and cohesive. After measuring the slump, the fresh mixture was poured down into standard plastic molds of 100 × 100 × 100 mm dimensions. The fresh mixture was poured into the molds and compacted in three layers using a steel rod. Later on, the molds were sealed from the ambient to prevent the moisture losing.

#### **3.7.2 Curing and Aging Conditions**

The optimum curing temperature and curing period of 70 °C for 24 hours were used in the curing regime of the LWAGC specimens which obtained from the results of actual design results presented in Chapter 4, sections 4.2.2. The wrapped molds were placed into a furnace and heated undisturbed until the end of curing. At the end of the curing process, the resulted specimens were wrapped again and aged at ambient conditions at ageing times of 3, 7, 28, 56, 91, 180 and 365 days.

### 3.8 Synthesizing of the Geopolymer Pastes and Mortar

The FA geopolymer paste and mortar materials were synthesized with respect to the final mix proportioning of the LWAGC illustrated in Table 3.5. In other words, the geopolymers paste and mortar were synthesized at the same Activator/FA mass ratio of 0.59, and the geopolymer mortar was prepared at the same sand/paste mass ratio of 1.51 which extracted from the final mix proportioning of the LWAGC showed in Table 3.5. The alkaline activator was prepared at the same way described earlier in section 3.5.1. The mix proportioning of this experiment is illustrated in Table 3.6. Furthermore, the synthesizing procedure of the geopolymer paste and mortar was also similar to the one used in LWAGC preparation mentioned in section 3.7. Consequently, the resulted specimens were aged for 3, 7 and 28 days. Figure 4.9 and 4.10 of Chapter 4 are illustrated the resulted FA geopolymer paste and mortar specimens, respectively.

Table 3.6: Mix proportion of the geopolymer paste and mortar (kg/m<sup>3</sup>).

<b>Constituents</b>	<b>Paste</b>	<b>Mortar</b>
FA	341.89	341.89
Na <sub>2</sub> SiO <sub>3</sub>	100.86	100.86
NaOH	100.86	100.86
Activator/FA mass ratio	0.59	0.59
LWA	-	-
Sand	-	823.39
Extra H <sub>2</sub> O	-	18.11

### 3.9 Preparation of FA Geopolymer Pastes and LWAGCs with Different Activator/FA Mass Mixing Ratios

This experiment was performed in order to investigate whether the Activator/FA ratio of 0.59 proposed by ACI standard provides the optimum activator content that leads to produce a maximum compressive strength to the LWAGC materials. At the same time, to investigate the effect of the Activator/FA mass mixing ratio on the geopolymerization reaction. Accordingly, LWAGCs and FA geopolymer paste systems were prepared at different Activator/FA mass ratios range of 0.3-0.7. Tables 3.7 and 3.8 are showing the mix proportioning of the FA geopolymer paste and LWAGC materials, respectively. The results of this experiment are presented in Chapter 4, section 4.2.4.

The alkaline activator solutions of this experiment were prepared at the same method described earlier in section 3.6. Furthermore, the geopolymer pastes and LWAGCs were synthesized and cured at the same procedure mentioned earlier in section 3.7, except the geopolymer paste mixtures were poured into 50 × 50 × 50 mm plastic molds. The LWAGCs of this experiment were aged at 28 days, while the paste specimens were aged at 3, 7 and 28 days.

Table 3.7: Mix proportioning of the LWAGCs prepared at different Activator/FA ratios

Mix no.	FA	Na <sub>2</sub> SiO <sub>3</sub>	NaOH	Activator/FA	LWA	Sand	Extra H <sub>2</sub> O
1	341.89	51.28	51.28	0.30	484.0	823.39	91.47
2	341.89	68.37	68.37	0.40	484.0	823.39	91.47
3	341.89	85.47	85.47	0.50	484.0	823.39	91.47
4	341.89	100.86	100.86	0.59	484.0	823.39	91.47
5	341.89	119.66	119.66	0.70	484.0	823.39	91.47

Table 3.8: Mix proportioning of the paste specimens prepared at different Activator/FA ratios (g).

Mix no.	FA(g)	Activator/FA ratio	Na <sub>2</sub> SiO <sub>3</sub> (g)	NaOH(g)
1	450	0.30	67.0	67.0
2	450	0.40	90.0	90.0
3	450	0.50	112.5	112.5
4	450	0.59	132.0	132.0

### 3.10 Synthesizing of LWAGCs with Different LWA Particle Size and Grading.

The graded LWA of 4-8 mm and another batch of graded LWA named batch 2 were used in the preparation of LWAGCs having different particle size and grading. The LWA of batch 2 shown in Figure 3.7 has a particle size of 8-16 mm as the particle size test shown (presented in Chapter 4 in Table 4.8). The results of this experiment are presented in Chapter 4, section 4.2.5.



Figure 3.7: Batch 2 LWA of 8-16 mm.

### **3.10.1 Synthesizing Procedure of LWAGCs with Different LWA Particle Size and Grading**

Targeted sizes of 4-5 mm and 5-8 mm were prepared from the original graded 4-8 mm by using a standard sieve sized of 5 mm in sieving portion of the 4-8 mm LWA. Figures 4.15 and 4.16 of Chapter 4 are showing the photographs of the targeted LWA of 4-5 mm and 5-8 mm, respectively. In addition, other targeted LWAs of 8-12 mm and 12-16 mm particle sizes shown in Chapter 4, Figures 4.17 and 4.18, respectively, were prepared from sieving a portion of the original graded 8-16 mm by using a standard sieve of 12 mm. Then, both the targeted and original graded LWAs (4-8 mm and 8-16 mm) were used to prepare LWAGCs possesses six different aggregate sizes and grading. In order to investigate the effect of the various LWAs size and grading on the resultant LWAGCs mechanical strength and physical properties, the mix design of all concretes was fixed constant. Accordingly, the mix design of the LWAGC made with LWA of 4-8 mm illustrated in Table 3.5 was used in the preparation of the LWAGCs of different particle size and grading. Furthermore, the liquid alkaline activator preparation procedure and the slump measurements of this experiment were similar to that used for the LWAGC manufacturing mentioned in section 3.7. In naming the concrete specimens, a LWAGC name was referred by its LWA size, i.e. L4-5 denotes the LWAGC prepared with LWA size of 4-5 mm. Also, the L4-8 and L8-16 of the graded 4-8 mm and 8-16 mm LWAs were used as graded control concretes.

### **3.11 Studies on the Thermal Behavior of the Geopolymeric Materials**

In these studies, the thermal behavior of the synthesized geopolymer paste, mortar and LWAGCs materials prepared in sections, 3.7, 3.8 and 3.10 were investigated at high heating temperatures (maximum 800 °C). Through these studies the residual compressive strength of the exposed geopolymeric materials was evaluated their thermal behavior. Furthermore, a microstructure study was conducting for one of these studies as well, to explore the microstructural changes that the exposed materials experienced during heating to elevated temperatures. The results and discussions of these experiments are presented in chapter 4, section 4.3.

#### **3.11.1 Study on the Effect of Elevated Temperatures on the Compressive Strength of the Geopolymer Paste, Mortar and LWAGC**

A part of the LWAGC prepared in section 3.7 and the FA geopolymer paste and mortar prepared in section 3.8 were further exposed to different high temperatures environment to investigate their effects on the compressive strength and microstructure of the geopolymer structure. The heating procedure applied for the geopolymers of this study was similar to one performed to the FA geopolymer paste and concrete reported by Kong et al., (2007) and Kong & Sanjayan (2008, 2010). The geopolymers were heated at elevated temperatures of 400 °C, 600 °C and 800 °C.

### **3.11.1.1 Procedure of Exposing to Elevated Temperatures**

The geopolymer paste, mortar and LWAGC specimens prepared of this experiment were exposed to the elevated temperatures at age of 27 days. In practice, the specimens were placed into a furnace and fired to the selected elevated temperature of 400 °C, 600 °C or 800 °C at fixed heating rate of 4.4 °C/minute. The geopolymers specimens were kept at each elevated temperature for 1 hour. After that, the geopolymers specimens were left undisturbed to cool down to room temperature inside the furnace. This heating procedure was required 24 hours to be complete, hence at the time of testing their strength they completed the aging period of 28 days.

### **3.11.2 Study on the Residual Strength of the LWAGC after Heating at Temperature Range of (100 °C to 800 °C)**

In this experiment, the resulted LWAGC prepared in section 3.7 was exposed to elevated temperatures ranged from 100 °C to 800 °C, in order to statistically investigate the thermal behavior of the concrete after exposure to each elevated temperature. In addition, to identify the exact elevated temperature at which the LWAGC would start to loss its strength continuously until the maximum elevated temperature of 800 °C.

#### **3.11.2.1 Test Procedure**

The LWAGC were exposed to elevated temperatures at the range of 100 °C to 800 °C with an increment of 100 °C. The age of specimens and the heating exposure procedure were similar to that performed in section 3.11.1.1.

### **3.11.3 Study on the Effect of the LWA Particle Size and Grading on the Thermal Behavior of the LWAGCs after Exposure to Elevated Temperature of 800 °C.**

A part of The LWAGCs prepared at different LWA particle size and grading mentioned in section 3.10 were further exposed to elevated temperature of 800 °C. The objective of this study was to investigate the effect of the different LWA particle size and grading on the thermal behavior of the exposed LWAGCs in term of residual compressive strength.

#### **3.11.3.1 Test Procedure**

The preparation of this experiment and heat exposure procedure were similar to the one performed to the geopolymers in section 3.11.1.1, except the elevated temperature was of 800 °C only.

### **3.12 Analysis Methods of the Geopolymeric Materials Properties**

This section presented the analysis methods and instruments used in the evaluation of the physical, mechanical, thermal and macro/microstructure properties of the geopolymer materials prepared in this work.

#### **3.12.1 Analysis Methods of the Geopolymeric Materials Physical Properties**

The investigated physical properties of the geopolymer materials prepared in this research were including the OD-density, water absorption, total porosity content and

slump value measurements. The OD-density, water absorption and total porosity content tests were conducting to the hardened geopolymer, while and the slump test was conducted to the fresh LWAGC mixtures. The details of these measurements as presented below.

#### **3.12.1.1 Slump Test**

This test was conducted to the fresh mixtures of the LWAGC prepared in sections 3.7 and 3.10. The test method was similar to the one described earlier in section 3.5.3.

#### **3.12.1.2 Density and Water Absorption Measurements**

The density and water absorption of the geopolymers were performed according to ASTM (C140-01) at age of 28 days. The test was conducted for the geopolymer pastes, mortars and LWAGCs prepared in section 3.7-3.10. The instrument used in this test which is composed of a high sensitively electrical balance (0.1 g or less) and a tank of water of 450 mm long, 300 mm width and 350 mm height. In practical, the geopolymer specimen was immersed undisturbed in the water filled tank at room temperature for 24 hours. Then, the immersed weight ( $W_i$ ) of the specimen was recorded while it suspended to the balance by a thin wire and completely submerged in water. After that, the specimen was removed from the water and placed in a wire mesh to allow water to drain for 1 minute, and the visible surface water was removed by using a damp cloth. The specimen was then weighted and the SSD weight ( $W_s$ ) was recorded. Afterward, the specimens was dried in a furnace at 105 °C for at least 24 hours, and the OD weight ( $W_d$ ) of the specimen was recorded when two successive weightings of the specimen at

intervals of 2 hours showed an increment of less than 0.2 % of the last previously determined weight. Thus, the water absorption and the OD-density of the geopolymers results presented in Chapter 4, sections 4.2.3 and 4.2.5 were calculated as:

$$OD\text{-density (kg/m}^3) = [W_d / (W_s - W_i)] \times 1000 \quad (3.10)$$

$$Water\ absorption\ (\%) = [(W_s - W_d) / W_d] \times 100 \quad (3.11)$$

where,  $W_s$  = weight of the SSD (kg);

$W_d$  = weight of the OD (kg);

$W_i$  = weight of the immersed specimen (kg).

### 3.12.1.3 Total Porosity Content Measurement

The total porosities of the 100 mm<sup>3</sup> cubic LWAGCs prepared in section (3.9) were measured at age of 28 days in accordance to the vacuum pump method similar to the one reported by Cabrera & Lynsdale (1988). In the practice, the specimens were placed in a vacuum saturated chamber and vacuumed for 3 hours using VCP 8101 single-impute pump, and then the water was allowed to flow into the chamber until the specimens were totally submerged. The negative pressure was applied for another 3 hours, to ensure that the specimens were fully filled with water. Afterward, the chamber was left overnight exposed to the atmospheric pressure, to balance the pressure and to ensure full saturation. Subsequently, the specimens were taken out from the chamber and weighed in water and in air, then placed in an oven at 105 °C for 24 hours. Finally, the dry weight was obtained after drying. The total porosity of the LWAGCs results that presented in Chapter 4, section 4.2.5, was calculated using the following equation:

$$\text{Total porosity} = \frac{W_s - W_d}{W_s - W_{ssw}} \times 100 \% \quad (3.12)$$

where,  $W_s$  = weight of the saturated surface dry specimen in air;

$W_d$  = weight of oven dry specimen in air;

$W_{ssw}$  = weight of saturated specimen in water.

### 3.12.2 Mechanical Compressive Strength Evolution

Compressive strength tests were conducted to investigate the ultimate strength of the prepared geopolymers materials from the actual design experiments mentioned in section 3.4, and for all resultant geopolymer specimens prepared in sections 3.7-3.11. The compressive strength tests of the specimens were measured after they completed their targeted ages. The strength tests of this work were performed using the Shimadzu Universal Testing Machine (UTM) having maximum loading of 1000 kN, Japan, at the School of Materials Engineering, University Malaysia Perlis (UniMAP). A minimum of three specimens was tested to evaluate the compressive strength of each test. During the test, the compression results were directory analyzed by a computer conducting to the instrument. Furthermore, for the 50 mm<sup>3</sup> geopolymer paste specimens, the compression test was held according to ASTM (C109/C 109 M), with speed rate of 50 mm/minute. While for the geopolymer specimens of 100 mm<sup>3</sup>, the compressive strength tests were performed in accordance with European standard EN (12390-3) at the same speed rate of 50 mm/minute. The details results of the compressive strength are presented and discussed in Chapter 4.

### **3.12.3 Microstructure Properties**

The microstructure properties of the geopolymers paste and LWAGC prepared in sections 3.7-3.8 and 3.11.1 were performed using the scanning electron microscopy (SEM). The SEM tests were carried out by using SEM JSM-6460 LA Jeol. Japan, at the School of Materials Engineering, University Malaysia Perlis (UniMAP). The specimen fragments for the geopolymer paste and LWAGC were mounted in an epoxy resin and further vacuumed and coated with platinum coat using JFC-1600 auto fine coater Jeol. Japan, prior to test. Then, the specimens were placed on the samples holder by using special carbon tape. Furthermore, the tests were carried out using secondary as well as backscattered electron (BSE) detectors. Energy dispersive spectrometry (EDS) test was also conducted to investigate the chemical composition of selected spots or micro-images of some resulted SEM micrographs. EDS test was carried out using BSE. The details results of the SEM has been shown and discussed in Chapter 4.

### **3.12.4 Thermogravimetric Analysis**

The weight loss with gradual temperature increasing was measured for the geopolymer paste specimens of the experiment mentioned in section 3.8, using the thermogravimetric analysis (TGA). The TGA was carried out using PerkinElmer Pyris diamond Thermogravimetric/ differential thermal analyser at the School of Materials Engineering, University Malaysia Perlis (UniMAP). In addition, the sub-analysis of the derivative thermogravimetric analysis (DTG) and differential thermal analysis (DTA) were also obtained from TGA test. In the analysis, Fragments of the geopolymer paste

specimens of the strength test analysis were powdered prior to test in order to ensure the thermal equilibrium during transient heating was achieved (Kong & Sanjayan, 2008).

### 3.12.5 Dilatometry Measurements

Dilatometry measurements were carried out in order to measure the thermal expansion of the geopolymer paste and LWA grains that used for preparation the geopolymers of the experiment mentioned in section 3.8. The test was carried out using Linseis, L75 Laser dilatometer, at the School of Materials Engineering, University Malaysia Perlis (UniMAP), at temperatures ranged from 20 °C to 800 °C with a constant heating rate of 5 °C/minute. The test was performed for both geopolymer paste and LWA specimens science they can present valuable information for the thermal expansion behavior of the LWAGC at high temperatures as reported by Kong & Sanjayan (2008, 2010). The test was carried out on 9 mm diameter × 3 mm height pellets specimens sliced from a geopolymer paste cylinder of 10 mm diameter × 70 mm height, shown in Figure 3.8. While the specimens of the LWA were prepared by mounted a LWA grains in an epoxy resin and then were further machined using a CY-S1860G, China lathe machine to obtained the test specimens size. The preparation of the test specimens were carried out at the School of Materials Engineering, University Malaysia Perlis (UniMAP).



Figure 3.8: Geopolymer paste cylinder used in the preparing the dilatometry test specimens.

Furthermore, prior to test, the pellets were pre-dried in oven at 50 °C until they maintained a constant weight (Uygunoğlu & Topçu, 2009), before performed the test according to ASTM (E831-03). The measurements were an average of two specimens. The linear length change values were calculated within the temperature range of 20 °C to 800 °C in accordance to the following equations:

$$\varepsilon = \Delta l / l_0 \quad (3.13)$$

$$\Delta l = \alpha \cdot l_0 \cdot \Delta T \quad (3.14)$$

where,  $\varepsilon$  is the thermal strain (mm/mm);

$\alpha$  is the coefficient of thermal expansion (1/ °C);

$\Delta l$  is the length change (mm) and  $l_0$  is the initial length of the specimens;

$\Delta T$  is the temperature difference, respectively.

### 3.12.6 Phase Composition Investigation

X-ray diffraction (XRD) test was performed to investigate the phase composition and the crystalline content of the FA geopolymers pastes before and after exposing to elevated temperatures of 400 °C, 600 °C and 800 °C as presented in section 3.11.1. The test was carried out using XRD-6000, X-ray Diffractometer Shimadzu, Japan at the School of Materials Engineering, University Malaysia Perlis (UniMAP). Samples of this test were prepared into powder form by cut small FA geopolymer paste slices and then grinded those into powder form suitable for the test requirement. The test was performed on a operating conditions of 40 kV and 30Mam, Cu-K $\alpha$  wavelengths: 1.54060 and 1.54439 Å. In collecting data sets, the 2 $\theta$  step size was 0.02°, the counting time step was 0.3 °/minute, and the 2 $\theta$  range between 10 to 80°. The obtained raw data was analyzed using XRD-6000 V 4.1(NT/98) licensed software.

### 3.13 Test Program of the Research Methodology

Table 3.9 summarized the test program of this research which included the testes performed through study and the numbers of the specimens used in each test.

Table 3.9: Test program of the current research.

<b>Test Type</b>	<b>Number of samples</b>
Mechanical compressive strength	294
%Water absorption	18
% Porosity	18
OD-Density	18
Slump of fresh LWAGC mixture	14
SEM	13
SEM-EDS	4
XRD	5
Dilatometry	4
Thermogravimetical	3
FA particle size	1
Sand particle size	1
LWA particle size	2

## CHAPTER 4

### RESULTS AND DISCUSSION

#### 4.1 Introduction

This Chapter presents the results of the analytical experiments conducted on the raw materials used in the preparation of the geopolymeric materials of this work which are mentioned in Chapter 3, section 3.2. Consequently, the results of the LWAGC's actual design which included the optimization of the preparation parameters mentioned in Chapter 3, section 3.4 are also reported in Chapter 4. In addition, the mechanical and physical results of all experiments mentioned in Chapter 3 and their discussions are also included in this Chapter.

#### 4.2 Evaluations of the Mechanical and Physical Properties of FA Geopolymer Materials at Room Temperature

This section is representing the results of the analytical experiments conducted to the raw materials used in the preparation of the geopolymeric materials of this research mentioned in Chapter 3, section 3.2. The results of the actual design of the LWAGC which included optimizing the preparation parameters mentioned in Chapter 3, section 3.4 are also reported here. In addition, the mechanical and physical results of all experiments mentioned in Chapter 3 and their discussions are also included in this Chapter, except those experiments which were dedicated to study the thermal behavior

of the geopolymeric materials at elevated temperatures of sections 3.11.1 to 3.11.3, which are presented in section 4.3.

#### **4.2.1 Analysis of the Raw Materials**

This section reports the chemical, physical and microstructural analysis results of the raw materials used in the geopolymer preparations of this work.

##### **4.2.1.1 Analysis of the FA**

The experiments conducted to the FA before it being used in the synthesis of the geopolymers is mentioned in chapter 3, section 3.2.1. The results of these experiments are presented in this section.

###### **4.2.1.1.1 The Chemical Composition of the FA (XRF Analysis)**

The XRF analysis of the FA is listed in Table 4.1. It can be observed that the FA composed mainly from the  $\text{Fe}_2\text{O}_3$ ,  $\text{SiO}_2$ , and  $\text{CaO}$  with relatively low  $\text{Al}_2\text{O}_3$ . These oxides occupied about 87% from the FA composition. The mass ratio of  $\text{SiO}_2/\text{Al}_2\text{O}_3=2.85$ . Furthermore, the FA contains  $\text{CaO}$  of 21.6 %, therefore, it can be classified as (Class-C) FA according to ASTM (C 681-08).

Table 4.1: XRF analysis data of FA composition

Chemical	Composition (%)
SiO <sub>2</sub>	26.4
Al <sub>2</sub> O <sub>3</sub>	9.25
Fe <sub>2</sub> O <sub>3</sub>	30.13
TiO <sub>2</sub>	3.07
CaO	21.6
MnO	0.27
CuO	0.14
K <sub>2</sub> O	2.58
P <sub>2</sub> O <sub>5</sub>	0.67
SO <sub>3</sub>	1.3
SrO	0.03
Loss on Ignition (LOI)	3.02

#### 4.2.1.1.2 Particle Size Distribution of the FA

The particle size analysis results and operation conditions as obtained from the test instrument are given in Figure 4.1 and Table 4.2. It can be seen that the high portion of FA having particle size of 10  $\mu\text{m}$ , with specific surface area of 0.463  $\text{m}^2/\text{gm}$ .

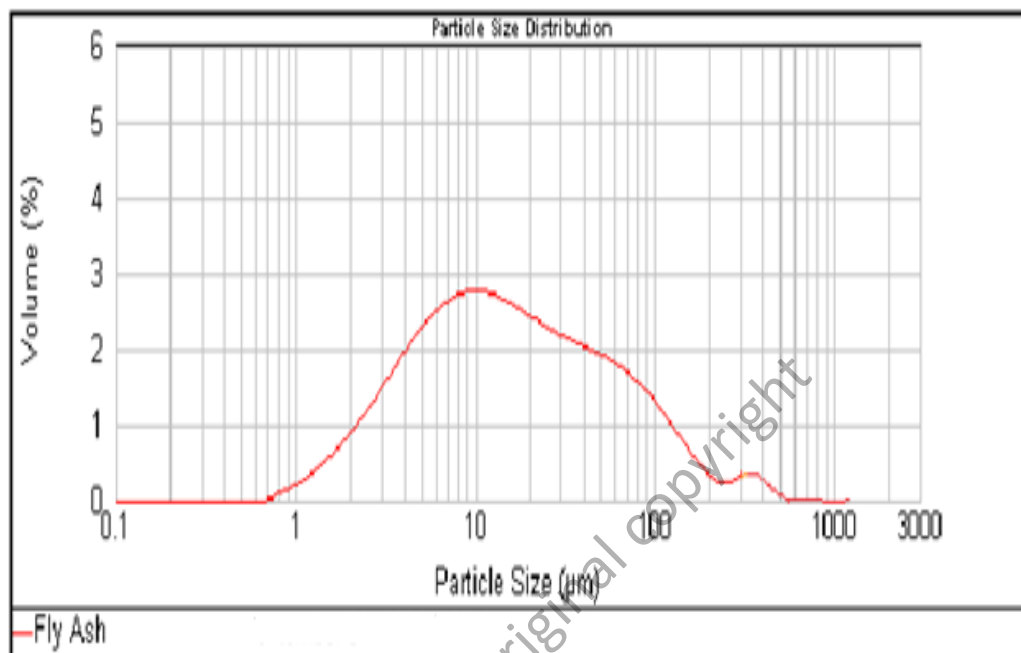


Figure 4.1: Particle size distribution of the FA

Table 4.2: Results of FA particle size analysis and operation conditions.

<b>Particle Name:</b>	<b>Accessory Name:</b>	<b>Analysis Model:</b>	<b>Sensitivity:</b>
Fly ash	Siroccos 2000 (A)	General Purpose	Enhanced
<b>Particle P.J:</b>	<b>Absorption:</b>	<b>Size Range:</b>	<b>Obscuration:</b>
1.500	0	0.020 to 200.00 µm	8.45 %
<b>Dispersant Name</b>	<b>Dispersant P.J:</b>	<b>Weight Residual:</b>	<b>Result</b>
-	1.000	2.268	<b>Emulation:</b>
			Off
<b>Concentration</b>	<b>Span:</b>	<b>Uniformity:</b>	<b>Result Units:</b>
0.0037 % Vol	21.074	6.75	Volume
<b>Specific Surface Area</b>	<b>Surface Weighted Mean</b>	<b>Volume Weighted Mean</b>	-
0.463 m <sup>2</sup> /g	12.964 µm	104.742 µm	-
d (0.1) 4.433 µm	d (0.5) 57.553 µm	d (0.9) 317.443 µm	

#### 4.2.1.1.3 Microstructure of the FA (SEM Analysis)

Figure 4.2 shows the SEM micrograph of the FA used in preparation of different FA geopolymer pastes, mortars and LWAGCs through this study. The FA consists mostly of glassy, hollow, spherical particles, which are cenospheres (thin walled hollow spheres). The microstructure appearance of the FA is well agreed with that reported by Davidovits (2008). Although, FA particles are essentially the same, variations do occur in shape (rounded to angular) with some crystals of mullite and iron (Fernandez-Jimenez & Palomo, 2003). Furthermore, surface texture appears to be smooth and dense to highly porous and present or absence of surface coatings likes magnetite.

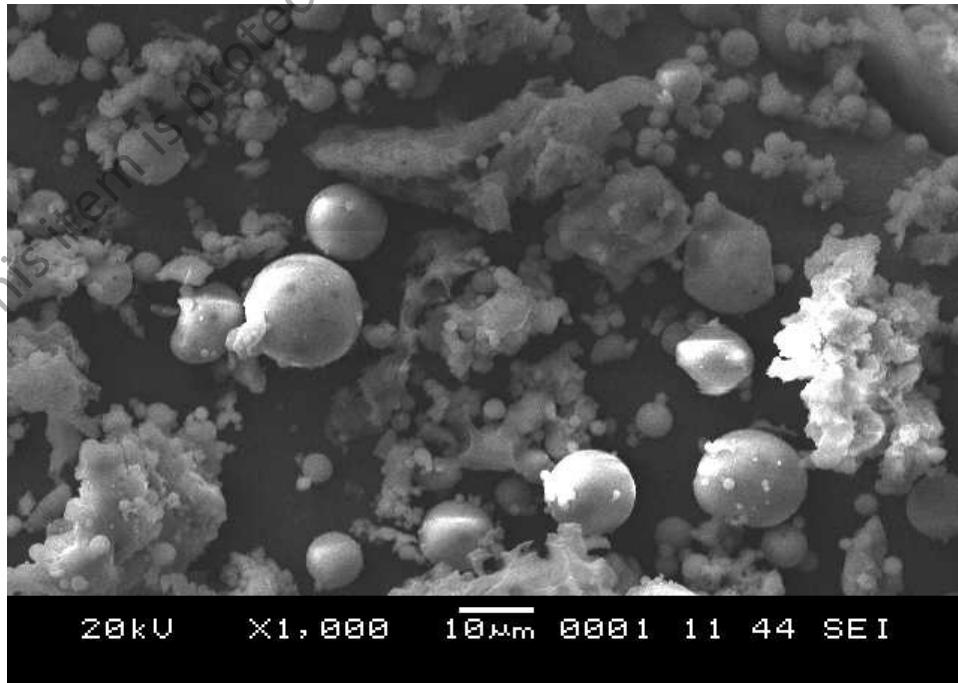


Figure 4.2: SEM micrograph of the source material (FA).

#### 4.2.1.1.4 The Phase Composition of the FA (XRD Analysis)

Figure 4.3 presents the XRD diffractogram of the FA. It can be seen that the FA is mainly an amorphous material with the appearance of a typical broad hallow at 16 to 38 2 $\theta$ . However, the FA diffractogram is also contains some of crystalline phases of quartz (SiO<sub>2</sub>) at 21, 26.6 and 65 2 $\theta$ , mullite (3Al<sub>2</sub>O<sub>3</sub>.2SiO<sub>2</sub>) at 17.1 and 28.3 2 $\theta$  and hematite (Fe<sub>2</sub>O<sub>3</sub>) at 24, 35 and 41 2 $\theta$ .

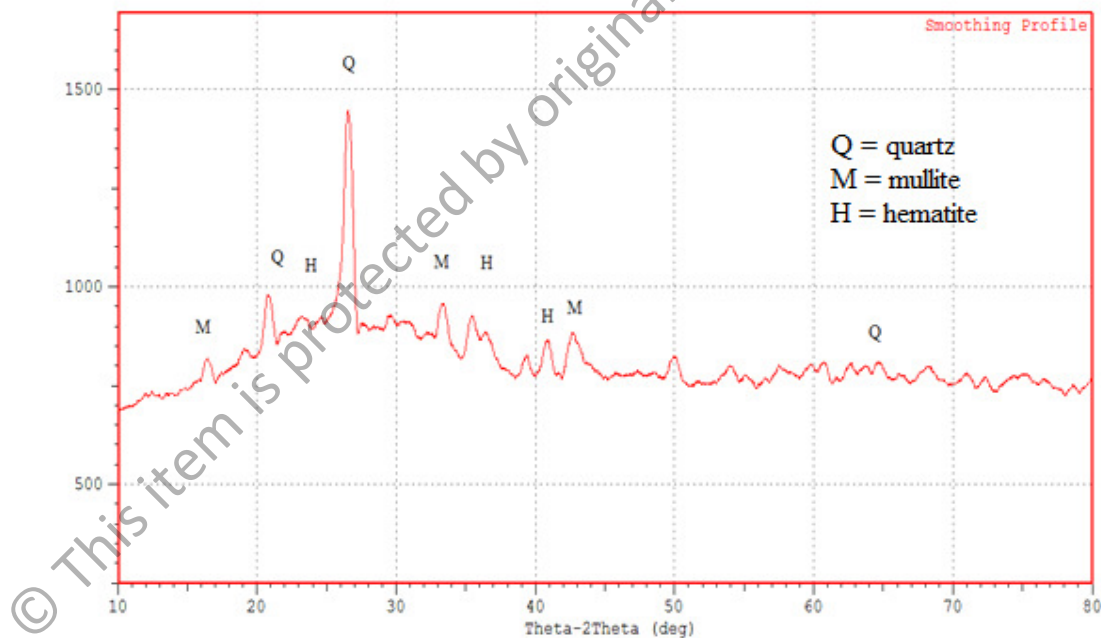


Figure 4.3: XRD diffraction pattern of the FA.

#### 4.2.1.2 Analysis of Sand

The details of the fine aggregate (sand) density and water absorption as well as the particle size analyses were mentioned in Chapter 3, section 3.2.3. The results of these experiments are given in this section.

#### 4.2.1.2.1 Density and Water Absorption of the Sand

The results of this experiment are the following weights:

- i. A: Mass of the OD = 490.7 g.
- ii. S: Mass of the SSD= 501.4 g.
- iii. B: mass of the flask filled with water = 953.5 g
- iv. C: the mass of flask with sample and water to the calibration or filling mark = 647.2 g.

The specific gravity of the sand is calculated by applying these weights in Equation (3.1) mentioned in Chapter 3, section 3.2.3, which equal to 2.5. The water absorption of the sand is also calculated from equation (3.2) mentioned in Chapter 3, section 3.2.3 and it is equal to 2.2%.

#### 4.2.1.2.2 Particle Size Analysis

Table 4.3 illustrates the results of the sand particle size analysis which calculated using equations of (3.3) to (3.7) mentioned Chapter 3, section 3.2.3 after obtained the IMR values of each used sieve form the test. The results indicated that the adopted sand possesses a maximum particle size of 2.38 mm. Thus, the sand is classified as a fine aggregate according to ASTM (C 136-06).

Table 4.3: Sieve analysis results for the sand.

Sieve (mm)	IMR (g)	IPR (%)	CMR (g)	CPR (%)	CPP (%)
4.75	0	0	0	0	100
2.38	5	1.25	5	1.25	98.75
1.19	15	3.70	20	5	95
0.59	100	25	120	30	70
0.30	120	30	240	60	40
0.15	120	30	360	90	10
0.075	30	7.50	390	97.50	2.50
Pan	10		400	-	-

#### 4.2.1.3 Analysis of LWA

The experiments were conducted to the LWA in order to analysis their physical properties such as density and water absorption as well as the particle size analysis as mentioned in Chapter 3, section 3.2.4. These results were used in the designing process of the LWAGC. The results of these experiments are given in this section.

##### 4.2.1.3.1 Density and Water Absorption Analysis

The results of this experiment are the following weights:

- i. A: Mass of the OD = 1880 g.
- ii. B: Mass of the SSD= 2205 g.
- iii. C: Mass of the apparent = 124 g.

Table 4.4 is listed the results of the density and water absorption of the aggregate which obtained by applying the resulted weights in the mentioned Equations of (3.8) to (3.14), in Chapter 3, section 3.2.4. Furthermore, the results show that the resultant aggregate has an OD-density of  $897.75 \text{ kg/m}^3$  which is less than the maximum LWA OD-density limit of  $1120 \text{ kg/m}^3$  reported by Mehta & Monteiro (2006), therefore, the used aggregate throughout this study is classified as LWA category. In addition, according to the LWA spectrum presented in Chapter 2, Figure 2.4, the adopted LWA is applicable for preparation a structural lightweight aggregate concrete LWAC. It is also observed that the LWA has a relatively high water absorption property of 17.2 %.

Table 4.4: Physical properties of LWA.

<b>Physical Property</b>	<b>Value</b>
<b>Specific gravity (OD)</b>	0.9
<b>Specific gravity (SSD)</b>	1.05
<b>Apparent specific gravity</b>	1.07
<b>Density (OD)</b>	$897.75 \text{ (kg/m}^3\text{)}$
<b>Density (SSD)</b>	$1047.37 \text{ (kg/m}^3\text{)}$
<b>Apparent density</b>	$1067 \text{ (kg/m}^3\text{)}$
<b>Water absorption (%)</b>	17.2

#### 4.2.1.3.2 Particle Size Distribution

The results of the LWA particle size analysis which were obtained from analyzing the sieve test raw data in similar method of analysis conducted to sand particle size data

presented in section 4.2.1.2.2. The LWA particle size analysis results given in Table 4.5 are revealing that the LWA have a particle size of 4-8 mm. Furthermore, the majority of the LWA of about 75 % is classified as coarse LWA, while the rest is considered as a fine LWA according to ASTM (C 136-06).

Table 4.5: Sieve analysis for the LWA.

<b>Sieve (mm)</b>	<b>CPP (%) LWA</b>
9.5	100
8	90
6.3	60
4.75	25
2.38	0

#### 4.2.2 Actual Design of the LWAGC

The actual design of the LWAGC was performed to obtaining the optimum preparation parameters which provides the optimum conditions to geopolymerization reaction and then leads to produce geopolymers with maximum compressive strength. As mentioned in Chapter 3, section 3.4, the actual design of the LWAGC was performed to the FA geopolymer paste to obtain the optimum curing temperature and curing period, as well as the optimum  $\text{Na}_2\text{SiO}_3/\text{NaOH}$  mass ratio. The significant effects of these preparation parameters on the geopolymerization reaction were already presented in details in Chapter 2, section 2.9.1. The details of these experiments were

also given in Chapter 3, section 3.4, and the results of these experiments are given in this section.

#### 4.2.2.1 Optimum $\text{Na}_2\text{SiO}_3/\text{NaOH}$ Mass Ratio

Figure 4.4 shows the resulted geopolymer paste specimens prepared at different  $\text{Na}_2\text{SiO}_3/\text{NaOH}$  mass ratios ranged of 0.5-3.0. While, Figure 4.5 is illustrating the effect of  $\text{Na}_2\text{SiO}_3/\text{NaOH}$  mass ratio on the compressive strength of the resultant geopolymer paste specimens at ages of 3, 7 and 28 days.



Figure 4.4: Geopolymer paste specimens prepared with different  $\text{Na}_2\text{SiO}_3/\text{NaOH}$  ratios.

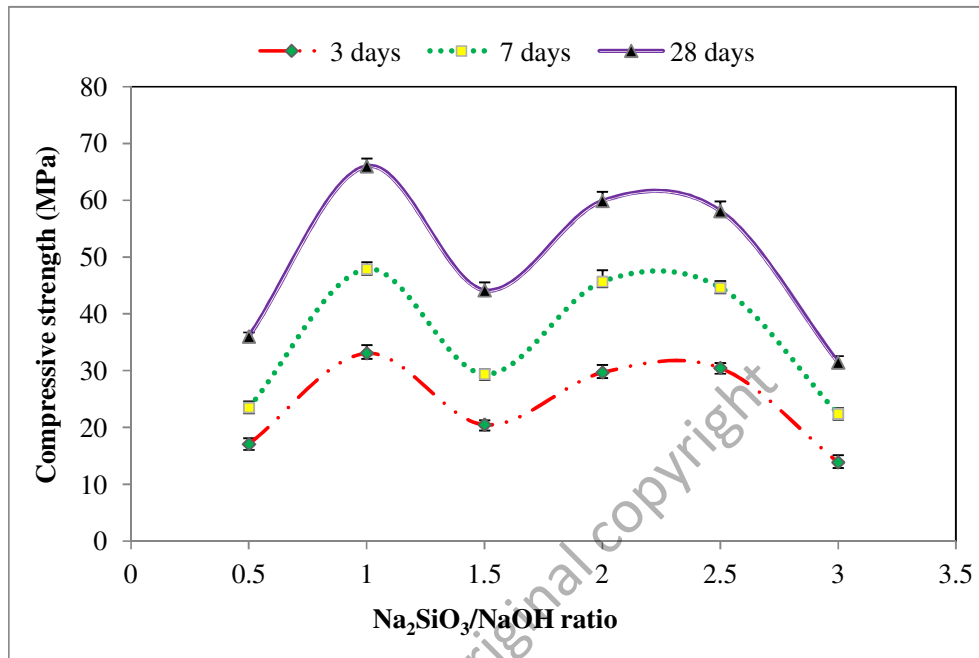


Figure 4.5: Effect of different Na<sub>2</sub>SiO<sub>3</sub>/NaOH mass ratios on the compressive strength development of the FA geopolymers paste.

It is observed that the Na<sub>2</sub>SiO<sub>3</sub>/NaOH mass ratio of 1.0 provides the highest compressive strength at all ages than other Na<sub>2</sub>SiO<sub>3</sub>/NaOH ratios. Correspondingly, as reported by Chindapasirt et al. (2007) that the Na<sub>2</sub>SiO<sub>3</sub>/NaOH mass ratios in the range of 0.67-1.0 produced the optimum strength for the resultant geopolymer, the results of this experiment are in good agreement with this statement. Furthermore, it can be seen that the Na<sub>2</sub>SiO<sub>3</sub>/NaOH mass ratios of 2 and 2.5 produces almost the same strength values at all the tested ages, which are approximately parallel to the optimum Na<sub>2</sub>SiO<sub>3</sub>/NaOH ratio of 1.0 strength values especially at the early ages of 3 and 7 days.

Nevertheless, high distinguish to the optimum value of Na<sub>2</sub>SiO<sub>3</sub>/NaOH ratio can be observed at the age of 28 days, which obviously clarified that the optimum value of Na<sub>2</sub>SiO<sub>3</sub>/NaOH ratio is 1.0. Whilst, the Na<sub>2</sub>SiO<sub>3</sub>/NaOH ratios of 0.5, 1.5 and 3.0 are developing low compressive strengths at the all tasted ages. Thus, according to the results of this experiment, the Na<sub>2</sub>SiO<sub>3</sub>/NaOH ratio of 1.0 has been selected in the

preparation the alkaline activator used in the preparation of the LWAGC, as it is leads to produce the highest (optimum) compressive strength for the FA geopolymers.

#### 4.2.2.2 Optimum Curing Temperature

Figure 4.6 illustrates the resultant FA geopolymers paste specimens cured at different curing temperatures ranged of 60 °C to 90 °C. Furthermore, Figure 4.7 shows the compressive strength development of the FA geopolymers paste cured at different curing temperatures of 60 °C to 90 °C, at aging periods of 3, 7 and 28 days.

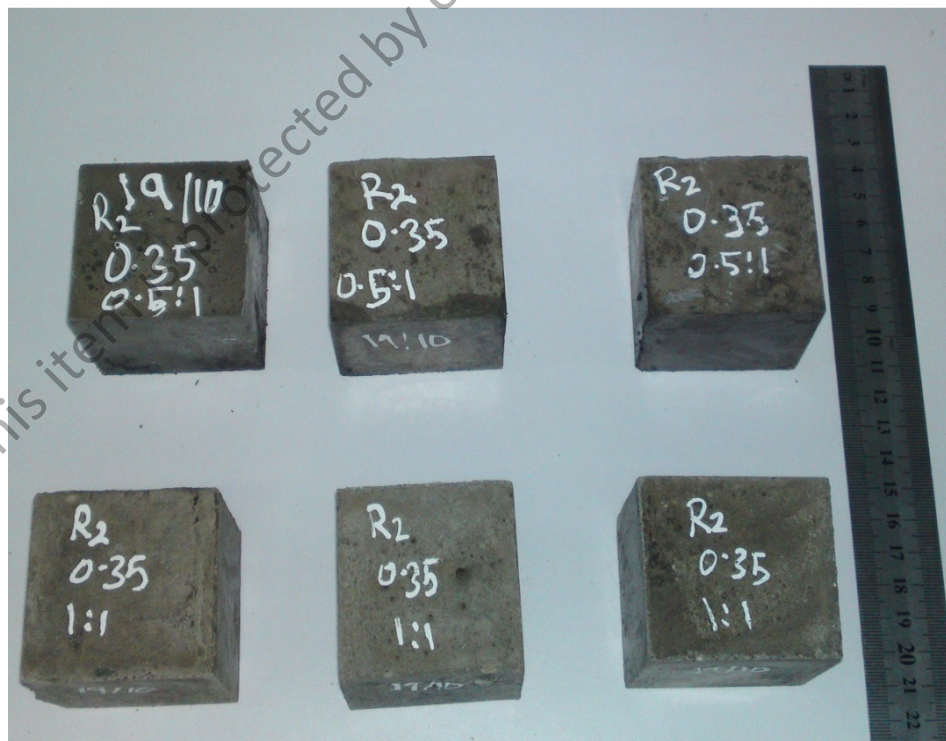


Figure 4.6: Geopolymer paste specimens cured at different temperatures ranged of 60-90 °C.

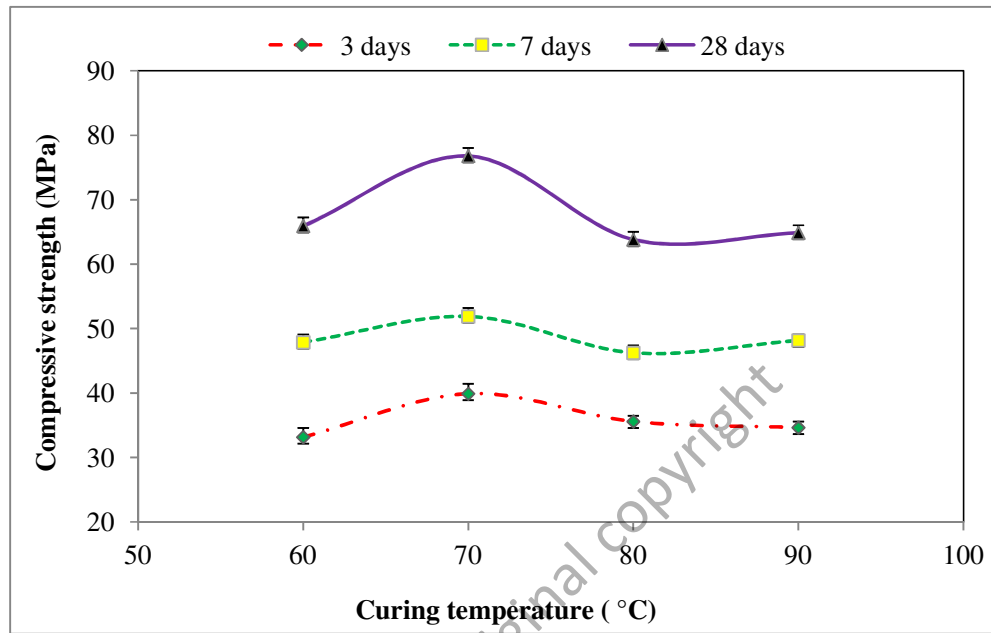


Figure 4.7: Effect of different curing temperatures on the compressive strength development of the FA geopolymers paste.

Although the curing temperature of 70 °C produces the highest compressive strength at all testing ages, it can be seen that the varied curing temperatures producing a comparable compressive strengths especially at age of 7 days. The results are also showing that the compressive strength of the geopolymer paste increases with increases the curing temperature from 60 °C to 70 °C. However, the strength is decreasing when the curing temperature increases higher that 70 °C and most significantly at the age of 28 days.

It is believed that the loss of moisture at temperatures of 80 and 90 °C is the cause behind the strength decreasing, as the geopolymerization reaction required the presence of moisture in order to develop a good strength (Chindapasirt et al., 2007). Based on results presented in Figure 4.7, the temperature of 70 °C has been chosen to be the curing temperature used in the curing process of the LWAGCs.

### 4.2.2.3 Optimum Curing Period

The resultant FA geopolymer paste specimens of this experiment were similar to that showed in Figure 4.6. In addition, Figure 4.8 presents the effect of curing periods ranged of 6 hours to 30 hours, on the compressive strength development of FA geopolymer paste specimens. It shows that the resultant compressive strength is increasing as the curing period increased up to 24 hours for all testing ages. This is revealing that the curing period of 24 hours developed a geopolymerization reaction of highest rate than other curing periods of 6 hours to 18 hours are leads to producing the maximum (optimum) strength to the resultant geopolymer.

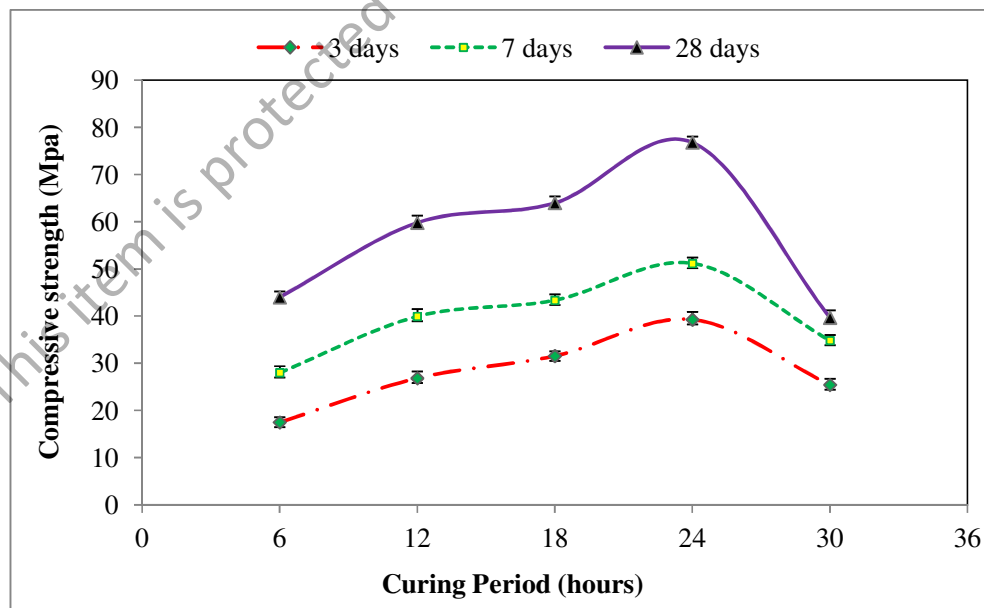


Figure 4.8: Strength development of the geopolymers paste at different curing periods.

Furthermore, curing the FA geopolymers further than 24 hours up to 30 hours has a negative effect on the strength development as the longer curing as 24 hours may result in breaking down the geopolymeric gel structure of the geopolymer matrix, leading to

lower the resultant strength ( van Jaarsveld et al., 2002). Thus, these results show that the curing periods of 24 hours producing the optimum compressive strength to the FA geopolymers and then it was utilized in the curing of the LWAGCs.

#### 4.2.3 Physical and Mechanical Properties of FA Geopolymer Paste, Mortar and LWAGC at 28 Days of Age

The resultant FA geopolymer pastes, mortars and LWAGCs prepared as mentioned in Chapter 3, sections 3.7 and 3.8 are shown in Figures 4.9-4.11, respectively. It observed that the geopolymers have sharp gray color which comes from the base material (FA) color.



Figure 4.9: Resultant FA geopolymer paste specimens (100×100×100 mm).



Figure 4.10: Resultant FA geopolymer mortar specimens (100×100×100 mm).



Figure 4.11: Resultant LWAGCs specimens (100×100×100 mm).

Furthermore, Table 4.6 illustrates some of physical and mechanical properties of the FA geopolymer paste, mortar and LWAGC obtained at age of 28 days, except the slump of the fresh concrete which was measured before casting process. The compressive strength (18.86 MPa) and unit weight (OD-density = 1438.70 kg/m<sup>3</sup>) results of the resultant LWAGC are attained the LWAGC design characteristics listed in Chapter 3, section 3.3. Furthermore, the resulted 28 days compressive strength and unit weight of the LWAGC values are permitting it to be classified as a structural LWAC could be used as a construction material according to the American Concrete Institute ACI (ACI 213R-87) and Mehta & Monteiro (2006).

Table 4.6: Physical and mechanical Properties of the resultant geopolymers.

<b>Property</b>	<b>Paste</b>	<b>Mortar</b>	<b>LWAGC</b>
<b>Compressive (MPa)</b>	44.83	46.32	18.86
<b>OD-Density (kg/m<sup>3</sup>)</b>	1935.70	1945.30	1438.70
<b>Water Absorption (%)</b>	15.20	18.40	10.70
<b>Fresh Slump (mm)</b>	-	-	95.00

It can be seen that the LWAGC has significantly lowest compressive strength than both the geopolymer paste and mortar. This is attributed to its low OD-density as well as to the low strength characteristics of its LWA. Correspondingly, compare the OD-density of the LWAGC with the densities of geopolymer paste and mortar; it observed that the LWAGC has OD-density of 25.6 % and 26 % lower than the densities of geopolymer paste and mortar, respectively. The decrease in the density value of the LWAGC than the geopolymer paste and mortar is likely the responsible for the decrease compressive strength, as the compressive strength of LWC is significantly dependent on its dry density (Neville, 1994; Kim & Harmon, 2006).

Figure 4.12 demonstrates the bulk characteristics of the adopted LWA as seen under the optical microscope. It can be seen the multi-fine micropours and voids are consistently exist within the interior structure of the LWA. These micropours and voids provides a lightweight and other thermal and acoustic insulation advantages, although these characteristics reduces the strength of the LWA and leads to weaken the resultant concrete (Yang et al., 2010; ACI 211.2).

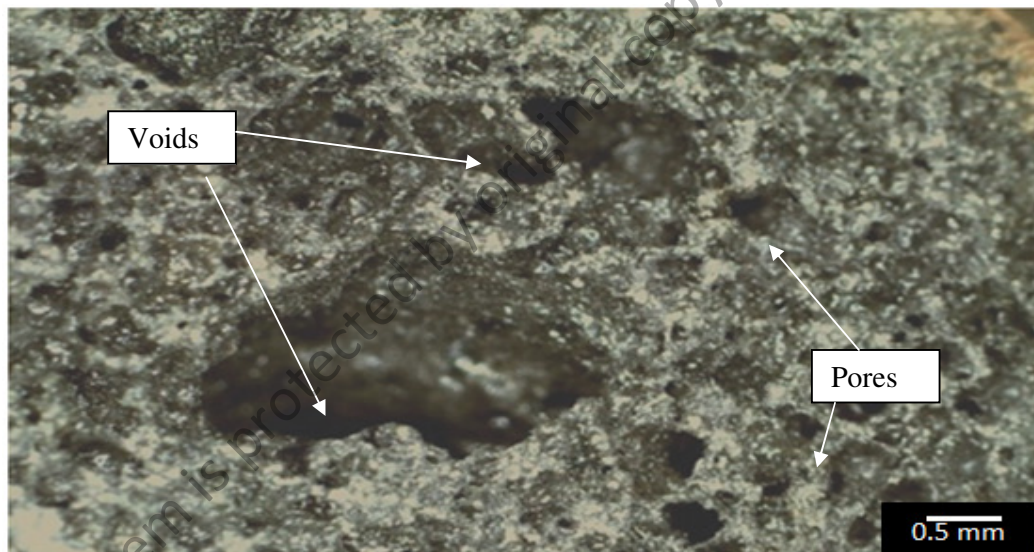


Figure 4.12: Microscopy image for the adopted LWA.

Nevertheless, the resulted LWAGC mechanical strength with respect to its OD-density of  $1438.70 \text{ kg/m}^3$  is considered as high-quality strength LWC, when it compared with similar structural LWAGC reported by Yang et al., (2010). According to their results, the LWAGC prepared by alkali-activation of ground granulate blast furnace slag (GGBS), by a powder sodium silicate activator and aggregates combination of normal sand and coarse LECA, possessed a compressive strength and OD-density of 19.1 MPa of  $1615.1 \text{ kg/m}^3$ , respectively, at 28 days of age, as mentioned in Chapter 2, section 2.10, Figure 2.2. Hence, since they used the same aggregates combination, the alkali-

activation of the FA with liquid activator appears to be better than the alkali-activated GGBS by a powder activator, as it produces almost the same strength, but with about 11% less density.

#### 4.2.4 LWAGC Compressive Strength Developing Versus Aging Times

The compressive strength development of LWAGC with aging times was studied as mentioned in Chapter 3, section 3.7.2, at ages of 3, 7, 28, 56, 91, 180 and 365 days. Figure 4.13 shows the LWAGC strength development versus the targeted ages, indicating that the LWAGC gains high rates of strength increasing at early ages of 3 and 7 days which are equivalent to about 66% and 81% of the 28 days aging strength, respectively. This trend is attributed to the fact that the geopolymerization process produces excellent early strength at early age stages (Hardjito & Rangan, 2005).

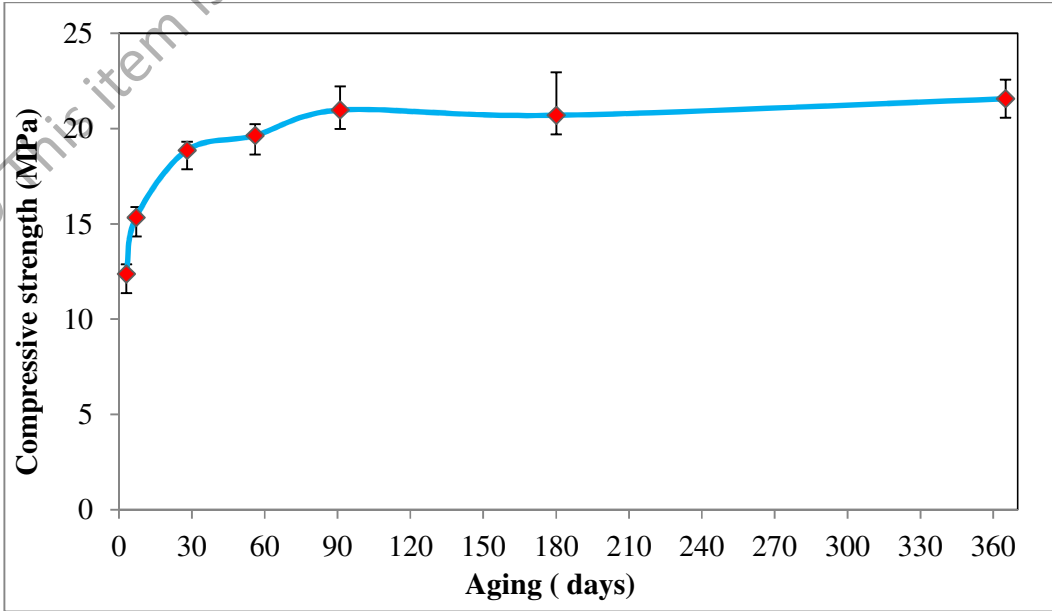


Figure 4.13: Compressive strength development of the LWAGC versus aging times.

However, the strength developing rate is slightly decreased beyond 28 days, although the strength developing is continued until the age of 365 days. Collins & Sanjayan (1999) reported that the absorbed water and/or activator liquid by the porous LWA during the fresh mixing may have a favorable effect on the strength development at the long-term age, due to the continuous activation of the source material (FA), while the moisture and/or absorbed liquid is released from the saturated aggregate. Therefore, the LWAGC is observed to gain compressive strength until the age of 365 days. The results of this experiment show another advantage of the geopolymeric materials represented by the strength gaining at long-term ageing with addition to the advantage of the high early strength reported at early ages of 3 and 7 days.

#### **4.2.5 Effect of Activator/FA Mass Ratio on the Workability and Compressive Strength of the FA Geopolymer Paste and LWAGC**

The details of the experiments carried out in order to address the effect of the Activator/FA mass mixing ratio on the compressive strength of the FA geopolymer paste and LWAGC were mentioned in Chapter 3, section 3.9. The geopolymeric materials were prepared at Activator/FA mass ratios range of 0.3-0.7.

Table 4.7 illustrates the effects of the Activator/FA mass ratios on the workability of the fresh LWAGC and the resulted compressive strength of the hardened concretes at age of 28 days. As expected, an increase in the ratio of Activator/FA enhanced the workability of the fresh concrete and increases the slump value, due to raise the liquid content in the mixture. Hence, it observed that the maximum slump of 117 mm is recorded for the Activator/FA ratio of 0.7. Nevertheless, after the fresh mixture poured into the molds, it was observed that the geopolymeric fresh mixture prepared at this

ratio (0.7) caused a severe segregation as the low density LWAs floated up to the surface of the specimen and further outside the molds, due to the excess liquid content that this ratio provided. Thus, this ratio failed to make a hardened LWAGC specimen and therefore no strength was possibly to be measured for this concrete.

Table 4.7: Effect of the Activator/FA mass ratios on the properties of LWAGC.

Activator/FA ratios	Slump (mm)	LWAGC strength (MPa) at 28 days
0.30	61	6.63
0.40	74	11.69
0.50	86	15.35
0.59	95	18.86
0.70	117	-

Table 4.7 is also showing the 28 days compressive strength results of the hardened LWAGC prepared at the Activator/FA ratios of 0.3-0.59. The highest rate of strength developing is observed when the ratio increases from 0.3-0.4 and from 0.4-0.5. Furthermore, the rate of strength developing is observed to be slightly decreases as the ratio increases from 0.5-0.59. Although, the compressive strength of the LWAGC prepared at Activator/FA ratio of 0.59 is approximately equal to about triple times the strength value resulted for the LWAGC of Activator/FA ratio of 0.3.

Moreover, as mentioned in Chapter 3, section 3.9, FA geopolymer paste specimens has been prepared at the same range of Activator/FA ratios of 0.3-0.59 used in the preparation of LWAGCs for further investigating the effect of the Activator/FA ratios

on the FA geopolymerization reaction. Figure 4.14 shows the effect of the Activator/FA ratio on the compressive strength of the FA geopolymer paste specimens prepared at different aging times of 3, 7 and 28 days. It observed that the compressive strength of the geopolymer paste is continuously increasing with raising the Activator/FA ratio from 0.3 up to 0.59 at all testing ages. This tendency makes the Activator/FA ratio of 0.59 which is containing the highest activator content than others ratios, an optimum ratio at the all three ages.

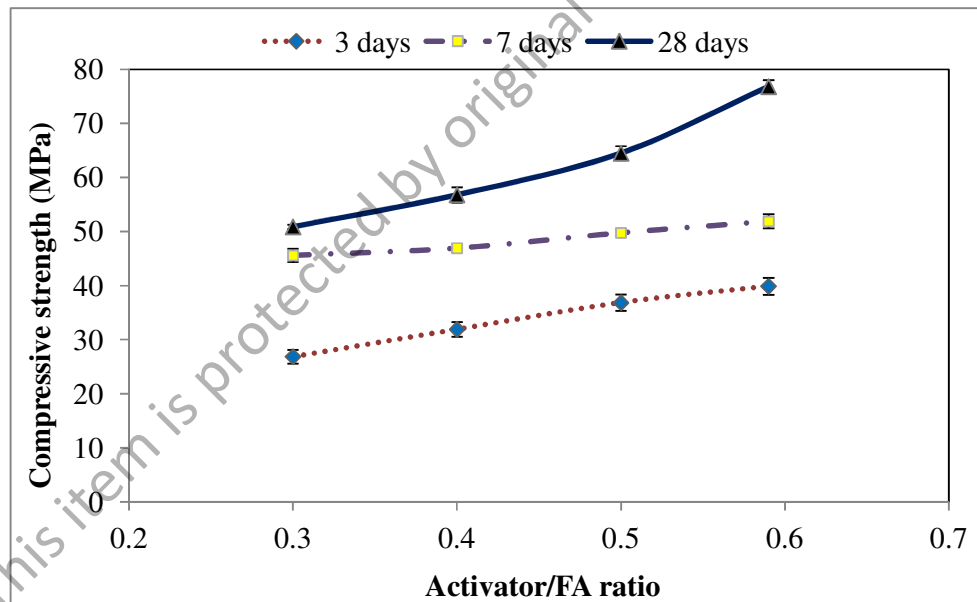


Figure 4.14: Effects of Activator/FA ratio on the compressive strength of FA geopolymer paste at different aging times.

As matter of fact, the more alkaline activator involves in the geopolymerization reaction, the more dissolution of the base material (FA) is results, leading to produce more geopolymeric products (Duxson et al., 2007a). Thus, at high geopolymerization reaction rates, the resulted compressive strength of the hardened material would be increased as well. However, further discussion about the effect of the selected Activator/FA ratio of 0.59 on the geopolymers microstructural and thermal properties is

presented in section 4.3. As a result, these experiments indicated that the Activator/FA ratio of 0.59 suggested by the ACI standard (ACI 211.2) is the optimum ratio that provides the optimum alkaline activator content lead to produce maximum compressive strength of the LWAGC. The compatibility of ACI standard (ACI 211.2) as a guidance used in the proportioning and designing of LWAGC systems in similar method used for designing an OPC lightweight aggregate structural concrete added another advantageous to the geopolymer materials.

#### 4.2.6 Effects of LWA Particle Size and Grading on the Physical and Mechanical Properties of LWAGC

Table 4.8 illustrates the second batch of LWA (batch 2) particle size distribution results show that this batch has a particle size of 8-16 mm. As mentioned in Chapter 3 section 3.10, the LWAGC systems were prepared with six different LWA size and grading in of 4-5 mm, 4-8 mm, 5-8 mm, 8-12 mm, 8-16 mm and 12-16 mm in order to study their effects on the physical and mechanical strength.

Table 4.8: Sieve analysis of batch 2 LWA.

Sieve (mm)	Passing (%) LWA batch 2
16	100
14	95
12.50	96
10	32
9.50	24
8	14
6.30	0
4.75	-

In accordance, the volume of the concrete, the mass of the aggregates (fine + coarse) and the mass ratio of Activator/FA are all kept constant in order to obtain the effect of particle size and grading on the workability of the fresh concrete mixtures and the density, compressive strength, water absorption and total porosity of hardened LWAGCs. Furthermore, the prepared LWAGC were named according to their LWA size which has been also mentioned in Chapter 3 section 3.10.1.

#### **4.2.6.1 Effect of LWA Particle Size and Grading on the Workability of the Fresh LWAGC Mixtures**

Table 4.9 illustrates the slump values of the fresh LWAGCs which indicate that the diversity in the LWAs size and grading leads to various workability or slump values. Compare the slump values of the fresh graded concrete mixtures of L4-8 and L8-16 indicated that the increasing of the maximum and minimum size of the LWA increase the slump value of the fresh mixture. Moreover, for the targeted concretes, decreasing the maximum size of the LWA results in reducing the fresh concrete workability as it observed for the targeted concretes of L4-5 and L8-12, which were prepared from the graded LWA of 4-8 mm and 8-16 mm, respectively. In addition, it is observed that increases the minimum size of the LWA for the targeted concretes of L5-8 and L12-16 which were prepared from the graded control concretes of L4-8 and L8-16, respectively; enhance the slump value of the fresh geopolymeric mixture.

Generally, as the maximum particle size of a bulk aggregate (NWA or LWA) decreases, the specific surface area of the bulk aggregate increases, and then more cement paste is needed to coat or bind the additional surfaces (ACI E-701). Accordingly, as the cement content is left constant, the thinner layers of paste

surrounding the aggregate particles result in a stiffer concrete that is hard to place and compact. Hence, it is observed that the slump values of LWAGC mixtures in general are decreased with decreasing the maximum size of the LWAs. Similarly, as the maximum size of the aggregate increases, the paste amount required to make the concrete decreased due to decreasing the specific surface area of the LWA, which leads to provide extra fresh geopolymeric mortar that increases the slump value. This phenomenon is observed in the higher slump value of the control graded L8-16 compared with the graded L4-8 as Table 4.9 illustrated.

Table 4.9: Slump values of fresh LWAGC prepared at different LWAs size and grading.

<b>Mixture</b>	<b>Slump (mm)</b>
L4-5	72
L4-8	95
L5-8	103
L8-12	125
L8-16	137
L12-16	146

On the other hand, as the minimum size of the LWA increases from 4-8 mm to 5-8 mm and 8-16 mm to 12-16 mm, it actually removed the intermediate aggregates smaller than 5 mm from the original graded 4-8 mm LWA, and the one smaller than 12 mm from the original graded 8-16 mm LWA. These intermediate aggregates were essentially occupied the spaces or voids between the largest aggregate particles. Hence, with the omission of these particles, the voids content in the fresh concrete mixture

increased (Mehta & Monteiro, 2006; ACI E-701). As the LWAGC ingredients quantities were fixed at the preparation process, the generated voids are the reason behind the slump values increases, which is observed for L5-8 and L12-16 prepared from the graded control concretes of L4-8 and L8-16, respectively. However, this is also affected the hardened LWAGCs properties at the similar aspects observed in the fresh stage as presented in section 4.2.5.2.

#### **4.2.6.2 Effects of LWA Particle Size and Grading on the Density and Mechanical Strength Properties of Hardened LWAGCs.**

Figure 4.15 illustrates the resulted L4-8, L4-5 and L5-8 LWAGCs prepared from the graded LWA batch 1 of 4-8 mm. While, Figure 4.16 shows the resulted L8-12, L8-16 and 12-16 concretes prepared from the graded LWA batch 2 of 8-16 mm. In general, it is observed that the surface texture of the resultant LWAGC is reflecting the size of its LWA by the increasing of the surface roughness as the LWA size increased.



Figure 4.15: LWAGCs of L4-8, L4-5 and L5-8 prepared from the graded LWA batch 1 of 4-8 mm.



Figure 4.16: LWAGCs of L8-16, L8-12 and L12-16 prepared from the graded LWA batch 2 of 8-16 mm.

Moreover, Figure 4.17 shows the resulted compressive strength of the LWAGCs prepared with various LWA size and grading at age of 28 days. For the control graded concretes, it can be seen that the L4-8 concrete has higher compressive strength than the L8-16. Furthermore, the density measurements showed that the L4-8 possesses an OD-

density of  $1438.7 \text{ kg/m}^3$ , higher than the L8-16 of  $1393.7 \text{ kg/m}^3$ . This increment in OD-density value of the L4-8 than the L8-16 is responsible for its higher strength, as the strength of LWAC generally increases with increase its OD-density (Yang et al., 2010; ACI 211-02).

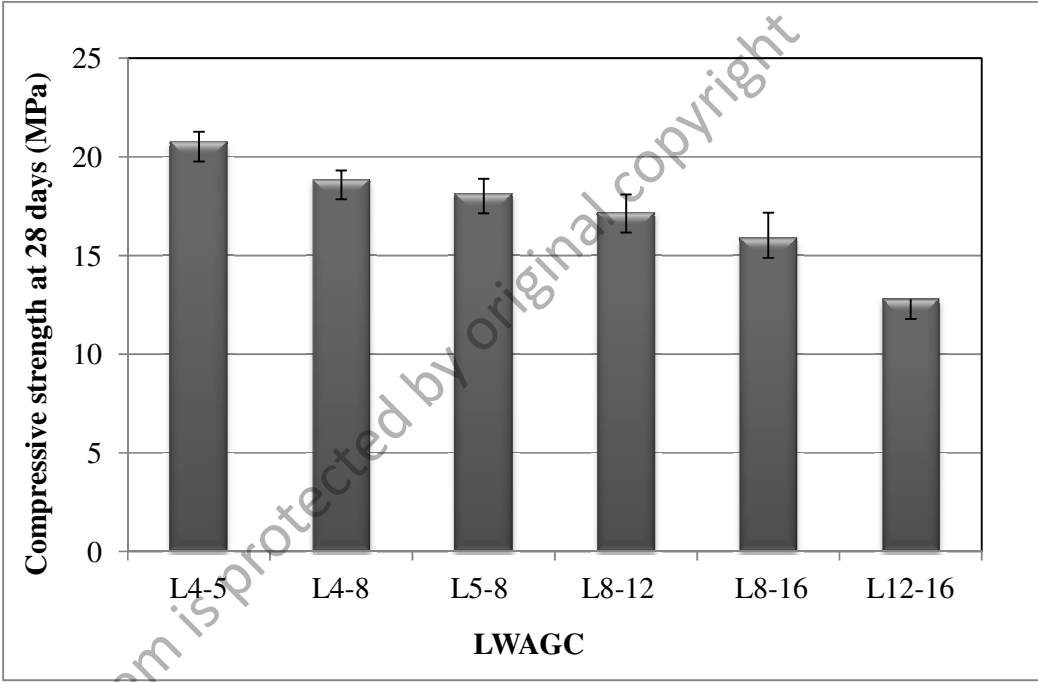


Figure 4.17: Compressive strength data of the LWAGCs prepared with different LWA sizes and grading.

It is also noticed that despite the fact that concrete ingredients quantities were fixed at the preparation process, the difference in the OD-density values of the L4-8 and L8-16 revealing that the L4-8 contains much more quantity of the geopolymer mortar than the L8-16. This is substantially attributed to the difference in their LWAs maximum size. The smallest surface area per unit volume of the 8-16 mm LWAs compared with 4-8 mm LWA required less quantity of the geopolymeric binder to cover the aggregate surfaces and the voids between them. Thus, with less geopolymeric binder, the resulted L8-16 possesses lower density and strength than L4-8.

Moreover, a similar behavior can be observed for the targeted L4-5 and L8-12 concretes which possess OD-densities of  $1531.85 \text{ kg/m}^3$  and  $1421.66 \text{ kg/m}^3$ , respectively, higher than their control graded concretes of L4-8 and L8-16 of  $1438.7 \text{ kg/m}^3$  and  $1393.7 \text{ kg/m}^3$ , respectively. Therefore, it observed that the compressive strength of the L4-5 is 9 % higher than its original graded L4-8 and the strength of the L8-12 is 8 % higher than the original graded L8-16 as indicated in Figure 4.17.

Additionally, a comparison in the strength results of L5-8 and L12-16 concretes with their original graded concretes of L4-8 and L8-16 illustrated in Figure 4.17 shows that the strength decreases with increases the minimum size of the LWAs. This is attributed to the highest voids content of the of L5-8 and L12-16 concretes than their original graded concretes of L4-8 and L8-16. This is due to the removal of the intermediate small aggregates which were occupied the spaces or the voids between the largest aggregate particles as well as the fixed geopolymeric binder as mentioned earlier in section 4.6.1. This is supported by the resulted OD-densities of the L5-8 and L12-16 concretes of  $1432.5 \text{ kg/m}^3$  and  $1356.11 \text{ kg/m}^3$ , respectively, which are lower than their control original concretes of L4-8 and L8-16 of  $1438.7 \text{ kg/m}^3$  and  $1393.7 \text{ kg/m}^3$ , respectively. The lowest OD-densities of the L5-8 and L12-16 than the original control concretes of L4-8 and L8-16 leads to decrease their compressive strength lower than the control original concretes.

#### **4.2.6.3 Effects of LWA Particle Size and Grading on the Water Absorption and Total Porosity Characteristics of Hardened LWAGCs.**

Table 4.10 shows the water absorption and the total porosity results of the prepared LWAGCs, illustrating that the water absorption and the total porosity of the LWAGCs

increase with increasing the maximum size of their LWAs. This trend is with good agreement with the results reported by Babu et al., (2006). For the targeted LWAGCs, the water absorption and the total porosity of the concretes increases with increasing the minimum size of their LWAs compared to the graded control concrete. Therefore, it is observed that L12-16 concrete has the highest water absorption and total porosity, while the lowest absorption and porosity content are resulted for L4-5 concrete.

Table 4.10: Water absorption and total porosity of the resulted LWAGCs.

<b>LWAGC</b>	<b>Water absorption (%)</b>	<b>Total porosity (%)</b>
L4-5	8.32	14.40
L4-8*	10.75	16.04
L5-8	10.82	16.17
L8-12	10.94	16.63
L8-16*	11.78	17.92
L12-16	12.60	18.74

\*The graded control concretes.

Accordingly, it is believed that the increases of the water absorption and total porosity of the resulted LWAGCs are depended significantly on their OD-densities. Figures 4.18 and 4.19 are displaying the relationships between the water absorption and total porosity, respectively, with the OD-densities of the resulted LWAGCs. It can be seen that the lower OD-density of the LWAGC, the higher water absorption and total porosity results. The L12-16 concrete has the highest water absorption and total porosity due to its lowest OD-density compared to other concretes, which, therefore, resulted in the lowest compressive strength as already presented in Figure 4.17. In addition, the

results of Figure 4.19 are explaining the dependency of the LWAGC strength on its OD-density due to the fundamentally inverse relationship between the porosity and the compressive strength of a concrete (Mehta & Monteiro, 2006).

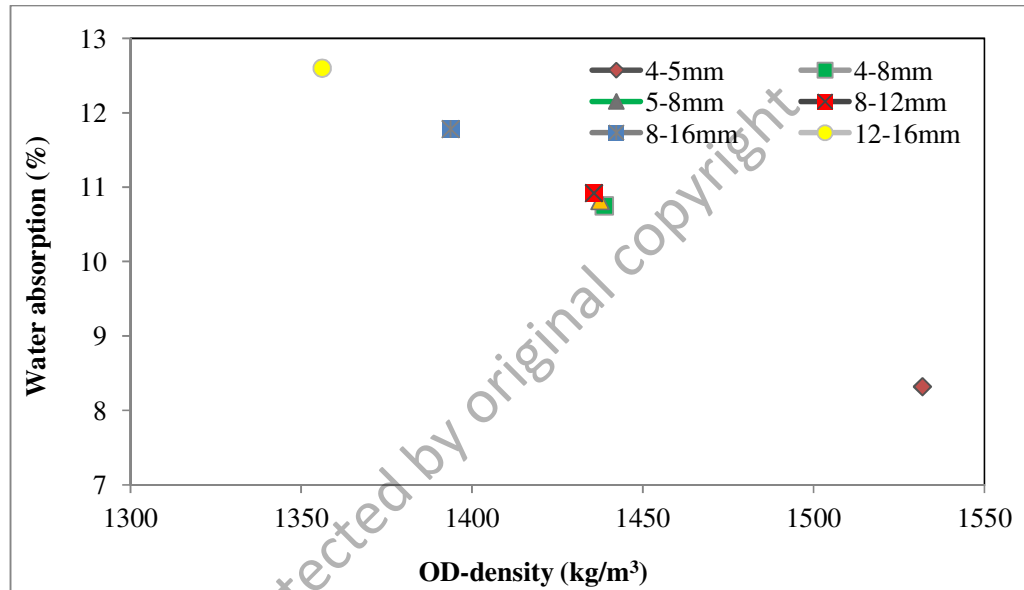


Figure 4.18: Relationship between the water absorption and OD-density of the resultant LWAGCs.

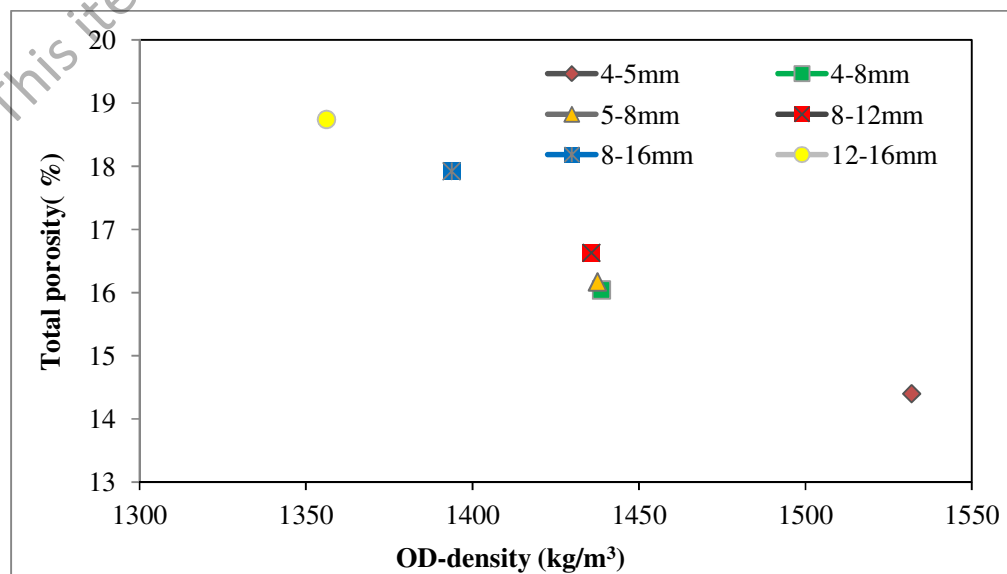


Figure 4.19: Relationship between total porosity and OD-density of the resultant LWAGCs.

### **4.3 FA Geopolymer Materials Thermo-Mechanical and Macro/Microstructure Evolution**

This section presents the results of the thermal behavior and heat resistance properties of the geopolymeric materials that tested through the exposing to elevated temperatures of maximum 800 °C according to the experimental studies mentioned in Chapter 3, section 3.11. Furthermore, it has been mentioned earlier in these studies that the resultant residual compressive strength of the exposed geopolymeric materials at elevated temperatures is the mechanical property that evaluated their thermal behavior. In addition, the results reported in this section are also including the thermo-physical properties of the geopolymeric matrix and the LWA as well as the macrostructural and microstructural observations analysis of the geopolymers before and after exposing to elevated temperatures.

#### **4.3.1 Effect of Elevated Temperatures on the Thermal Behavior of the FA Geopolymer paste, Mortar and LWAGC**

This section presents the thermal behavior evaluation of the FA geopolymer paste, mortar and LWAGC after exposing to elevated temperatures of 400 °C, 600 °C and 800 °C as described earlier in Chapter 3, section 3.10.1. Furthermore, the thermal behavior of the geopolymers are compared to the unexposed FA geopolymer paste, mortar and LWAGC mechanical and physical properties which have been already reported in section 4.2.3.1 with addition to macro/microstructural observation comparisons.

Figure 4.20 shows the initial compressive strength of the unexposed FA geopolymer paste, mortar and LWAGC specimens and their residual strength after exposed to the

elevated temperatures of 400 °C, 600 °C and 800 °C. It can be observed that the compressive strength of all geopolymers decreases as the elevated temperatures increases. The geopolymer paste undergoes the highest rate of strength loss with increasing the elevated temperature. Whereas, the LWAGC shows the lowest rate of strength loss compared to other geopolymer paste and mortar.

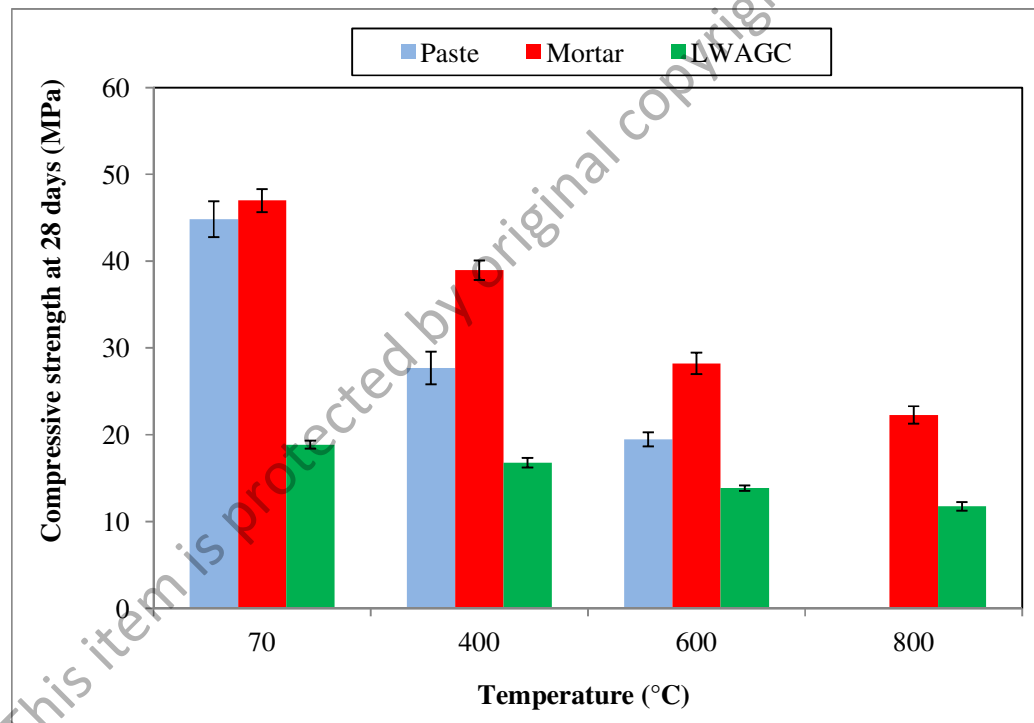


Figure 4.20: Initial strength data of the unexposed geopolymers and the residual strength of geopolymers after exposed to the elevated temperatures 400 °C, 600 °C and 800 °C.

Table 4.11 shows the strength loss of the FA geopolymers paste, mortar and LWAGC after being exposed to each elevated temperatures. It can be observed that the geopolymer paste possesses the highest strength loss at 400 °C and 600 °C. Further, the geopolymer paste lost its strength (failed) after exposure to elevated temperatures of 800 °C. Nevertheless, Kong & Sanjayan, (2010) reported that the FA geopolymer paste has superior fire resistance over an equivalent OPC paste system which lost its strength at

temperature of 400 °C (presented in Chapter 2, section 2.9.4, Figure 2.15). In addition, the geopolymer paste of their study showed a 73.4% of strength loss at 800 °C, unlike the thermal performance of the geopolymer paste in this work which lost its strength at temperature range of 600 °C to 800 °C. This is attributed to the highest alkaline activator liquid content adopted in the geopolymer paste preparation in this study which is the foremost responsible for the thermal performance differences as it will be discussed later on.

Table 4.11: Strength loss of the geopolymers after exposure to elevated temperatures.

<b>Temp.</b> (°C)	<b>Strength loss (%)</b>		
	<b>Paste</b>	<b>Mortar</b>	<b>LWAGC</b>
400	37.8	16.7	13
600	56.5	38.6	26.7
800	100	52.3	39

Moreover, the thermal performance of the geopolymer mortar and LWAGC at elevated temperature of 800 °C are much better than the geopolymer paste. The geopolymer mortar and LWAGC maintained residual compressive strengths at 800 °C of 22.07 and 11.93 MPa as shown in Figure 4.20, respectively, recording a strength loss of 52.3 % and 39 %, respectively, as illustrated in Table 4.11. These results indicated that the inclusion of the aggregates (fine or fine + LWA) substantially enhanced the performance of the FA geopolymers at the elevated temperatures. It can be seen that the LWAGC undergoes the minimum strength loss at all elevated temperatures.

In general, the loss in compressive strength with increasing the elevated temperature is attributed to the substantial increase in the thermal shrinkage resulting from the structural water evaporation from the geopolymer structure (Davidovits, 2008). The water in the geopolymer structure is transformed to vapor when the geopolymer is heated, and its pressure increases continuously with increasing the elevated temperature beyond 100 °C. When the water vapor pressure reaches the maximum limit, the dense matrix with less permeability would be unable of restrain the high thermal stresses, results in intensive thermal cracks on the specimen surfaces due to the thermal shrinkage and this phenomenon is called the vapor effect (Hu et al., 2009). The thermal behavior and strength loss characteristics of the geopolymeric materials are discussed in details below.

#### **4.3.1.1 Thermo-Physical Properties of the Geopolymer Paste**

For better understanding to the effect of the high temperature environment on the properties of the FA geopolymeric materials and the results reported in section 4.3.1, it is likely to investigate elevated temperature effect on the FA geopolymer paste as it is the cementitious material (binder) used for making the geopolymer mortars and LWAGCs.

As mentioned in Chapter 2, section 2.9.4, that the geopolymeric materials contains three types of water of the physically bonded water or free water, the chemically bounded water and the hydroxyl groups OH. Each type of this mentioned water evaporates at a specific range of temperatures when the geopolymeric material is heated at temperatures above 100 °C (Davidovits, 2008). The evaporation of water from the

geopolymer structure is associated with mass loss that could cause the formation of cracks due to the thermal shrinkage.

Figures 4.21 and 4.22 represent the thermogravimetric analysis (TGA) and the derivative thermogravimetric analysis (DTG) curves for the geopolymer paste, respectively. These tests used for measuring the mass loss as a function of temperature from 25 °C to 800 °C, and the details of these tests are mentioned in Chapter 3, section 3.11.4. The TGA/DTG curves illustrate a sharp decrease in mass before 150 °C which is attributed to the evaporation of both the free water and part of the chemically bonded water from the geopolymer. The sharp mass loss before 150 °C indicates that the free water contributed about 55 % to 60 % of the total water content in the geopolymer structure, which evaporates before 100 °C. Furthermore, the mass loss rate stabilizes after 150 °C up to 780 °C, which is attributed to the evaporation of both chemically bonded water and hydroxyl groups OH. Consequently, no mass loss was detected between 780 °C to 800 °C and the average of the mass remaining after the geopolymer being heated to 800 °C was about 79.8%.

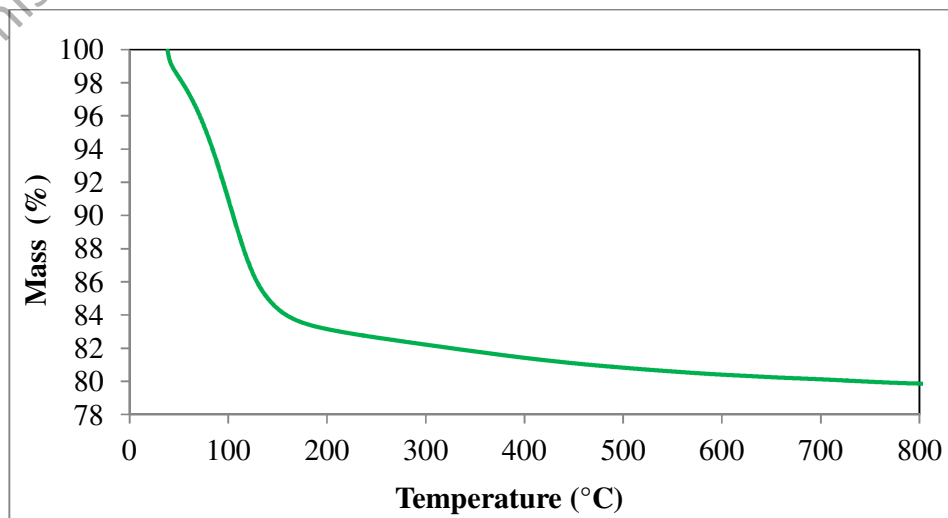


Figure 4.21: TGA curve of the unexposed FA geopolymer paste.

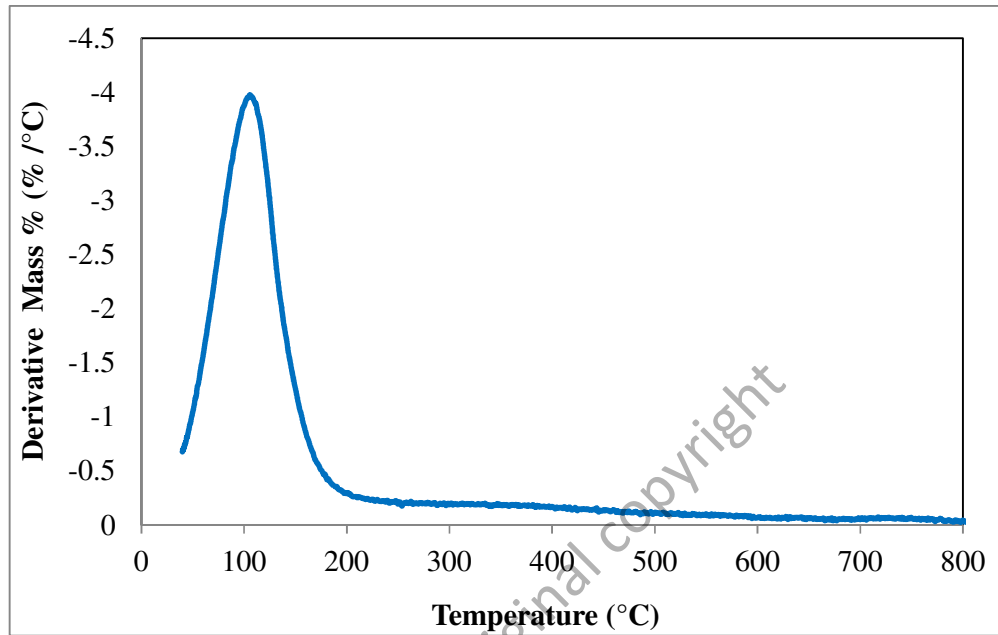


Figure 4.22: DTG curve of the unexposed FA geopolymer.

Moreover, Figure 4.23 illustrates the differential thermal analysis (DTA) thermogram of the geopolymer paste showing an endothermic phase between 25 °C to 220 °C which is attributed to the evaporation of the free water and part of the chemically bonded water from the geopolymeric structure. Davidovits (2008) estimated that the evaporation of the free water is not the cause of the damaging stresses except a very small shrinkage, although the free water contributes about 60 % of the total water content in the geopolymer structure. However, the remaining 40 % of the water content evaporation is contributing about 90 % of the total shrinkage at high temperatures. Therefore, the small intensity and broad exothermic phase in the DTA curve in the temperature range of 220 °C to 700 °C is detected due to the partial and gradual destruction of the geopolymer matrix as a result of the liberation of the residual water. Thus, the 90 % of the total shrinkage in the geopolymer paste occurs in the temperature range of 220 °C to 700 °C.

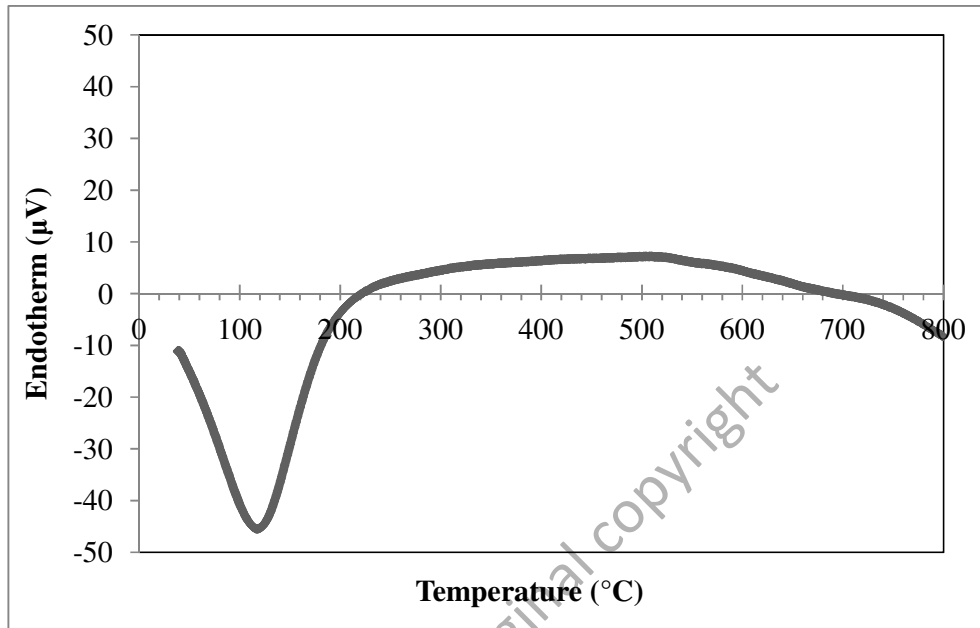


Figure 4.23: DTA curve of the FA geopolymer.

Furthermore, an endothermic phase is detected at the range of 700 °C to 800 °C, which associated with minimal mass loss observed in the TGA/DTG data of Figures 4.21 and 4.22. The existing of this endothermic phase is believed to be as a result of the viscous sintering process of the high silicate secondary phases that caused extreme densification to the geopolymer paste at 700 °C to 800 °C when high content of these phases existed in the geopolymeric gel (Provis et al., 2009; Rickard et al., 2012). This extreme expansion is the reason of the geopolymer paste failure when it is exposed to 800 °C (Figure 4.20 and Table 4.11) as will be discussed further in the next sections.

Figure 4.24 is presenting the thermal expansion of the geopolymer paste at the temperatures between 20 °C and 800 °C obtained by dilatometry analysis mentioned in Chapter 3, section 3.11.5. A Slight expansion is observed in the geopolymer paste as the temperature increased from 70 °C to 100 °C. Subsequently, the paste then undergoes a sharp thermal shrinkage occurred in the range of temperatures of 100 °C to 700 °C. This shrinkage is related to the evaporation of the structural water as

previously detected by the TGA curve shown in Figure 4.21. Furthermore, a significant expansion has been detected in the geopolymer paste instead of the shrinkage experienced earlier in the range of temperatures of 700 °C to 800 °C. It is likely that a portion of the activating solution remained unreached or partially reacted during the geopolymer formation (Rickard et al., 2012). These residual silicates experienced a thermal expansion at the range of 700 °C to 800 °C due to the swelling of the high silicate secondary phases as described by Provis et al. (2009). Therefore, the geopolymer paste exposed to the elevated temperature of 800 °C fail to return any residual strength as shown in Figure 4.20, due to the extremely swelling.

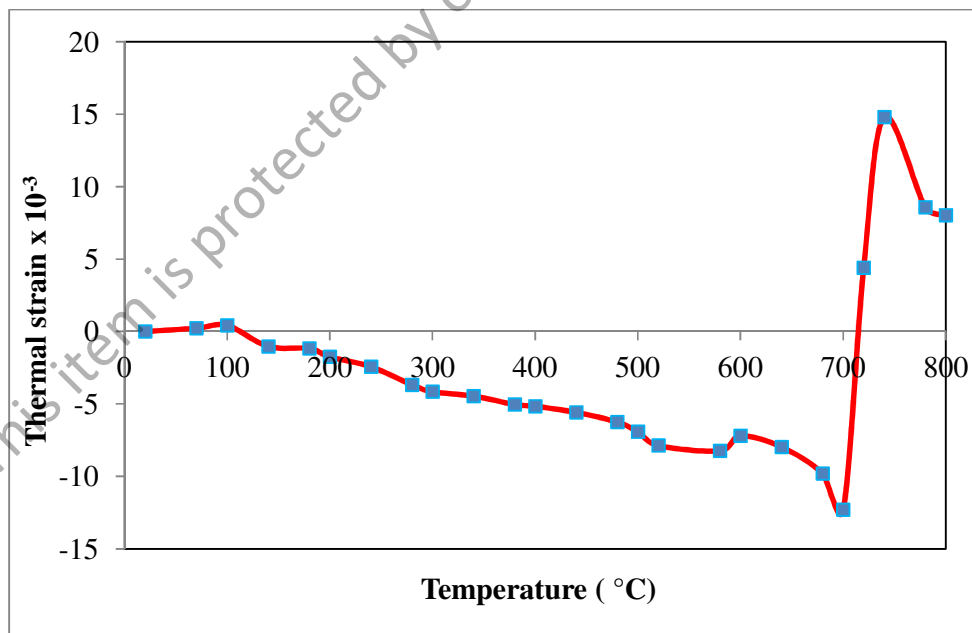


Figure 4.24: Thermal expansion of the unexposed geopolymer paste.

Comparing the thermal behavior of FA geopolymer paste material with an OPC paste system subjected to heat up to 800 °C shows some similarity especially in trend of loss the structural water in vapor form at temperatures higher than 100 °C. However, the OPC paste system does not experience any sintering or swelling processes in its

essential phase composition which consists mainly of calcium silicate hydrate (C-S-H) gel when exposing to elevated temperature up to 800 °C. Instead, the OPC paste systems undergoes from dehydration of the interlayer C-S-H water at 105 °C and dehydroxylation process resulted from the breakdown of  $\text{Ca}(\text{OH})_2$  into  $\text{CaO}$  and  $\text{H}_2\text{O}$  at about 400 °C to 500 °C (Guerrieri et al. 2010; Khaliq & Kodur, 2011). Consequently, the dehydration process is continued beyond 500 °C although the complete decomposition of the C-S-H phase is require a temperature higher than 800 °C of about 900 °C ( Mehta & Monteiro, 2006).

#### **4.3.1.2 Physical Observation of the Exposed FA Geopolymer Paste, Mortar and LWAGC to the Elevated Temperatures**

Figure 4.25 illustrates photographs showing the physical observation of the unexposed and exposed FA geopolymer pastes to the elevated temperatures of 400 °C, 600 °C and 800 °C. It can be seen that the thermal cracks distribution and width appearing on the specimen's surfaces are developed with increasing the elevated temperatures from 400 °C up to 800 °C. It is also observed that the color of specimens exposed to elevated temperatures of 400 °C and 600 °C has been changed and converts to light gray. This is attributed to the oxidation changes in the  $\text{Fe}_2\text{O}_3$  of the FA as reported by Temuujin & van Riessen (2009). Nevertheless, the specimens exposed to 600 °C keep their original dimension despite the thermal shrinkage at this temperature and they are able to maintain about 44.5% of their original strength. Furthermore, the deterioration in the geopolymers paste structure increases seriously as the specimen exposed to elevated temperature of 800 °C. The dense matrix of the geopolymer paste swelled producing extensive superficial and internal cracks visually observed through

the specimens as seen in Figure 4.25. The sharp swelling and extensive cracks lead to change the specimen's size and shape; therefore, it is not possible to measure the compressive strength for the exposed geopolymer paste. In addition, it can be observed the specimens color is much altered to a brightly gray. These observations clearly demonstrate the effect of the high sintering and densification processes of the unreacted silicate portion discussed in Figure 4.23 when the geopolymer exposed to elevated temperature of 800 °C. Sintering and densification processes led to the structural failure with respect to the damages caused by the dehydration during heating.



Figure 4.25: Photographs of the unexposed and exposed FA geopolymer pastes to elevated temperatures of 400 °C, 600 °C and 800 °C.

Moreover, much higher heat resistance and thermal durability are observed for the exposed geopolymer mortars and LWAGCs compared with the geopolymer paste, especially when they exposed to highest elevated temperature of 800 °C. Figure 4.26 shows the geopolymer mortars appearance before and after exposing to the elevated temperatures of 400 °C, 600 °C and 800 °C, respectively. Comparison the physical observation of the exposed geopolymer paste and mortar to elevated temperature of 800 °C (Figures 4.25 and 4.26) shows that the geopolymer mortar experienced significantly less thermal cracks and it is able to maintain its original dimension as well. This is attributed to the sand particles incorporated in the geopolymeric matrix which increased the thermal conductivity and decreased the specific heat of the resulted mortar structure (Xu & Chung, 2000).



Figure 4.26: Photographs of the unexposed and exposed FA geopolymer mortars to elevated temperatures of 400 °C, 600 °C and 800 °C.

Accordingly, as the thermal conductivity increases, the thermal stresses in the mortar structure would decrease due to the reduction of the temperature gradient. In addition, decreasing the specific heat of the geopolymer mortar would constrain the swelling of the unreacted silicate secondary phase. Hence, the geopolymer mortar specimens show better thermal durability and lower strength loss compared to the geopolymer paste at all elevated temperatures as it can be observed in Figure 4.20 and Table 4.11.

Figure 4.27 shows the unexposed and exposed LWAGCs to elevated temperatures of 400 °C, 600 °C and 800 °C, respectively. It can be observed that the minimum deterioration in the appearances of the geopolymers exposed to the elevated temperatures is for the LWAGCs. Apart from decolorization which is similarly experienced by the geopolymer paste and mortar, the LWAGC does not show any spalling or visible swelling. In addition, the concrete shape and size appear to be unaffected by the high temperature environment. This is suggested that the incorporation of the LWAs to the geopolymeric structure enhance the fire resistance of the geopolymer system. This can be attributed to the microstructure and the physical properties of the LWAs which are characteristics of high pores and voids content as illustrated in Figure 4.12, section 4.2.3.1. These micro-pores and voids reduce the thermal conductivity of the aggregate significantly, which in turn decreases the thermal conductivity of the LWAGC as the LWAs occupied about 75% of the LWAGC volume. Thus, the heat diffusion into the LWAGC specimen's core would be much less than the heat diffusion that the geopolymer paste and mortar experiences (Sancak et al. 2008). Decreasing the heat diffusion into the LWAGC effects, firstly, on reducing the evaporation of the structural water and thermal shrinkage due to restrain the mass loss at high temperatures. Secondly and most significantly, the rate of sintering and

densification processes occur in the temperature range of 700-800 °C is also decreased as the heat diffusion through the LWAGC structure decreased.



Figure 4.27: Photographs of the unexposed and exposed LWAGCs to elevated temperatures of 400 °C, 600 °C and 800 °C.

Furthermore, the high porosity of the LWAGC structure that is resulted from the incorporation of porous LWAs provides channels inside the concrete to facilitate the dispersion of the water vapor from the structure at high temperatures. Therefore, the LWAGC structure experienced the lowest damage in the physical and mechanical properties when exposed to elevated temperatures than the paste and mortar.

### **4.3.1.3 Microstructural Analysis of the Exposed FA Geopolymer Paste and LWAGC to the Elevated Temperatures**

This section presents the microstructure analysis conducted to the FA geopolymer paste and LWAGC before and after exposure to elevated temperatures 400 °C, 600 °C and 800 °C.

#### **4.3.1.3.1 Microstructural Analysis of the Exposed FA Geopolymer Paste to the Elevated Temperatures**

SEM micrographs for the geopolymers paste, samples before and after exposing to the elevated temperatures of 400 °C, 600 °C and 800 °C are summarized in Figure 4.28. The unexposed geopolymer paste shows typical microstructure of dense and homogeneous matrix consisting mainly from aluminosilicate gel (Si/Al molar ratio = 2.89) resulted from the geopolymerization process as indicated by the EDS test presented in Figure 4.29. The micrograph shows the absence of the unreacted fly ash microspheres portion which implies that the adoption of high Activator/FA ratio result in high activation to the FA, thus high geopolymeric products (Duxson et al., 2007a). In addition, the dense matrix contains small microcracks resulting from the evaporation of water during curing and aging processes exist with little quantities of bright crystals.

However, the initial matrix formed at 70 °C, deteriorates as it is exposed to the elevated temperatures. Figure 4.28 presents the SEM micrograph of the geopolymer paste exposed to 400 °C shows the development in the microcracks width due to the high water evaporation rate from the dense structure. Further, the evaporated water leaves micro-pores in the matrix which are responsible for the strength declination observed in

the compressive strength measurements. It can be seen that exposing the geopolymer to 400 °C increases the content of the bright crystals that distributed on the microcracks and pores. In addition, the EDS test of this sample given in Figure 4.30 illustrates an increasing in the molar ratio of Si/Al to 3.68 as the geopolymer paste exposed to 400 °C. Moreover, Figure 4.32 shows that the geopolymer paste exposed to 600 °C undergoes higher deterioration in the microstructure due to increasing in the microcracks dimensions and crystals content.

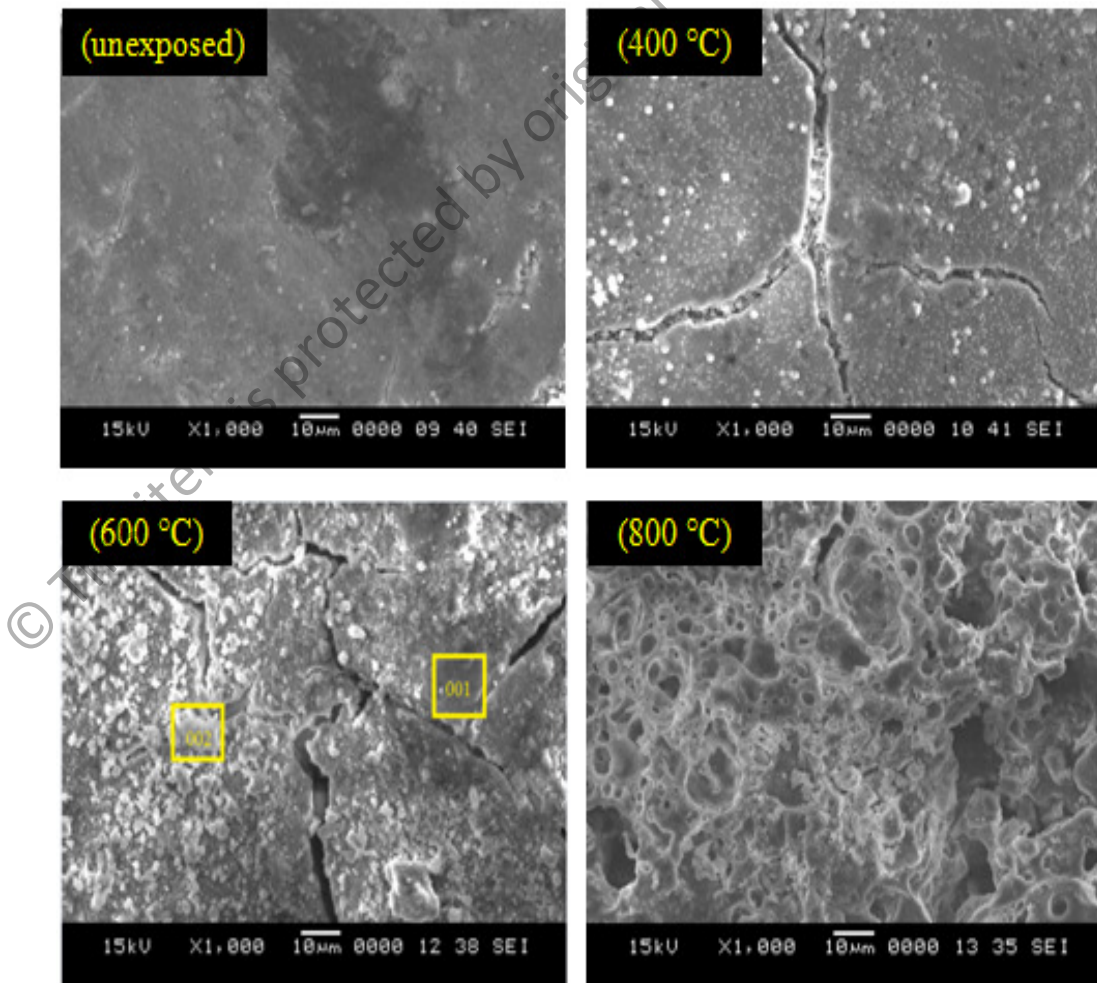


Figure 4.28: SEM micrographs of unexposed and exposed FA geopolymer paste to elevated temperatures 400 °C, 600 °C and 800 °C.

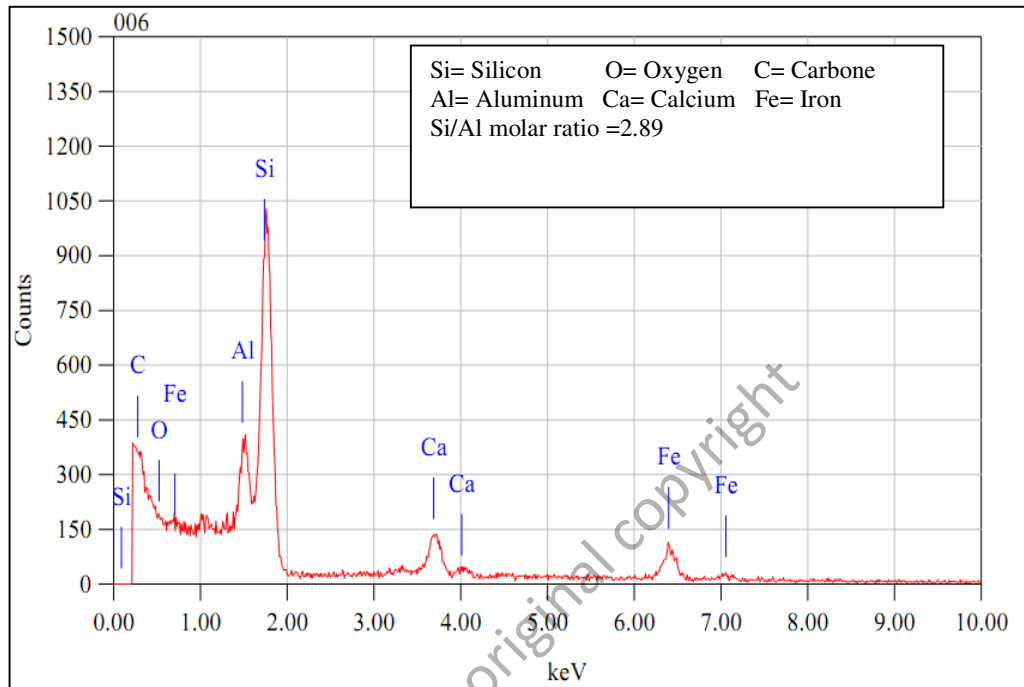


Figure 4.29: EDS analysis of the unexposed geopolymeric paste gel of Figure 4.28.

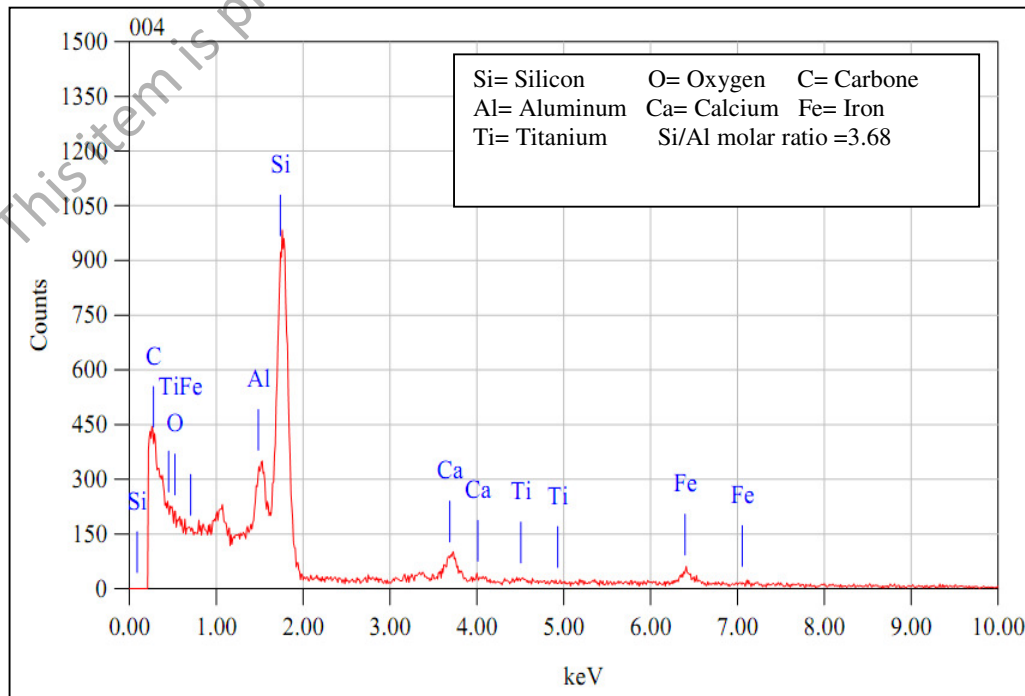


Figure 4.30: EDS analysis of the exposed geopolymer paste to 400 °C of Figure 4.28.

Consistently, Figures 4.31 and 4.32 represent the EDS spot analyses of the geopolymeric gel matrix (zone 001) and crystal particles (zone 002) exist in the SEM micrograph of the geopolymer paste exposed to 600 °C (Figure 4.28), respectively. From these Figures it is observed that the geopolymeric gel consists of high silicate phase (Si/Al molar ratio of 3.60) and the crystals composed mainly from high silicate portion having Si/Al molar ratio of 6.5. This silicate portion mentioned earlier in the dilatometrical analysis shown in section 4.3.1.1, Figure 4.24, is believed to be the responsible for the densification and sintering processes occurs in the geopolymer paste while exposing to 800 °C.

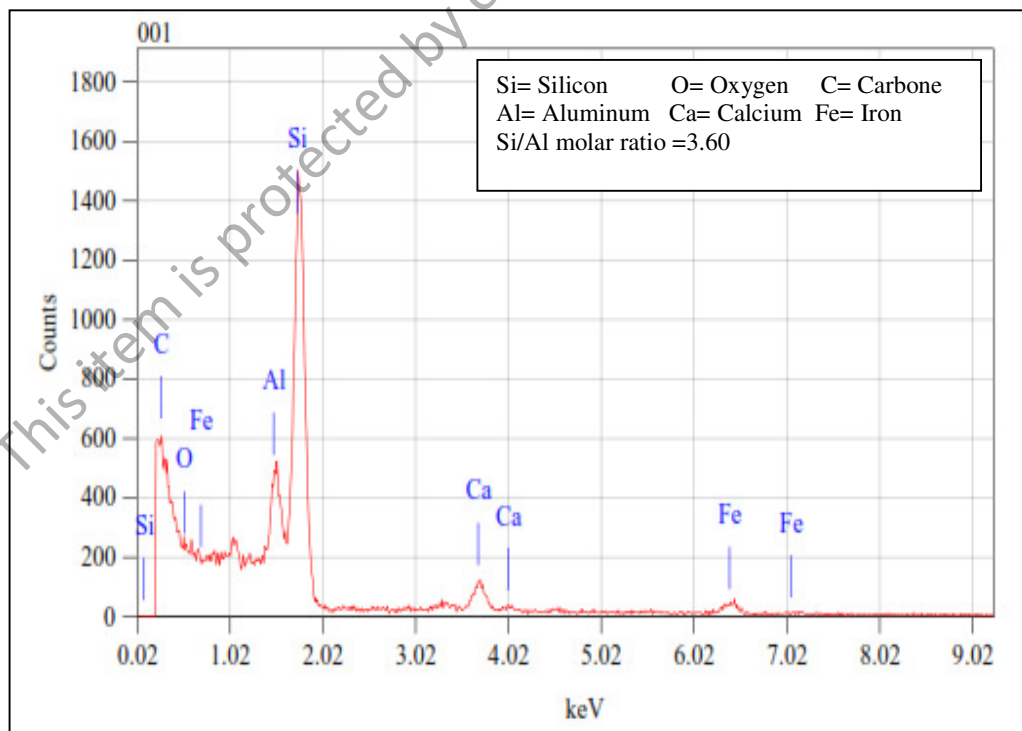


Figure 4.31: EDS analysis of geopolymeric gel zone (001) of the exposed geopolymer paste to 600 °C of Figure 4.28.

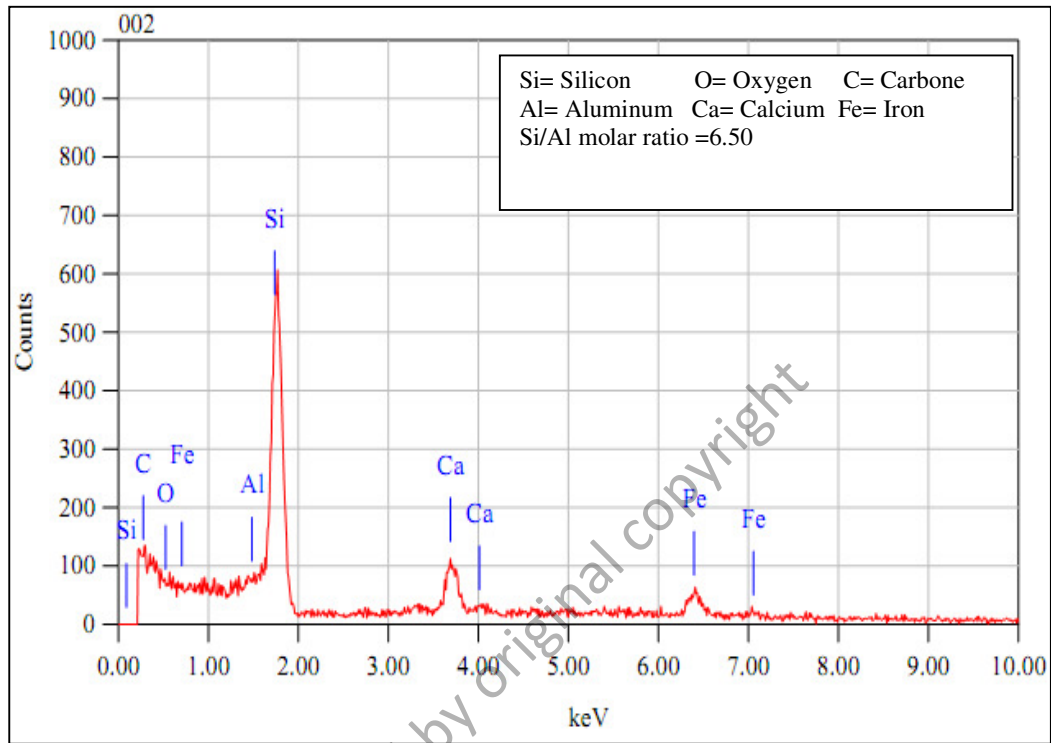


Figure 4.32: EDS spot analysis of the crystal particles zone (002) of the exposed geopolymer paste to 600 °C of Figure 4.28.

Correspondingly, Figure 4.28 indicates that the SEM micrograph of the geopolymer paste exposed to 800 °C shows severe deterioration in the microstructure appearance by the obvious destruction of the homogeneous aluminosilicate gel matrix formed at 70 °C.

Furthermore, the EDS analysis given in Figure 4.33 shows that the molar ratio of Si/Al is dramatically decreased to 1.43 as compared to the initial Si/Al ratio of 2.89 (Figure 4.29).

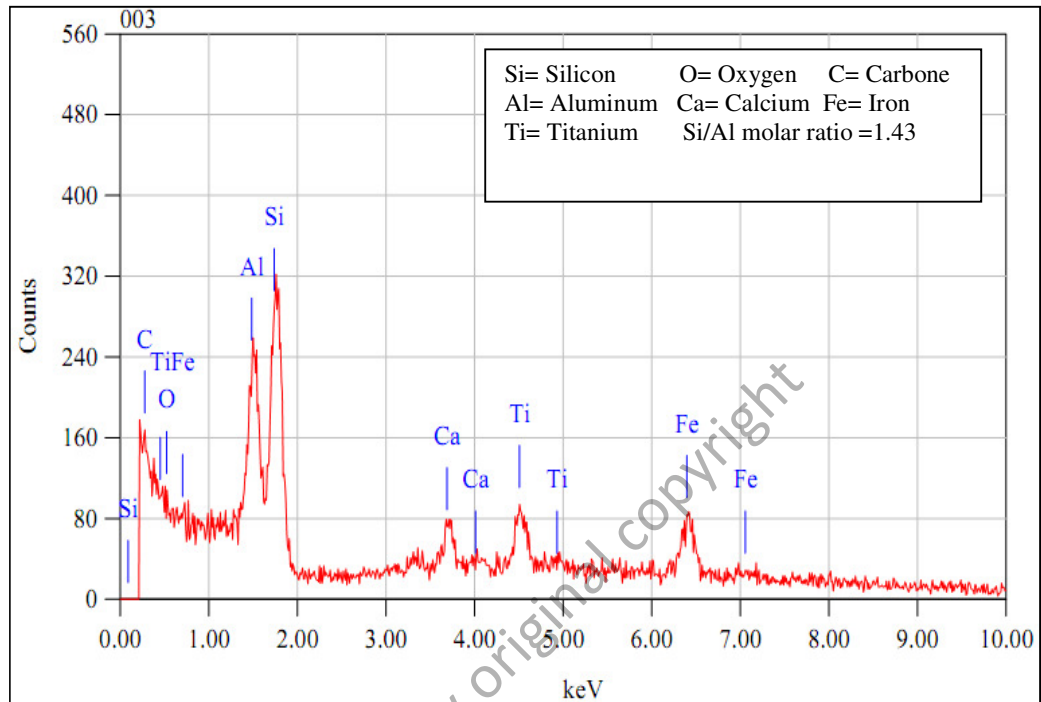


Figure 4.33: EDS analysis of the exposed geopolymer paste to 800 °C of Figure 4.28.

Moreover, Figures 4.34 to 4.36 shows the XRD diffractograms of the FA geopolymer pastes exposed to elevated temperatures 400 °C, 600 °C and 800 °C versus the XRD pattern of the unexposed FA geopolymers paste, respectively. The phase composition of the unexposed geopolymer paste shows a typical amorphous to semi-crystalline composition reflecting its source FA by having the same crystalline phases of quartz ( $\text{SiO}_2/\text{Q}$ ), mullite ( $\text{Al}_6\text{Si}_2\text{O}_{13}/\text{M}$ ), magnetite ( $\text{Fe}+2\text{Fe}_2+3\text{O}_2/\text{Ma}$ ), hematite ( $\text{Fe}_2\text{O}_3/\text{H}$ ), wollastonite ( $\text{CaSiO}_3/\text{W}$ ), Aegirine [ $\text{NaFe}+3(\text{SiO}_3)_2/\text{A}$ ], calcium iron silicate ( $\text{CaFe}_3\text{O}_5/\text{C}$ ) and hercynite ( $\text{Fe}+2\text{Al}_2\text{O}_4/\text{He}$ ). The highest crystalline phases in the FA are due to the highest iron and calcium contents in its composition as Table 4.1 illustrated. The XRD pattern also has a broad hump, characteristic of an amorphous component. In addition, the phase composition of the unexposed geopolymers paste contains some zeolitic phases of hydroxysodalite ( $\text{Na}_4\text{Al}_3\text{Si}_3\text{O}_{12}\text{OH}$ ) and herschelite ( $\text{NaAl-Si}_2\text{O}_6\cdot 3\text{H}_2\text{O}$ ) which are difficult to be sited at the XRD pattern as they have low

peak intensity and excessive peaks overlapping with other phases. These zeolitic phases are reported to be resultant from the geopolymerization reaction (Bakharev, 2006).

Furthermore, after exposing to elevated temperatures of 400 °C, 600 °C and 800 °C the crystalline phase compositions are subjected to mild to significant changes comparing with unexposed patterns. Figures 4.34 and 4.35 are illustrating the XRD pattern of the exposed geopolymer pastes to elevated temperatures of 400 °C and 600 °C, respectively, shows some changes in the crystalline phase of increasing the iron oxides contents and peaks intensities. Other formed phases of tridymite ( $\text{SiO}_2/\text{T}$ ) and sodium silicate ( $\text{Na}_2\text{Si}_2\text{O}_5/\#$ ) are detected especially at the exposed geopolymer pastes to elevated temperatures of 600 °C (Figure 4.35). It is observed that the mullite and quartz peaks intensities are reduced after firing similarly to the observations reported by Rickard et al. (2012), though, the fired samples at 400 and 600 °C are retained their characteristics amorphous hump and the major geopolymeric material XRD typical pattern features. This is suggesting that the geopolymers at these elevated temperatures are experiencing iron oxides phase changes and crystallization of the excess alkaline activator species as well as to destruction of the zeolitic phases which are composed of high silicate content. It is expected that these crystallized phases were detected in form of white crystals in the SEM investigations of Figure 4.28.

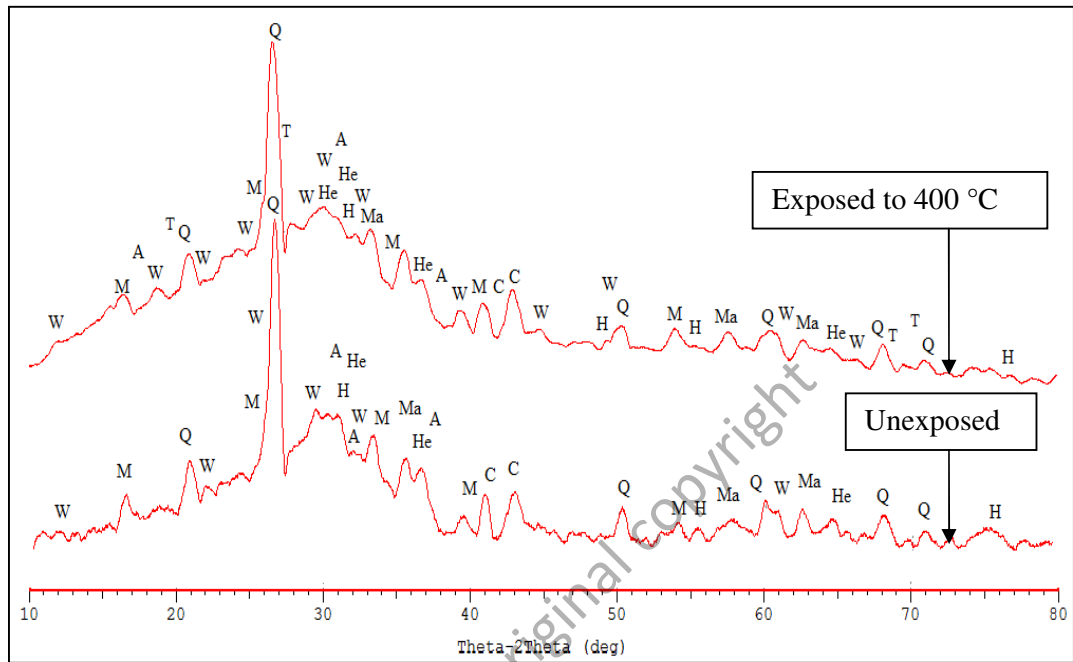


Figure 4.34: XRD diffraction patterns of the unexposed and exposed geopolymer paste to 400 °C. (All peaks symbols are defined in the main text).

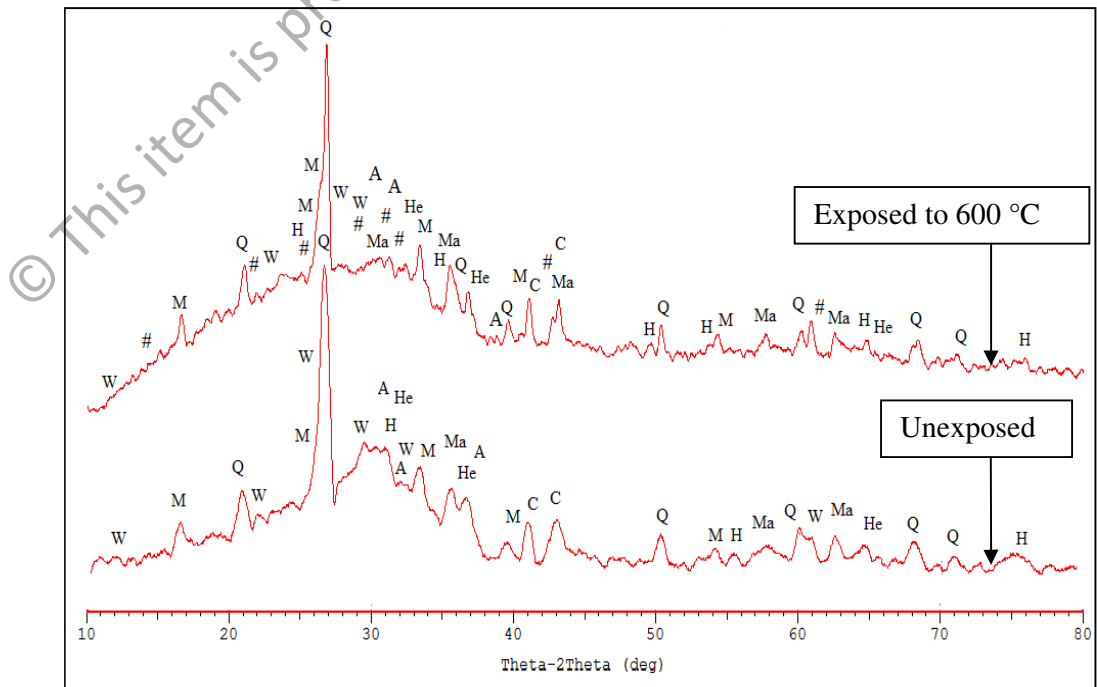


Figure 4.35: XRD diffraction patterns of the unexposed and exposed geopolymer paste to 600 °C. (All peaks symbols are defined in the main text).

Additionally, Figure 4.36 shows the significant changes in the phase composition of geopolymer paste as exposed to elevated temperatures 800 °C. Sodium based feldspars phases of nepheline ( $\text{NaAlSi}_3\text{O}_8/\text{N}$ ) and sodium aluminum silicate ( $\text{NaAlSi}_2\text{O}_6/\text{S}$ ) are formed in high peaks intensities with the presence of other original crystalline phases of the unexposed sample. The formed phases of nepheline and tridymite are known in improving the thermal resistance of the geopolymers due to their high melting point of 1257 °C and 1670 °C, respectively (Rickard et al., 2012). It is believed that the bulk of the crystallization observed in this sample derives from the free Na, Si and Al species after the decomposition of the amorphous geopolymeric gel matrix contains high unreacted or partially reacted aluminosilicate species which swelled at temperatures ranged of 600 °C to 800 °C. This is supported by the significant reduction and deterioration in the amorphous hump existed in the unexposed sample after exposing to 800 °C as well as to the white crystals composed of high silicate content detected in the SEM and EDS tests showed in Figures 4.28 and 4.32, respectively. These findings are explaining the FA geopolymer paste specimen fail in return any strength after exposing to 800 °C. Such reduction in the amorphous hump of fired FA geopolymer paste at 800 °C was not reported by other phase studies of the fired FA geopolymer pastes to elevated temperatures of 800 °C to 1000 °C (Rickard et al., 2012; Bakharev, 2006; Rashad & Zeedan, 2011). This is due to the highest alkaline activator content used in the preparation of the FA geopolymer specimen of this study which led to form high content of unreacted aluminosilicate compounds.

In addition, the presented thermal behavior of geopolymer at the elevated temperatures indicates the significant effect of the Activator/FA ratio on the geopolymer performance at high temperature environments. Although, the high activator content produces high-reacted dense aluminosilicate gel matrix at 70 °C, it produces high

portion of unreacted silicate products which are significantly weaken the fire-resistance of the geopolymer at temperatures of 600 °C to 800 °C.

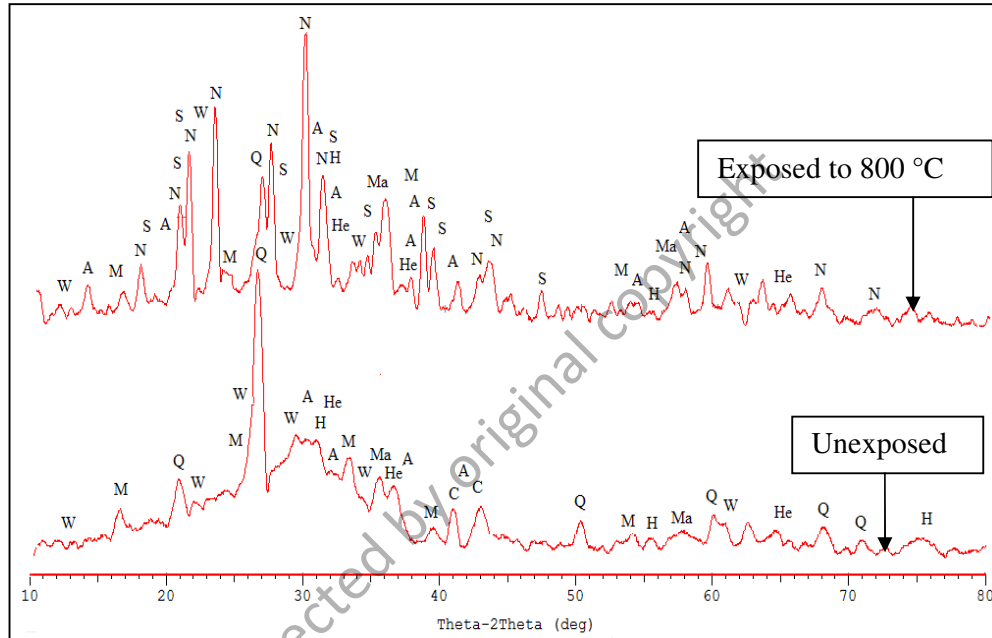


Figure 4.36: XRD diffraction patterns of the unexposed and exposed geopolymer paste to 800 °C. (All peaks symbols are defined in the main text).

#### 4.3.1.3.2 Microstructural Analysis of the Exposed LWAGC to the Elevated Temperatures

Figure 4.37 illustrates the SEM micrographs of the cured LWAGC at 70 °C (unexposed) as well as the exposed specimens to the elevated temperatures of 400 °C, 600 °C and 800 °C. For the unexposed LWAGC, it can be seen that the interface transition zone (ITZ) between the aggregate/mortar is indistinct in the LWAGCs microstructure. This is attributed to the porous nature of the LWAs surfaces which provides interlocking sites for the geopolymer mortar to form a better interfacial bond between aggregate/mortar at the ITZ (Mouli & Khelafi, 2008). Therefore, it can be seen

that the geopolymer mortar infiltrates the aggregate surface to a certain depth. This impregnation phenomenon has been also observed by other researchers (Ke et al., 2010; Topçu & Uygunoğlu, 2007).

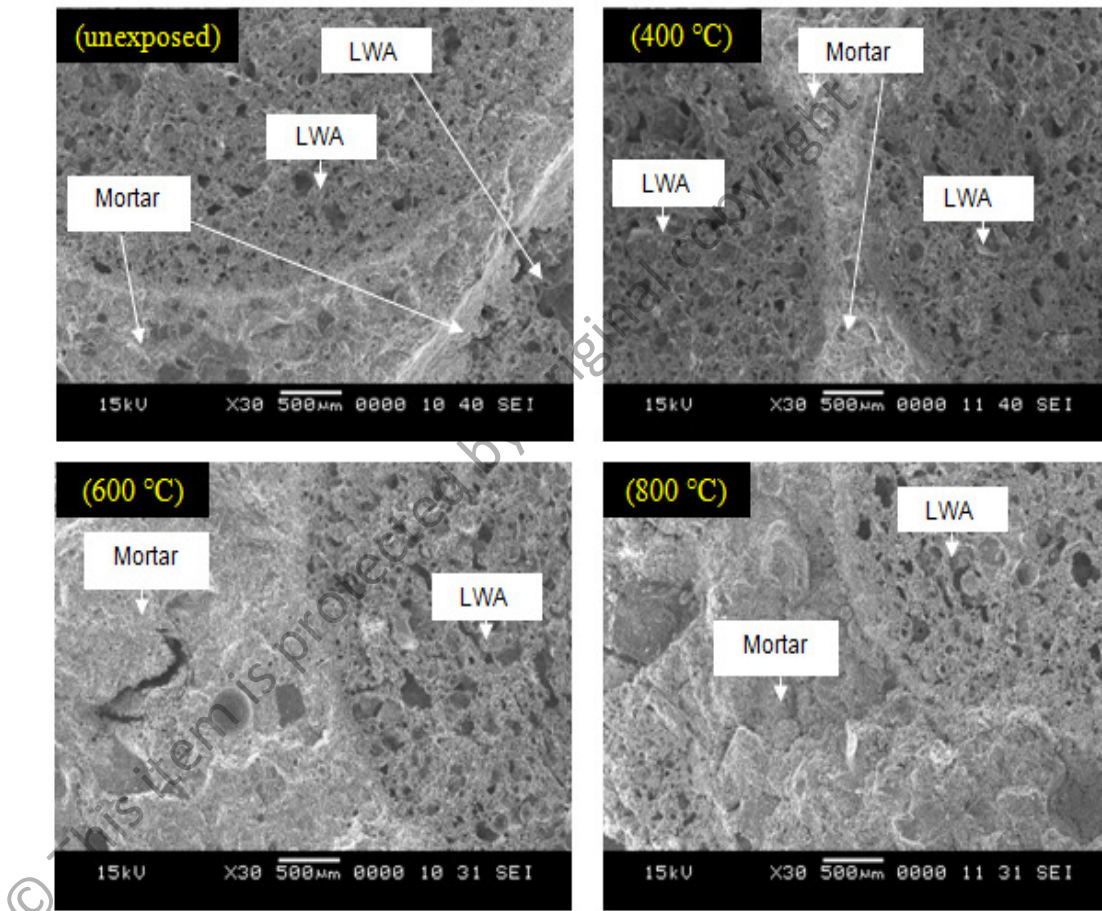


Figure 4.37: SEM micrographs of unexposed and exposed LWAGCs to elevated temperatures of 400 °C, 600 °C and 800 °C.

Furthermore, Figure 4.37 is also shows the microstructure of the LWAGC exposed to 400 °C. It can be seen that the microstructure appearance does not show much changes from the unexposed concrete and appears to be unaffected by the elevated temperature. This can explain the low strength deterioration obtained to the LWAGC when exposed to 400 °C as shown in Figure 4.20. On the other hand, the microstructure

of the LWAGC exposed to 600 °C shown in Figure 4.37, illustrates the deterioration in the geopolymer mortar due to the high dehydration of the structural water as well as the formation of microcracks in the ITZ. Furthermore, Figure 4.37 shows the swelling traces of the unreacted silicate phases in the aggregate/mortar bond zone for the LWAGC exposed to 800 °C as well as the high microcracks content in the aggregate/mortar bond zone.

#### **4.3.1.4.3 Thermal Expansion Behavior of the LWA**

Basically, as mentioned in Chapter 2, section 2.9.4, that the thermal shrinkage and the swelling of the unreacted silicate phase are not only the reasons behind the strength deterioration when the LWAGCs exposed to the elevated temperatures. The difference in the thermal expansion between the LWA and the geopolymer paste during heating up to each elevated temperature is also contributing significantly in the strength loss (Kong & Sangayan, 2010; Sancak et al., 2008; Andiç-Çakır & Hizal, 2012).

The thermal strain data for the adopted LWA for temperatures between 20 and 800 °C are represented in Figure 4.38 and they show that the LWA had a minimal thermal expansion up to 800 °C. The low thermal expansion of the LWA is attributed to their low coefficient of thermal expansion (CTE), since they were exposed to a pre-heating process at high temperature during their formation (Topçu & Uygunoğlu, 2007).

Accordingly, by comparing the thermal expansion behavior of the LWA and the geopolymer paste shown in Figure 4.24, the essential difference in the thermal expansion behavior can be distinguished. This difference in the thermal expansion behavior is also responsible for the strength loss when the LWAGC is exposed to the elevated temperatures. The mismatching in thermal expansion of the paste and the LWA

results in microcracks in the interface transition zone (ITZ) as it is observed in Figure 4.39 which representing a high magnification SEM micrograph for the ITZ of the LWAGC exposed to 800 °C. These microcracks declines the compressive strength significantly and this phenomenon known as ‘thermal inconsistency of the concrete ingredients’ (Topçu & Uygunoğlu, 2007; Sancak et al., 2008; Saad et al., 1996; Andiç-Çakır & Hizal, 2012). Nevertheless, the low CTE of the LWA results in low CTE for the resultant LWAGC which leads to experience low thermal expansion and low strength loss at elevated temperatures as the LWAs occupied about 75 % of the concrete volume.

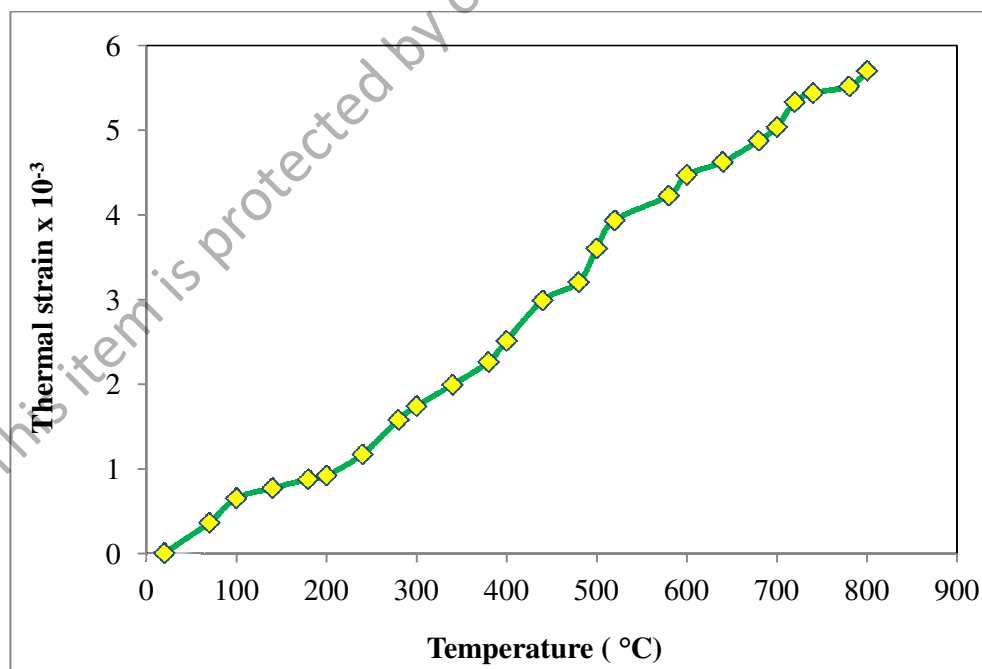


Figure 4.38: Thermal expansion of LAW.

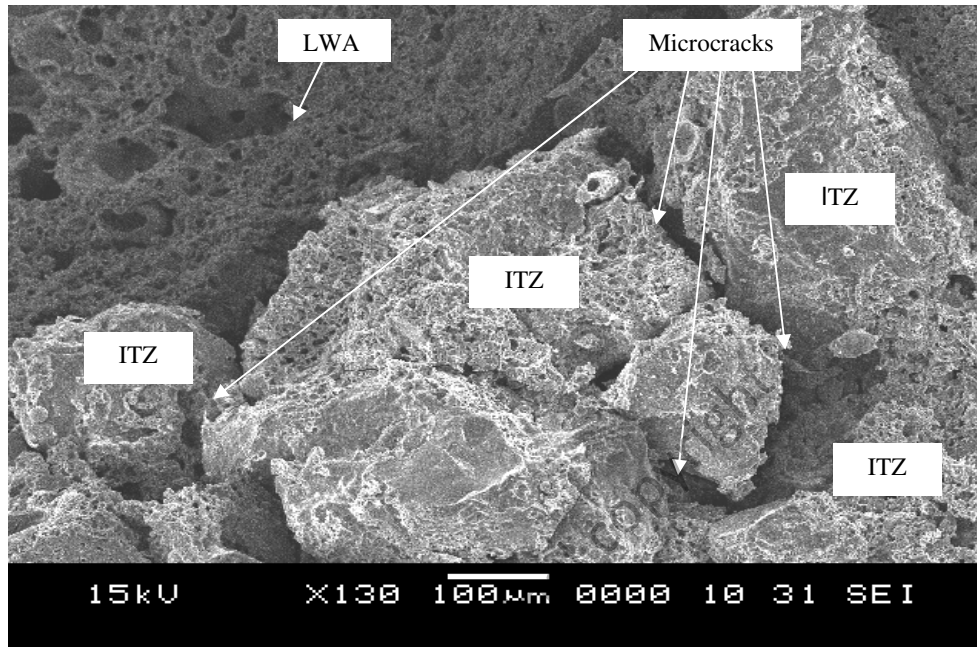


Figure 4.39: High magnification SEM micrograph for the ITZ of the LWAGC exposed to 800 °C.

#### 4.3.2 Effect of Elevated Temperatures of 100 °C to 800 °C on the Residual Strength of LWAGC

As mentioned in Chapter 3, section 3.11.2 that this experiment was carried out in order to statistically investigate the effect of the elevated temperatures ranged of 100 °C to 800 °C with increment of 100 °C on the residual strength of the LWAGC. The test procedure of this study is also presented in Chapter 3, section 3.11.2.1.

Figure 4.40 illustrates the residual compressive strength ( $f_c$ ) of the LWAGCs exposed to elevated temperatures ranged of 100 °C to 800 °C with an increment step of 100 °C. It can be seen that the compressive strength of the LWAGC increases after exposure to elevated temperatures of 100 °C to 300 °C. The LWAGCs exposed to elevated temperatures of 100, 200 and 300 °C attained relative residual compressive strengths of 103.54%, 105.83% and 108.32%, respectively, compared to the compressive strength of

the unexposed LWAGC of 18.86 MPa. The strength gaining of the exposed FA-based geopolymers to elevated temperatures of 100 °C to 300 °C has been already reported in previous investigations (Kong & Sanjayan, 2010; Rashad & Zeedan, 2011).

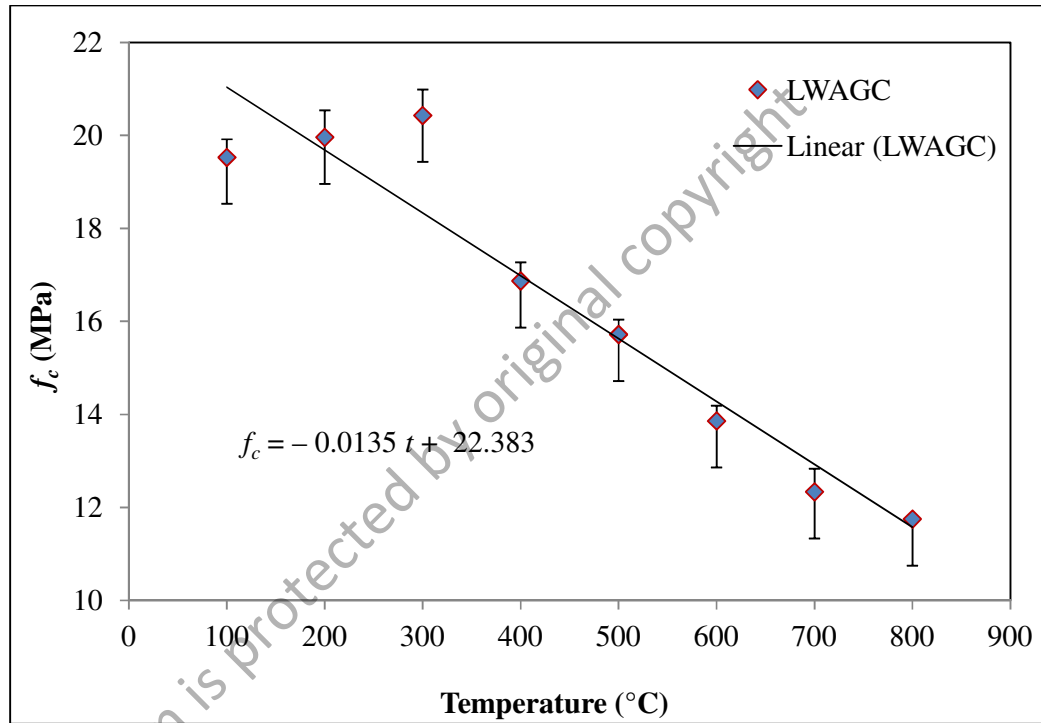


Figure 4.40: Residual compressive strength of the LWAGCs after being exposing to elevated temperatures of 100 °C to 800 °C.

Subsequently, the compressive strength of the LWAGC is observed to decrease gradually after being exposed to elevated temperatures of 400 °C and further up to 800 °C. The strength losses of 13%, 16.6%, 26.7%, 34.6% and 39 %, respectively, are recorded for the LWAGC after exposed to 400 °C, 500 °C, 600 °C, 700 °C and 800 °C, respectively. The loss in the compressive strength of the exposed LWAGC to elevated temperatures of 400 °C to 600 °C is attributed to the thermal shrinkage caused by the evaporation of the structural water and the difference in the thermal expansion between the paste and LWA as mentioned in section 4.3.1. Whereas, the strength loss of the

exposed LWAGC to elevated temperatures of 700 °C and 800 °C is attributed to the swelling of the unreacted or partially reacted silicate secondary phase as reported earlier in section 4.3.1. Furthermore, Figure 4.40 demonstrates the relationship between the exposure temperatures ranged from 100-800 °C and the residual compressive strength of LWAGC, based on the results of 24 LWAGC specimens exposed to elevated temperatures ranging of 100 °C to 800 °C with an increment step of 100 °C, which can be fitted as:

$$f_c = -0.0135 t + 22.383 \quad (4.1)$$

where  $f_c$  is the residual compressive strength (MPa);

$t$  is the exposure temperature (100 °C to 800 °C);

with fitting error of (1.1048).

### **4.3.3 Effect of LWA Particle Size and Grading on Residual Compressive Strength of the LWAGC**

This section is presenting an investigation on the effect of different LWA particle sizes and grinding of 4-5 mm, 4-8 mm, 5-8 mm, 8-12 mm, 8-16 mm and 12-16 mm on the thermal behavior of the LWAGCs (L4-5 , L4-8 , L5-8 , L8-12, L8-16 and L12-16) after exposed to elevated temperature of 800 °C. The preparation and test procedure details of this experiment are described earlier in Chapter 3, section 3.11.3. Furthermore, the resultant residual mechanical strengths of these LWAGCs after their exposure to elevated temperature of 800 °C are compared with the unexposed LWAGCs mechanical strengths which have been already reported in section 4.2.6.2.

Figure 4.41 illustrates the photographs of the exposed L4-5, L4-8, and L5-8 to elevated temperature of 800 °C. While, Figure 4.42 illustrates the photographs of the exposed, L8-12, L8-16 and L12-16 to similar elevated temperature. Comparing the physical observation of the exposed LWAGCs to elevated temperature of 800 °C with the unexposed LWAGCs shown in section 4.2.6.2, Figures 4.15 and 4.16, shows similar trend of color change after exposure to high temperature reported for the exposed FA geopolymers in section 4.3.1.

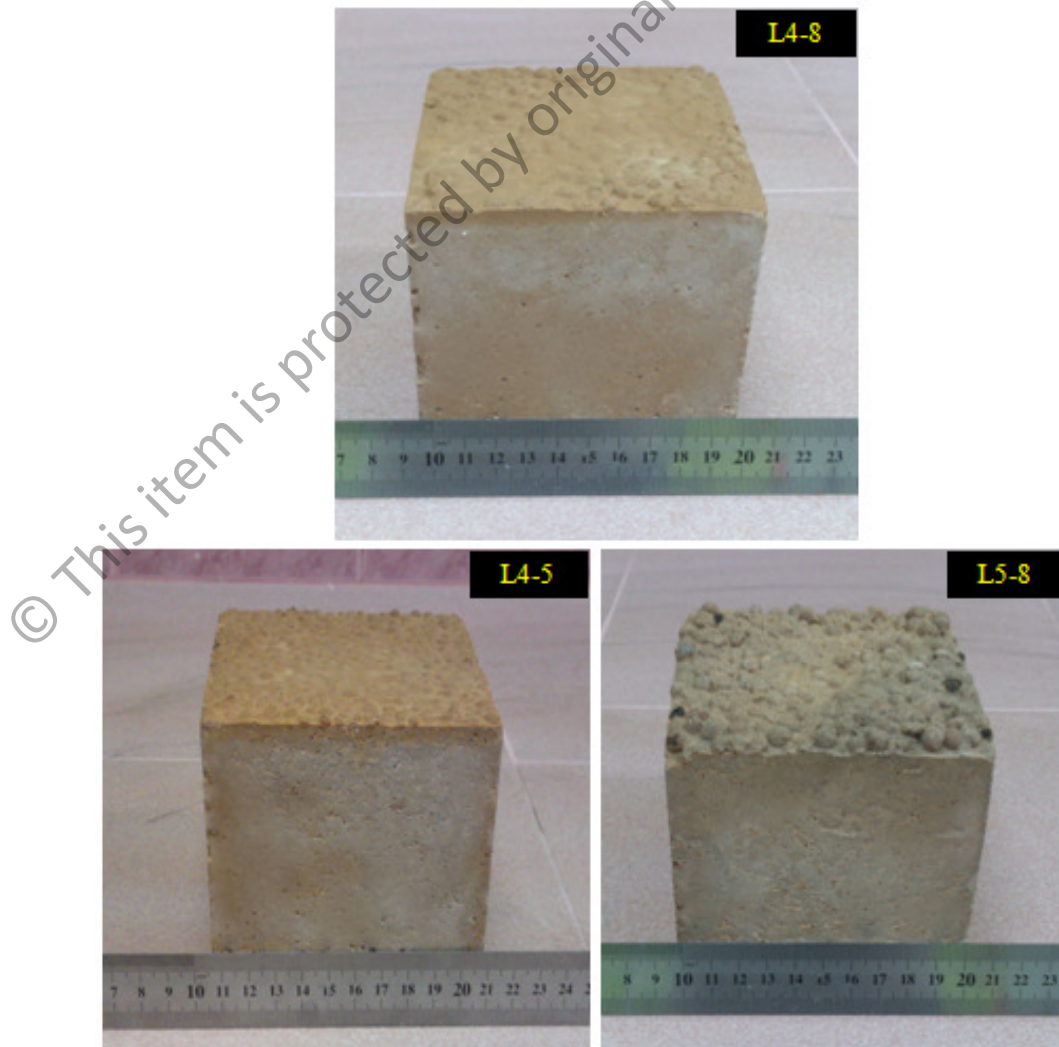


Figure 4.41: LWAGCs of L4-8, L4-5 and L5-8 prepared from the graded LWA batch 1 of 4-8 mm after exposed to 800 °C.



© Figure 4.42: LWAGCs of L8-16, L8-12 and L12-16 prepared from the graded LWA batch 2 of 8-16 mm after exposed to 800 °C.

Moreover, Figure 4.43 illustrates the mechanical residual strength results of the exposed LWAGCs to 800 °C. Comparing the residual strengths with the concretes initial strengths given in section 4.2.6.2, Figure 4.17, shows that the compressive strength of all LWAGCs decreased after the exposure to 800 °C. Consistently, it has been mentioned earlier in section 4.3.1, that this behavior is attributed to the thermal shrinkage caused by the evaporation of the structural water and the difference in the

thermal expansion behavior between the paste and LWA as well as to the swelling of the unreacted or partially reacted silicate secondary phase.

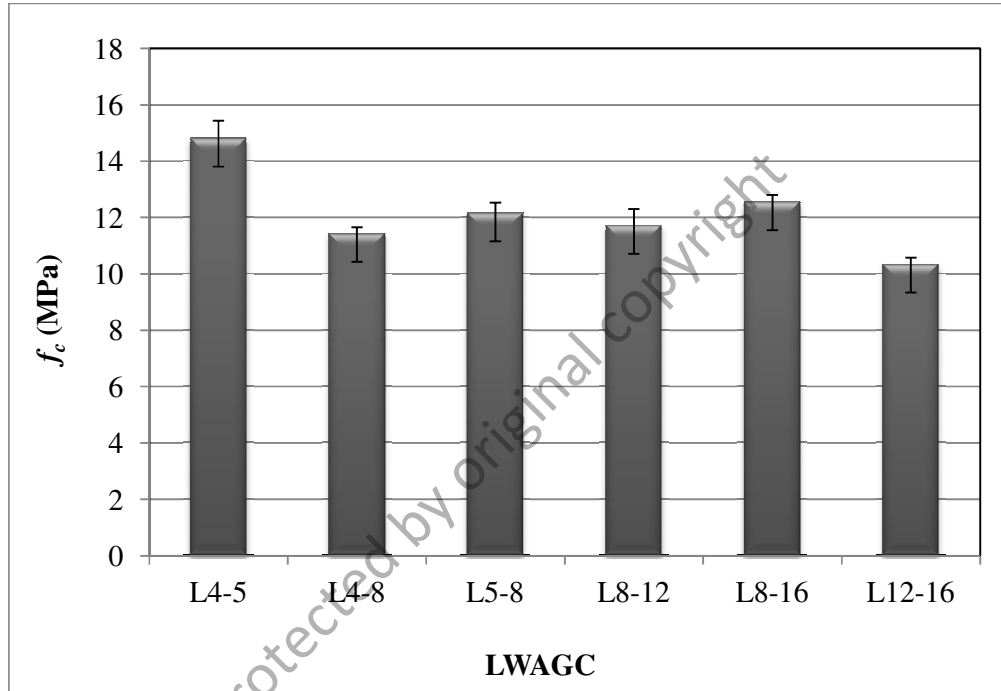


Figure 4.43: Residual compressive strength of the L4-5, L4-8, L5-8, L8-12, L8-16 and L12-16 after exposure to elevated temperature of 800 °C.

Nevertheless, the rates of the strength loss of the exposed LWAGCs to 800 °C are observed to be varied according to the concretes LWA sizes and grading as presented in Figure 4.44. For the original graded concretes of L4-8 and L8-16 prepared with the original graded LWAs of 4-8 mm and 8-16 mm, respectively, increasing of the minimum sizes of LWAs to 5-8 mm and 12-16 mm, respectively, the strength losses of the exposed L5-8 and L12-16 to 800 °C are decreased. While decreasing the maximum size of 8-16 mm LWA to 8-12 mm, the resultant L8-12 exposed to elevated temperature possesses higher strength loss compared with the original graded L8-16 exposed to 800 °C. Although, the L4-5 which prepared from the graded LWA of 4-8 mm by decreasing the LWA maximum size to 4-5 mm shows different strength loss behavior after exposed

to 800 °C compared to L8-12, by possessing lower strength loss than its original graded L4-8.

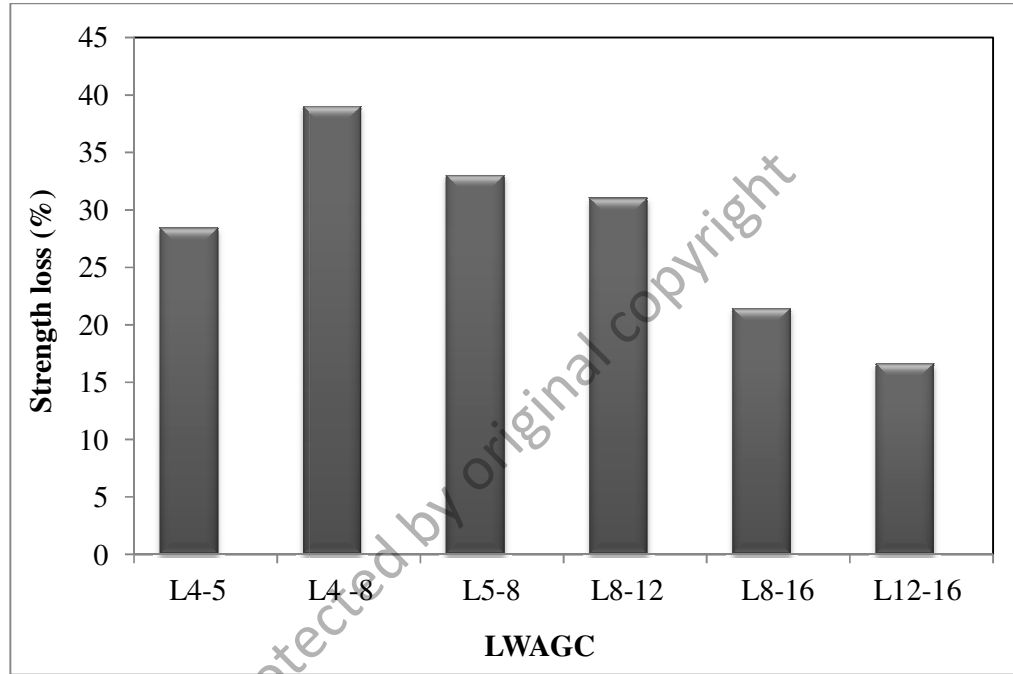


Figure 4.44: Strength loss of the L4-5, L4-8, L5-8, L8-12, L8-16 and L12-16 after exposure to elevated temperature of 800 °C.

It has been mentioned in section 4.2.6.2 that increasing the minimum sizes of LWA decreases the LWAGCs OD-densities, as well as decreasing the maximum sizes of LWA increases the LWAGCs OD-densities. Based on the results of the strength loss illustrated in Figure 4.43, it is observed that the L12-16 which possesses the lowest OD-density of 1356 kg/m<sup>3</sup> than other concretes (as presented in section 4.2.6.2) has the lowest strength loss compared to other concretes. Thus, with exceptional of the L4-5 thermal behavior, the lowest LWAGC OD-density, results in lowest strength loss after being exposed to 800 °C. This is believed to be due to the better permeability characteristics that the low OD-density LWAGC possesses compared with high OD-density concrete.

Basically, the water absorption and the porosity characteristics of a LWAGC are indirectly imply the concrete permeability. Furthermore, it has been mentioned earlier in section 4.2.6.3 that the water absorption and total porosity of the LWAGCs are increased with decreasing the LWAGCs OD-densities (Figures 4.18 and 4.19). Thus, during heating the LWAGCs to 800 °C, the dispersion of the water vapor from the geopolymeric concrete structure possessed high porosity content would causes less deterioration to the resultant strength compared with low porosity structure (high density structure). A similar finding has been reported by Sancak et al. (2008) showing that the weight loss in term of water vapor at high temperatures is increasing with increasing the porosity content. Therefore, it is observed that the L12-16 possesses lowest OD-density (high porosity and water absorption characteristics) has the lowest strength loss after exposed to the elevated temperatures of 800 °C.

However, this explanation of the strength loss observed for the exposed LWAGCs to 800 °C is incompatible to the thermal behavior of the L4-5 concrete. As mentioned in section 4.2.6.3, the L4-5 has the highest OD-density of 1531.85 kg/m<sup>3</sup> than other concretes and the results of Figure 4.44 shows that this concrete attains relatively lower strength loss than its original graded L4-8 as well as L5-8. This is attributed to the fact that the thickness of the geopolymer mortar per unit surface of the LWA of 4-5 mm is thinner than other LWAs. This is due to the highest specific surface area of the 4-5 mm LWA than other LWAs and the fixed quantity of the geopolymer mortar as mentioned in the preparation procedure (Chapter 3, section 3.10.1). Accordingly, during heating, the gentle releasing of the water vapor from the geopolymeric structure, due to low geopolymer mortar thickness, would cause less thermal shrinkage (less thermal stresses) which reduces the deterioration in the resultant strength comparing with the original graded L4-8 and other LWAGCs of L5-8 and L8-12 (Hu et al, 2009).

#### **4.4 Summary of Results and Discussion**

The results presented in chapter 4 showed that the designed LWAGC achieved the specific characteristics proposed prior to selecting the mix proportioning listed in Chapter 3, section 3.3. The mechanical and physical properties of the prepared LWAGC are permitting to classify it as a structural LWAC according to American concrete institute ACI (213R-87). In addition, the comparison of the mechanical and physical properties of the LWAGC with its constituents (FA paste and mortar) showed that the concrete possessed significantly lower strength and density than its constituents due to the microstructural characteristics of its LWA. However, these characteristics improved the fire resistance of the LWAGC considerably after exposed to the elevated temperatures compared to FA paste and mortar. The results also highlighted the essentially significant phase composition changes when the FA geopolymer materials exposed to elevated temperatures ranged from 400-800 °C, which is significantly affected the thermal behavior of all geopolymers prepared in this research. Furthermore, investigation the thermal behavior of LWAGC at temperatures of 100-800 °C showed an excellent fire resistance of the concrete exposed to these range of temperatures.

#### **4.5 Guide of LWAGC Mix Design**

This research provides fundamental recommendations and guidance to the designers who aim to design a mix proportioning of LWAC based on the geopolymerization technology. The reported mix design here for LWAGC is unavailable in any published research or work based on the recommendations reported by American concrete institute ACI committee 211-standard (ACI 211.2) used for designing and proportioning

of a structural OPC lightweight aggregate concrete. Based on the design method known as weight method or specific gravity pycnometer, a LWAGC contains a normal weight-sand, fly ash activated by 12 M NaOH solution and liquid  $\text{Na}_2\text{SiO}_3$  and lightweight expanded clay aggregate (LECA) have an OD-density of  $897.75 \text{ kg/m}^3$  as a LWA, the mix proportioning of the LWAGC is given in Table 4.12.

Table 4.12: Recommended Mix Design for LWAGC

<b>Constituents</b>	<b>(<math>\text{kg/m}^3</math>)</b>
FA	341.89
$\text{Na}_2\text{SiO}_3$	100.86
NaOH	100.86
Activator/FA	0.59
LWA	484.00
Sand	823.39
Extra $\text{H}_2\text{O}$	91.47

© This item is protected by original copyright

## CHAPTER 5

### CONCLUSIONS AND FUTURE WORK

#### 5.1 Conclusions

This work was aimed to study the designing and preparation procedures of a structural lightweight aggregate concrete (LWAC) based on the utilization of the geopolymerization technology. A geopolymer binder was used to bind a mixture of aggregates consisting of lightweight expanded clay aggregate (LECA) and normal weight sand to prepare a lightweight aggregate concrete (LWAGC). The geopolymer binder was prepared by the alkali-activation of locally source fly ash (FA) without any additives materials. The alkaline activator used in the FA activation process is a mixture of liquid sodium silicate ( $\text{Na}_2\text{SiO}_3$ ) and 12M sodium hydroxide (NaOH) solution.

Furthermore, the designing process was based on the recommendations of the American Concrete Institute (ACI) committee 211-standard (ACI 211.2) used for designing and proportioning of a structural OPC lightweight aggregate concrete. This is due to the lack of standard documents dealing with the geopolymers as a cementitious material. The design processes also involves the optimization of the preparation parameters that the ACI 211.2 standard did not specified or what's known as 'actual design'.

The second approach of this work was to investigate and addressing the thermal behavior as well as the significant changes in the geopolymeric phase composition of the LWAGC after exposed to elevated temperatures ranging of 100 °C to 800 °C.

The designing and preparation procedures that included in this thesis represents the fundamental and solid ground of future standardized document that described in details the utilization of the FA-based geopolymer binder as a cementitious material in making of a structural lightweight aggregate geopolymer concrete (LWAGC). The designing and extensive work reported here are unavailable in any published work by any institute or individual researchers. In relation to the objectives of this research, the following conclusions have been made:

- The ACI 211.2 standard used for the designing and mix proportioning of OPC lightweight aggregate structural concrete was compatible and reliable for designing a structural LWAGC and provides the optimum Activator/FA mass mixing ratio. The resulted LWAGC had the required 28 days compressive strength (18.86 MPa) and unit weight (1438.70 kg/m<sup>3</sup>) proposed by the ACI 213R (28 days strength higher than 17 MPa and unit weight less than 1850 kg/m<sup>3</sup>).
- The actual design experiments revealed that the optimum preparation parameters of a fly ash-based geopolymer binder are: Na<sub>2</sub>SiO<sub>3</sub>/NaOH ratio of 1.00, curing temperature of 70 °C and curing period of 24 hour at different tested ages of 3,7 and 28 days.
- The physical and mechanical properties of FA geopolymers paste, mortar and LWAGC showed that the LWAGC had significantly lower strength and unit weight than the FA geopolymer paste and mortar. This is due to the

microstructural and physical characteristics of the LWAs used in the LWAGC preparation process.

- The LWAGC showed excellent compressive strength development versus aging times of 3, 7, 28, 56, 91 and 365 days. This tendency added a noticeable advantage to these novel materials.
- Decreasing the LWAs maximum size decreases the workability of the fresh LWAGC mixture and increases the density as well as the compressive strength of hardened LWAGC. While, increasing the LWAs minimum particle size increasing the workability of the fresh LWAGC mixture and decreases the density as well as compressive strength of hardened LWAGC.
- The lower OD-density of the LWAGC, the higher water absorption and total porosity resulted for the hardened LWAGC.
- FA geopolymers paste, mortar and LWAGC exposed to elevated temperatures of 400 °C, 600 °C and 800 °C underwent strength deterioration. The thermo-physical results of the FA geopolymer paste indicated that both dehydration and dehydroxylation processes were the reasons behind the strength loss after exposure to 400 and 600 °C. While, the sintering and densification processes of the unreacted silicate secondary phases detected by the DTA and dilatometry analysis were responsible for the paste structure failure after exposed to 800 °C.

- The SEM micrographs and XRD analysis showed that the high activator content produced a highly reacted dense aluminosilicate gel matrix at 70 °C. Although, it is led to produce high portion of unreacted silicate products which are significantly weaken the fire-resistance of the geopolymer at range of temperatures of 600 °C to 800 °C.
- The exposed FA geopolymer mortar to the elevated temperatures of 400 °C, 600 °C and 800 °C showed better thermal durability and lower strength loss compared with FA geopolymer paste. This is attributed to the sand particles incorporated in the geopolymeric matrix which decreased the thermal stresses as well as the sintering and densification processes.
- LWAGC has shown remarkable thermal performance and minimum strength loss upon the exposure to the elevate temperatures of 400 °C, 600 °C and 800 °C. This is specifically attributed to the microstructural characteristics of its LWA. The voids and micro-pores appeared in LWA microstructural analysis decreased the heat flow through the concrete core which led to decrease the thermal stresses as well as the sintering and densification processes to the lowest rates compared to the FA geopolymer paste and mortar.
- SEM results of the unexposed LWAGC to elevated temperatures of 400 °C, 600 °C and 800 °C illustrated the good bond between the aggregate/mortar in the indistinct ITZ due to the porous texture of LWA shell which provides better interfacial bonding. However, at elevated temperatures of 600 °C and 800 °C

the bonding zone was deteriorated due to the dehydration of the structural water as well as the swelling of the unreacted silicate phase.

- The dilatometerical analysis indicated the mismatching in the thermal expansion between the geopolymer paste and the LWA which caused the formation of microcracks in the ITZ zone when the LWAGC exposed to elevated temperatures as the SEM analysis indicated. These microcracks caused the strength deterioration observed as the LWAGC exposed to elevated temperatures of 400 °C, 600 °C and 800 °C.
- The LWAGC exposed to elevated temperatures of 100 °C to 800 °C showed a compressive strength gaining after exposing to elevated temperatures of 100 °C, 200 °C and 300 °C. This made the prepared LWAGC an excellent refractory material to an application when the high strength and thermal durability up to 300 °C is desired. In addition, The strength was started to deteriorate after exposing to elevated temperature of 400 °C up to 800 °C, due to vapor effect, the different in the thermal expansion between the aggregate and the geopolymeric paste as well as the sintering of the unreacted silicate species.
- Increasing the minimum size of LWAs increased the thermal durability of the resulted LWAGC exposed to elevated temperature of 800 °C. While, decreasing the maximum size of LWAs decreased the thermal durability of the LWAGC exposed to elevated temperature of 800 °C.

## 5.2 Future Work

This thesis has dealt with an investigation on the designing and preparation of a green structural LWAC prepared by using of the geopolymerization technology without the utilization of OPC or any other additives material. In addition, the prepared lightweight aggregate geopolymer concrete (LWAGC) by the alkali-activation of a fly ash (FA) source as the only source material was subjected for elevated temperatures ranged of 100 °C to 800 °C in order to investigate its thermal behavior. The thermal behavior of the LWAGC at selected elevated temperatures of 400 °C, 600 °C and 800 °C was compared with its constituents of FA geopolymer paste and mortar exposed to similar elevated temperatures range to explore the effect of LWA incorporating on the thermal behavior of the geopolymer material. In general, the geopolymer concrete showed superior advantages compared to the normal OPC concrete representative by its higher mechanical strength and thermal durability as well as the essential environmentally-friendly benefits that the geopolymeric materials offers. While, much information regarding the character, strength as well as the thermal behavior of the LWAGC has been elucidated in this work, a number of issues could not be addressed due to equipment and time constraints. Therefore, future work should need to be undertaken to get better understanding and knowledge to other mechanical and chemical resistance characteristics of the LWAGC before these materials can be widely adopted as a construction material for industrial and commercial applications. The following recommendations are made for future work:

1. To characterize the mechanical properties of the LWAGC other than the compressive strength reported in this thesis like the tensile strength, splitting tensile strength, modulus of rupture, modulus of elasticity, shrinkage strain, ect...
2. To developing LWAGCs synthesized by the utilization of other by-products or waste industrial materials base on the essential designing principles that this thesis reported, to achieve new building materials that might cost less and obtained another commercial and environmental advantages.

© This item is protected by original copyright

## REFERENCES

- Abdullah, M., Kamarudin, H., Bnhussain, M., Khairul Nizar, I., Rafiza, A., & Zarina, Y. (2011a). The relationship of NaOH molarity,  $\text{Na}_2\text{SiO}_3/\text{NaOH}$  ratio, fly Ash/Alkaline activator ratio, and curing temperature to the strength of fly ash-based geopolymer. *Advanced Materials Research*, 328, 1475-1482.
- Abdullah, M. M. A. B., Hussin, K., Bnhussain, M., Ismail, K. N., Abdul Razak, R. & Yahya, Z. (2011b). Microstructure of different NaOH molarity of fly ash-based green polymeric cement. *Journal of Engineering and Technology Research*, 3(2), 44-49.
- Abdullah, M. M. A. B., Hussin, K., Bnhussain, M., Ismail, K. N., Yahya, Z., & Abdul Razak, R. (2012). Fly Ash-based Geopolymer Lightweight Concrete Using Foaming Agent. *International journal of molecular sciences*, 13(6), 7186-7198.
- ACI, B. (1998). 211.2-Standard Practice for Selecting Proportions for Structural Lightweight Concrete. American Concrete Institute International.
- ACI, B. (1987). 213R-87, Guide for structural lightweight aggregate concrete. American Concrete Institute International, (reapproved 1999).
- ACI education bulletin E1-07 (2007). Aggregate for concrete. American Concrete Institute International.
- Álvarez-Ayuso, E., Querol, X., Plana, F., Alastuey, A., Moreno, N., Izquierdo, M., et al. (2008). Environmental, physical and structural characterisation of geopolymer matrixes synthesised from coal co-combustion fly ashes. *Journal of Hazardous Materials*, 154(1), 175-183.
- Andiç-Çakir, Ö., & Hizal, S. (2012). Influence of elevated temperatures on the mechanical properties and microstructure of self consolidating lightweight aggregate concrete. *Construction and Building Materials*, 34, 575-583.
- Arellano Aguilar, R., Burciaga Díaz, O., & Escalante García, J. (2010). Lightweight concretes of activated metakaolin-fly ash binders, with blast furnace slag aggregates. *Construction and Building Materials*, 24(7), 1166-1175.

ASTM C618-08a. Standard specification for coal fly ash and raw or calcined natural pozzolan for use in concrete, ASTM international; 2008.

American Coal Ash Association (ACAA) (2004). Fly ash facts for highway Engineers. American Coal Ash Association.

ASTM C330/C330M-09. Standard Specification for Lightweight Aggregates for Structural Concrete. ASTM international; 2009.

ASTM C140-01. Standard test method for sampling and testing concrete masonry units and related units. ASTM international; 2001.

ASTM C127-01. Standard Test Method for Density, Relative Density (Specific Gravity), and Absorption of Coarse Aggregate. ASTM international; 2001.

ASTM C136-06. Standard Test Method for Sieve Analysis of Fine and Coarse Aggregates. ASTM international; 2006.

ASTM C109/C109M-12. Standard Test Method for Compressive Strength of Hydraulic Cement Mortars (Using 2-in. or [50-mm] Cube Specimens). ASTM international; 2012.

ASTM E 831-03, Standard test method for linear thermal expansion of solid materials by thermomechanical analysis. ASTM international; 2003.

Babu, D. S., Ganesh Babu, K., & Tiong-Huan, W. (2006). Effect of polystyrene aggregate size on strength and moisture migration characteristics of lightweight concrete. *Cement and Concrete Composites*, 28(6), 520-527.

Bakharev, T. (2005). Geopolymeric materials prepared using Class F fly ash and elevated temperature curing. *Cement and Concrete Research*, 35(6), 1224-1232.

Bakharev, T. (2006). Heat resistance of geopolymer materials prepared using class F fly ash. *Journal of Australian Ceramic Society* (1), 36-44.

Bakharev, T. (2006). Thermal behaviour of geopolymers prepared using class F fly ash and elevated temperature curing. *Cement and Concrete Research*, 36(6), 1134-1147.

- Barbosa, V. F., & MacKenzie, K. J. (2003a). Synthesis and thermal behaviour of potassium sialate geopolymers. *Materials Letters*, 57(9), 1477-1482.
- Barbosa, V. F., & MacKenzie, K. J. (2003b). Thermal behaviour of inorganic geopolymers and composites derived from sodium polysialate. *Materials Research Bulletin*, 38(2), 319-331.
- Barbosa, V. F., MacKenzie, K. J., & Thaumaturgo, C. (2000). Synthesis and characterisation of materials based on inorganic polymers of alumina and silica: sodium polysialate polymers. *International Journal of Inorganic Materials*, 2(4), 309-317.
- CEN/TC 104. EN 12390-3. Testing hardened concrete-part 3: compressive strength of testing specimens. Brussels; 2009.
- Cabrera, J., & Lynsdale, C. (Eds.). (1988). Proceedings from: *the International Conference on Measurements and Testing in Civil Engineering*. Lyon, France. 279-291.
- Chandra, S., & Berntsson, L. (Eds.). (2002). *Lightweight Aggregate Concrete: Science, Technology and Application*, New York, William Andrew.
- Cheng, T., & Chiu, J. (2003). Fire-resistant geopolymer produced by granulated blast furnace slag. *Minerals Engineering*, 16(3), 205-210.
- Chindapasirt, P., Chareerat, T., & Sirivivatnanon, V. (2007). Workability and strength of coarse high calcium fly ash geopolymer. *Cement and Concrete Composites*, 29(3), 224-229.
- Chindapasirt, P., Jaturapitakkul, C., Chalee, W., & Rattanasak, U. (2009). Comparative study on the characteristics of fly ash and bottom ash geopolymers. *Waste Management*, 29(2), 539-543.
- Collins, F., & Sanjayan, J. (1999). Workability and mechanical properties of alkali activated slag concrete. *Cement and Concrete Research*, 29(3), 455-458.
- Criado, M., Palomo, A., & Fernández-Jiménez, A. (2005). Alkali activation of fly ashes. Part 1: Effect of curing conditions on the carbonation of the reaction products. *Fuel*, 84(16), 2048-2054.

- Davidovits, J. (1988). Geopolymers of the first generation: SILIFACE-Process, Proceedings from Geopolymer '88: *The First European Conference on Soft Mineralogy*, Compiegne, France, 49-67.
- Davidovits, J. (1991). Geopolymers. *Journal of Thermal Analysis and calorimetry*, 37(8), 1633-1656.
- Davidovits, J. (1994). Global warming impact on the cement and aggregates industries. *World Resource Review*, 6, 263-278.
- Davidovits, J. (1982). Mineral polymers and methods of making them, *United State Patent, No. 4,349,386*. Washington, DC: U.S. Patent.
- Davidovits, J. (1999). Chemistry of geopolymeric systems, terminology. Proceedings from Geopolymere '99: International Geopolymer Conference, Saint-Quentine, France, 9-93.
- Davidovits, J. (2008). *Geopolymer Chemistry and Applications*. 1<sup>nd</sup> ed. Institut Geopolymere, Saint-Quentin, France.
- Davidovits, J. (1979). Synthesis of new high-temperature Geopolymers for reinforced plastics and composites, *SPE PACTEC'79*, Costa Mesa, California, *Society of Plastics Engineers, USA*. 151-154.
- Davidovits, J. & Sawyer, J. L. (1985) Early-high strength mineral polymer, *United State Patent No. 4, 509.958*, Washington, DC: U.S. Patent.
- Detphan, S., & Chindapasirt, P. (2009). Preparation of fly ash and rice husk ash geopolymer. *International Journal of Minerals, Metallurgy and Materials*, 16(6), 720-726.
- Dombrowski, K., Buchwald, A., & Weil, M. (2007). The influence of calcium content on the structure and thermal performance of fly ash based geopolymers. *Journal of Materials Science*, 42(9), 3033-3043.
- Duxson, P., Lukey, G. C., & Van Deventer, J. S. J. (2007a). Physical evolution of Na-geopolymer derived from metakaolin up to 1000 °C. *Journal of Materials Science*, 42(9), 3044-3054.

- Duxson, P., Fernández-Jiménez, A., Provis, J. L., Lukey, G. C., Palomo, A., & Van Deventer, J. S. J. (2007b). Geopolymer technology: The current state of the art. *Journal of Materials Science*, 42(9), 2917-2933.
- Duxson, P., Provis, J. L., Lukey, G. C., Mallicoat, S. W., Kriven, W. M., & Van Deventer, J. S. (2005). Understanding the relationship between geopolymer composition, microstructure and mechanical properties. *Colloids and Surfaces A: Physicochemical and Engineering Aspects*, 269(1), 47-58.
- EN, B. (2000). 12350-2. Testing of fresh concrete–slump test. London: British Standards Institution.
- EN, B. (2003). 12390-3, Testing hardened concrete. *London: British Standards Institution*. Part, 3, 21.
- EN, B. (2000). 12350-2. Testing of fresh concrete–slump test. *London: British Standards Institution*.
- Fernandez-Jimenez, A., & Palomo, J. (2002). Alkali activated fly ash concrete: Alternative material for the precast industry. Proceedings from 2002 *Geopolymer Conference*. Melbourne, Australia. 117-125.
- Fernández-Jiménez, A., & Palomo, A. (2003). Characterisation of fly ashes. Potential reactivity as alkaline cements. *Fuel*, 82(18), 2259-2265.
- Fernández-Jiménez, A., & Palomo, A. (2005). Composition and microstructure of alkali activated fly ash binder: effect of the activator. *Cement and Concrete Research*, 35(10), 1984-1992.
- Fernandez-Jimenez, A. M., Palomo, A., & Lopez-Hombrados, C. (2006). Engineering properties of alkali-activated fly ash concrete. *ACI Materials Journal*, 103(2), 106-112.
- Fernández-Jiménez, A., Garcia-Lodeiro, I., & Palomo, A. (2007). Durability of alkali-activated fly ash cementitious materials. *Journal of Materials Science*, 42(9), 3055-3065.
- Glukhovskiy, V. (1981). Slag-alkali concretes produced from fine-grained aggregate. Kiev: Vishcha Shkolay. USSR (1981) in Russian.

- Gourley, J. (2003). Geopolymers; opportunities for environmentally friendly construction materials. Proceedings from *Materials 2003 Conference: Adaptive Materials for a Modern Society, Sydney, Institute of Materials Engineering Australia*.
- Gourley, J., & Johnson, G. (2005). Developments in geopolymer precast concrete. Proceedings of Geopolymer 2005, World Congress. Geopolymer Green Chemistry and sustainable development solutions. Saint-Quentin, France. 139-143.
- Guerrieri, M., Sanjayan, J., & Collins, F. (2010). Residual strength properties of sodium silicate alkali activated slag paste exposed to elevated temperatures. *Materials and Structures*, 43(6), 765-773.
- Guo, X., Shi, H., & Dick, W. A. (2010). Compressive strength and microstructural characteristics of class C fly ash geopolymer. *Cement and Concrete Composites*, 32(2), 142-147.
- Hanjitsuwan, S., Chindapasirt, P., & Pimraksa, K. (2011). Electrical conductivity and dielectric property of fly ash geopolymer pastes. *International Journal of Minerals, Metallurgy, and Materials*, 18(1), 94-99.
- Hardjito, D., Wallah, S., & Rangan, B. (2002). Study on engineering properties of fly ash-based geopolymer concrete. *Journal of the Australasian Ceramic Society*, 38(1), 44-47.
- Hardjito, D., & Rangan, B. V. (2005). Development and properties of low-calcium fly ash-based geopolymer concrete. Research Report GC1, Curtin University of Technology, Perth, Australia.
- Hos, J., McCormick, P., & Byrne, L. (2002). Investigation of a synthetic aluminosilicate inorganic polymer. *Journal of Materials Science*, 37(11), 2311-2316.
- Hu, S. G., Wu, J., Yang, W., He, Y. J., Wang, F. Z., & Ding, Q. J. (2009). Preparation and properties of geopolymer-lightweight aggregate refractory concrete. *Journal of Central South University of Technology (English Edition)*, 16(6), 914-918.
- Jahanian, S., & Rostami, H. (2001). Alkali ash material, a novel material for infrastructure enhancement. *Engineering Structures*, 23(6), 736-742.

- Jiang, W., & Roy, D. (1992). Hydrothermal processing of new fly ash cement. *American Ceramic Society Bulletin* ;( United States), 71(4), 642–647.
- Jo, B.-w., Park, S.-k., & Park, J.-b. (2007). Properties of concrete made with alkali-activated fly ash lightweight aggregate (AFLA). *Cement and Concrete Composites*, 29(2), 128-135.
- Ke, Y., Ortola, S., Beaucour, A. L., & Dumontet, H. (2010). Identification of microstructural characteristics in lightweight aggregate concretes by micromechanical modelling including the interfacial transition zone (ITZ). *Cement and Concrete Research*, 40(11), 1590-1600.
- Khaliq, W., & Kodur, V. (2011). Thermal and mechanical properties of fiber reinforced high performance self-consolidating concrete at elevated temperatures. *Cement and Concrete Research*, 41(11), 1112-1122.
- Kim, Y.-J., & Harmon, T. G. (2006). Analytical model for confined lightweight aggregate concrete. *ACI structural Journal*, 103(2), 263-270.
- Kong, D. L., Sanjayan, J. G., & Sagoe-Crentsil, K. (2007). Comparative performance of geopolymers made with metakaolin and fly ash after exposure to elevated temperatures. *Cement and Concrete Research*, 37(12), 1583-1589.
- Kong, D. L. Y., & Sanjayan, J. G. (2008). Damage behavior of geopolymer composites exposed to elevated temperatures. *Cement and Concrete Composites*, 30(10), 986-991.
- Kong, D. L. Y., & Sanjayan, J. G. (2010). Effect of elevated temperatures on geopolymer paste, mortar and concrete. *Cement and Concrete Research*, 40(2), 334-339.
- Kovalchuk, G., Fernández-Jiménez, A., & Palomo, A. (2007). Alkali-activated fly ash: Effect of thermal curing conditions on mechanical and microstructural development–Part II. *Fuel*, 86(3), 315-322.
- Krivenko, P. (1997). Alkaline cements: terminology, classification, aspects of durability. Paper presented at the Proceeding of the Tenth International Congress on Chemistry of Cement, Amarkai and Cöngrex, Göteborg, Gothenburg, Sweden. 6-4Iv046.

- Li, Z., Ding, Z., & Zhang, Y. (2004). Development of sustainable cementitious materials. Proceedings from *the International Workshop on Sustainable Development and Concrete Technology*, Beijing, China. 20-21.
- Malek, R., & Roy, D. (1997). Synthesis and Characterization of New Alkali-activated Cements. Proceedings from *the 10th International Congress on the Chemistry of Cement*, Amarkai and Cöngrex, Göteborg, Gothenburg, Sweden 8-1i024.
- Malhotra, V. (1999). Making concrete "greener" with fly ash. *Concrete International-Detroit*-, 21(5), 61-66.
- Malhotra, V. (2002). High-performance high-volume fly ash concrete. *Concrete International-Detroit*-, 24(7), 30-34.
- Malhotra, V. M., & Ramezani pour, A. (1994). *Fly ash in concrete*: CANMET. Energy, Mines and Resources, Canada.
- Mehta, P. K., & Burrows, R. W. (2001). Building durable structures in the 21st century. *Concrete International*, 23(3), 57-63.
- Mehta, P. K., & Monteiro, P. D. (2006). CONCRETE (Microstructure, Properties, and Materials, *MacGraw-Hill, New York*.
- Mouli, M., & Khelafi, H. (2008). Performance characteristics of lightweight aggregate concrete containing natural pozzolan. *Building and Environment*, 43(1), 31-36.
- Nazari, A., Riahi, S., & Bagheri, A. (2012). Designing water resistant lightweight geopolymers produced from waste materials. *Materials and Design*, 35, 296-302.
- Neville, A. (1994). *Concrete in the Year 2000. Advances in Concrete Technology*, 2nd Edition (Editor: VM Malhotra), Canada Centre for Mineral and Energy Technology, Ottawa, Ontario, Canada, 1-17.
- Ng, T. S., & Foster, S. J. (2010). Shear strength of lightweight fibre reinforced geopolymer concrete composite, In Sujeeva Setunge. Editor (Eds.), *Incorporating Sustainable Practice in Mechanics and Structures of Materials* (77-82), London. CRC Press, Taylor & Francis Group.

- Palomo, A., Blanco-Varela, M., Granizo, M., Puertas, F., Vazquez, T., & Grutzeck, M. (1999a). Chemical stability of cementitious materials based on metakaolin. *Cement and Concrete Research*, 29(7), 997-1004.
- Palomo, A., Grutzeck, M., & Blanco, M. (1999b). Alkali-activated fly ashes: a cement for the future. *Cement and Concrete Research*, 29(8), 1323-1329.
- Pinto, A. (2004). Alkali-activated metakaolin based binders. PhD Thesis. University of Minho, Portugal. [Only in Portuguese].
- Provis, J. L., Yong, C. Z., Duxson, P., & van Deventer, J. S. (2009). Correlating mechanical and thermal properties of sodium silicate-fly ash geopolymers. *Colloids and Surfaces A: Physicochemical and Engineering Aspects*, 336(1), 57-63.
- Provis, J. L., Yong, C. Z., Duxson, P., & van Deventer, J. S. J. (2009). Correlating mechanical and thermal properties of sodium silicate-fly ash geopolymers. *Colloids and Surfaces A: Physicochemical and Engineering Aspects*, 336(1-3), 57-63.
- Puertas, F., Martínez-Ramírez, S., Alonso, S., & Vazquez, T. (2000). Alkali-activated fly ash/slag cements: strength behaviour and hydration products. *Cement and Concrete Research*, 30(10), 1625-1632.
- Rahier, H., Van Mele, B., Biesemans, M., Wastiels, J., & Wu, X. (1996). Low-temperature synthesized aluminosilicate glasses. Part I: Low-temperature reaction stoichiometry and structure of a model compound. *Journal of Materials Science*, 31(1), 71-79.
- Rashad, A. M., & Zeedan, S. R. (2011). The effect of activator concentration on the residual strength of alkali-activated fly ash pastes subjected to thermal load. *Construction and Building Materials*, 25(7), 3098-3107.
- Reshi, W. F. (2011). Evaluation of stone mastic asphalt using fly ash, cement and hydrated lime as mineral filler. Master Thesis, Universiti Teknologi Malaysia, Faculty of Civil Engineering, Malaysia.
- Rickard, W. D., Van Riessen, A., & Walls, P. (2010). Thermal Character of Geopolymers Synthesized from Class F Fly Ash Containing High Concentrations of Iron and  $\alpha$ -Quartz. *International Journal of Applied Ceramic Technology*, 7(1), 81-88.

- Rickard, W. D., Williams, R., Temuujin, J., & Van Riessen, A. (2011). Assessing the suitability of three Australian fly ashes as an aluminosilicate source for geopolymers in high temperature applications. *Materials Science and Engineering: A*, 528(9), 3390-3397.
- Rickard, W. D. A., Temuujin, J., & Van Riessen, A. (2012). Thermal analysis of geopolymer pastes synthesised from five fly ashes of variable composition. *Journal of Non-Crystalline Solids*, 358(15), 1830-1839.
- Rickard, W. D. A., Van Riessen, A., & Walls, P. (2010). Thermal character of geopolymers synthesized from class F Fly ash containing high concentrations of iron and  $\alpha$ -quartz. *International Journal of Applied Ceramic Technology*, 7(1), 81-88.
- Roberts, F. L., Kandhal, P. S., Brown, E. R., Lee, D.-Y., & Kennedy, T. W. (1996). Hot mix asphalt materials, mixture design and construction. National Asphalt Pavement Association Education Foundation. Lanham.
- Roy, D. M. (1999). Alkali-activated cements opportunities and challenges. *Cement and Concrete Research*, 29(2), 249-254.
- Rukzon, S., Chindapasirt, P., & Mahachai, R. (2009). Effect of grinding on chemical and physical properties of rice husk ash. *International Journal of Minerals, Metallurgy and Materials*, 16(2), 242-247.
- Saad, M., Abo-El-Enainf, S. A., Hanna, G. B., & Kotkata, M. F. (1996). Effect of temperature on physical and mechanical properties of concrete containing silica fume. *Cement and Concrete Research*, 26(5), 669-675.
- Sancak, E., Dursun Sari, Y., & Simsek, O. (2008). Effects of elevated temperature on compressive strength and weight loss of the light-weight concrete with silica fume and superplasticizer. *Cement and Concrete Composites*, 30(8), 715-721.
- Sindhunata, A, Lukey, G., Xu, H. & van Deventer, J. (2004). The effect of curing conditions on the properties of Geopolymeric materials derived from fly ash, Proceedings from: *The 1st International RILEM Symposium on Advances in Concrete Through Science and Engineering*, North-western University, Evanston, IL, USA. DOI: 10.1617/2912143926.011

- Song, X., Marosszky, M., Brungs, M., & Munn, R. (2005). Durability of fly ash based geopolymer concrete against sulphuric acid attack. Proceedings From: The 10<sup>th</sup> DBMC, International Conference on Durability of Building Materials and Components, Lyon, France. 123-129.
- Subaer, Van Riessen, A. 2007. Thermo-mechanical and microstructural characterisation of sodium-poly (sialate-siloxo)(Na-PSS) geopolymers. *Journal of Materials Science*, 42, 3117-3123.
- Swamy, R. N., & Lambert, G. H. (1981). The microstructure of Lytag aggregate. *International Journal of Cement Composites and Lightweight Concrete*, 3(4), 273-282.
- Swamy, R. N., & Lambert, G. H. (1983). Mix design and properties of concrete made from PFA coarse aggregates and sand. *International Journal of Cement Composites and Lightweight Concrete*, 5(4), 263-275.
- Swamy, R., & Jiang, E. (1993). Pore Structure and Carbonation of Lightweight Concrete after 10 Years' Exposure. *ACI Special Publication*, 136. 377-396
- Swanepoel, J., & Strydom, C. (2002). Utilisation of fly ash in a geopolymeric material. *Applied Geochemistry*, 17(8), 1143-1148.
- Teixeira-Pinto, A., Fernandes, P., & Jalali, S. (2002). Geopolymer manufacture and application-Main problems when using concrete technology. Proceedings from the *Geopolymers 2002 International Conference, Melbourne, Australia*. 223-229.
- Temuujin, J., & Van Riessen, A. (2009). Effect of fly ash preliminary calcination on the properties of geopolymer. *Journal of Hazardous Materials*, 164(2-3), 634-639.
- Temuujin, J., & Van Riessen, A. (2009). Effect of fly ash preliminary calcination on the properties of geopolymer. *Journal of Hazardous Materials*, 164(2), 634-639.
- Thakur, R. N., & Ghosh, S. (2006). Effect of mix composition on compressive strength and microstructure of fly ash based geopolymer composites. *ARPJ Journal of Engineering and Applied Sciences*, 4(4), 68-74.

- Topçu, I. B., & Uygunoğlu, T. (2007). Properties of autoclaved lightweight aggregate concrete. *Building and Environment*, 42(12), 4108-4116.
- Uygunoğlu, T., & Topçu, I. B. (2009). Thermal expansion of self-consolidating normal and lightweight aggregate concrete at elevated temperature. *Construction and Building Materials*, 23(9), 3063-3069.
- Van Jaarsveld, J., Van Deventer, J., & Lorenzen, L. (1997). The potential use of geopolymeric materials to immobilise toxic metals: Part I. Theory and applications. *Minerals Engineering*, 10(7), 659-669.
- Van Jaarsveld, J., Van Deventer, J., & Lorenzen, L. (1998). Factors affecting the immobilization of metals in geopolymerized fly ash. *Metallurgical and Materials Transactions B*, 29(1), 283-291.
- Van Jaarsveld, J., Van Deventer, J., & Lukey, G. (2002). The effect of composition and temperature on the properties of fly ash-and kaolinite-based geopolymers. *Journal of Chemical Engineering*, 89(1), 63-73.
- Van Jaarsveld, J., Van Deventer, J., & Lukey, G. (2003). The characterisation of source materials in fly ash-based geopolymers. *Materials Letters*, 57(7), 1272-1280.
- Wallah, S., Hardjito, D., Sumajouw, D., & Rangan, B. (2005). Creep and Drying Shrinkage Behaviour of Fly Ash-Based Geopolymer Concrete. proceedings from: The 22nd Biennial Conference Concrete. New South Wales, Australia. 153-159.
- Wallah, S., & Rangan, B. V. (2006). Low calcium fly ash based geopolymer concrete—Long term properties. Research Report-GC2, Curtin University, Australia. 76-80.
- Wan, X., Wang, W., Ye, T., Guo, Y., & Gao, X. (2006). A study on the chemical and mineralogical characterization of MSWI fly ash using a sequential extraction procedure. *Journal of Hazardous Materials*, 134(1), 197-201.
- Wang, H., Li, H., & Yan, F. (2005). Synthesis and mechanical properties of metakaolinite-based geopolymer. *Colloids and Surfaces A: Physicochemical and Engineering Aspects*, 268(1), 1-6.

- Wu, H.-C., & Sun, P. (2007). New building materials from fly ash-based lightweight inorganic polymer. *Construction and Building Materials*, 21(1), 211-217.
- Xie, Z., & Xi, Y. (2001). Hardening mechanisms of an alkaline-activated class F fly ash. *Cement and Concrete Research*, 31(9), 1245-1249.
- Xu, H., & Van Deventer, J. (2000). The geopolymerisation of aluminosilicate minerals. *International Journal of Mineral Processing*, 59(3), 247-266.
- Xu, H., & Van Deventer, J. S. (2002). Geopolymerisation of multiple minerals. *Minerals Engineering*, 15(12), 1131-1139.
- Xu, Y., & Chung, D. D. L. (2000). Effect of sand addition on the specific heat and thermal conductivity of cement. *Cement and Concrete Research*, 30(1), 59-61.
- Yang, K. H., Song, J. K., & Lee, J. S. (2010). Properties of alkali-activated mortar and concrete using lightweight aggregates. *Materials and Structures*, 43(3), 403-416.
- Zhang, L., Ahmari, S., & Zhang, J. (2011). Synthesis and characterization of fly ash modified mine tailings-based geopolymers. *Construction and Building Materials*, 25(9), 3773-3781.
- Zuda, L., Drchalová, J., Rovnaník, P., Bayer, P., Keršner, Z., & Černý, R. (2010). Alkali-activated aluminosilicate composite with heat-resistant lightweight aggregates exposed to high temperatures: Mechanical and water transport properties. *Cement and Concrete Composites*, 32(2), 157-163.
- Zuhua, Z., Xiao, Y., Huajun, Z., & Yue, C. (2009). Role of water in the synthesis of calcined kaolin-based geopolymer. *Applied Clay Science*, 43(2), 218-223.

## APPENDIX A

### LIST OF PUBLICATION AND EXHIBITION

#### Journal papers

1. **Omar A. Abdulkareem, A.M. Mustafa Al Bakri, H. Kamarudin. Khairul Nizar, and Ala'ddin A. Saif.** “*Effects of Elevated Temperatures on the Thermal Behavior and Mechanical Performance of Fly Ash Geopolymer Paste, Mortar and Lightweight Concrete*”. *Construction and Building Materials*, V.50, pp. 377–387. 2014. (Elsevier Publisher).
2. **Omar A. Abdulkareem, A.M. Mustafa Al Bakri, H. Kamarudin. Khairul Nizar, and Mohammed Binhussain.** “*Mechanical and Microstructural Evaluations of Lightweight Aggregate Geopolymer Concrete Before and After Exposed to Elevated Temperatures*”. *Materials*, V.6, No.10, pp. 4450-4461. 2013. (MDPI Publisher).
3. **Omar A. Abdulkareem, Mohd Mustafa Al Bakri, H. Kamarudin and I. Khairul Nizar,** “*A Study on the Synthesis of Fly Ash-Based Lightweight Aggregate Geopolymer Concrete*”, *Advanced Science Letters*, V.19, No.1 pp. 282-285. 2013. (ASP Publisher).
4. **Omar A. Abdulkareem, Mohd Mustafa Al Bakri, H. Kamarudin and I. Khairul Nizar,** “*The Influence of Curing Periods on the Compressive Strength Of Fly Ash-Based Geopolymer at Different Aging Times* ”, *Journal of Advanced Materials Research*, V. 479-48,1 No. 1, pp. 512-516. 2012. (TTP Publisher).
5. **Omar A. Abdulkareem, Mohd Mustafa Al Bakri, H. Kamarudin and I. Khairul Nizar,** “*Alteration in the Microstructure of Fly Ash Geopolymers Upon Exposures to Elevated Temperatures*”. *Advanced Materials Research*, V. 795, pp 201-205. (2013). (TTP Publisher).
6. **Omar A. Abdulkareem, Mohd Mustafa Al Bakri, H. Kamarudin and I. Khairul Nizar,** “*Fire Resistance Evaluation of Lightweight Geopolymer Concrete System Exposed to Elevated Temperatures of 100-800 °C*”. *Key Engineering Material*. V. 594-595, pp 427-432. (2014). (TTP Publisher).

7. Omar A. Abdulkareem, Mohd Mustafa Al Bakri, H. Kamarudin and I. Khairul Nizar, "Lightweight Fly Ash-Based Geopolymer Concrete", *Journal of Advanced Materials Research*, V. 626, No. 1, pp. 781-785. 2013. (TTP Publisher).
8. Omar A. Abdulkareem, Mohd Mustafa Al Bakri, H. Kamarudin and I. Khairul Nizar, "Effect of Lightweight Aggregate Size and Grading on the Residual Strength of Lightweight Geopolymer Concrete Exposed to Elevated Temperature", *Materials Science Forum*, (Accepted), 2014. (TTP Publisher).
9. A.M. Mustafa Al Bakri, Omar A. Abdulkareem, A.R. Rafiza, Y. Zarina, M.N. Norazian and H. Kamarudin. "Review on Processing of Low Calcium Fly Ash Geopolymer Concrete". *Australian Journal of Basic and Applied Sciences*, V.7, NO.5, pp. 342-349, ISSN 1991-8178. 2013. (SJR Publisher).
10. A.M. Mustafa Al Bakri, Omar A. Abdulkareem, H. Kamarudin I. Khairul Nizar, A.R. Rafiza, Y. Zarina and A. Alida." Microstructure Studies on the Effect of the Alkaline Activators of Fly Ash-Based Geopolymer at Elevated Heat Treatment Temperature". *Applied Mechanics and Materials* V. 421, pp. 342-348. (2013). (TTP Publisher).
11. A.M. Mustafa Al Bakri, H. Kamarudin, Omar A. Abdulkareem, C.M. Ruzaidi, A.R. Rafiza and M.N. Norazian. "Optimization of Alkaline Activator/Fly Ash Ratio on the Compressive Strength of Manufacturing Fly Ash-Based Geopolymer". *Applied Mechanics and Materials*, V. 110-116, pp.734-739, 2011. (TTP Publisher).
12. A.M. Mustafa Al Bakri, H. Kamarudin, Omar A. Abdulkareem, M.N. Norazian C.M. Ruzaidi and A.R. Rafiza. "The Effect of Alkaline Activator Ratio on the Compressive Strength of Fly Ash-Based Geopolymers". *Australian Journal of Basic and Applied Sciences*. V.5 No. 9, pp.1916-1022. 2011. (SJR Publisher).
13. Ali Basheer Azeez , Kahtan S. Mohammed, A.M. Mustafa Al Bakri, Hana Ihsan Hasan, Omar A. Abdulkareem "Radiation Shielding Characteristics of Concretes Incorporates Different Particle Sizes of Various Waste Materials" *Advanced Materials Research*, V. 925, pp. 190-194. 2014. (TTP Publisher).

#### Conference paper

1. Omar A. Abdulkareem, A.M. Mustafa Al Bakri, H. Kamarudin and I. Khairul Nizar. "The Effect of Damp Sand Content on the Geopolymerization

*Reaction of Fly Ash-Based Geopolymer Mortars". The 2<sup>nd</sup> international Malaysia-Ireland Joint Symposium on Engineering, Science and Business (IMiEJS2012). Kuala Lumpur, Jun 2012.pp. 235-240.*

#### **EXHIBITIONS & AWARDS:**

- **Prof. Dr. Kamarudin Hussin, Mohd Mustafa Al Bakri Abdullah, Omar A.K.A. Abdulkareem, Assoc. Prof. Dr. Khairul Nizar Ismail, Assoc. Prof. Che Mohd Ruzaidi Ghazali, Mohammad Tamizi Selimin.** Lightweight Aggregate Geopolymer Concrete (LWAGC). EXSPO, Rekacipta dan Pameran Penyelidikan Unimap 2012. *Perlis, Malaysia. 3-4 JAN 2012. Bronze Medal.*
- **Prof. Dr. Kamarudin Hussin, Mohd Mustafa Al Bakri Abdullah, Assoc. Prof. Dr. Khairul Nizar Ismail, Assoc. Prof. Che Mohd Ruzaidi Ghazali, Mohammad Tamizi Selimin, Omar A.K.A. Abdulkareem.** Novel Lightweight Geopolymer Concrete. *23<sup>rd</sup> International Invention, Innovation & Technology Exhibition ITEX 12. Kuala Lumpur, Malaysia. 5 May 2012. Bronze Medal.*
- **Prof. Dr. Kamarudin Hussin, Omar A.K.A. Abdulkareem, Mohd Mustafa Al Bakri Abdullah, , Assoc. Prof. Dr. Khairul Nizar Ismail, Assoc. Prof. Che Mohd Ruzaidi Ghazali, Mohammad Tamizi Selimin Muhammad Faheem B. Mohd Tahir.** Lightweight Aggregate Geopolymer Concrete (LWAGC). EXSPO, Rekacipta dan Pameran Penyelidikan Unimap 2013. *Perlis, Malaysia. 3-4 JAN 2013. Gold Medal.*
- **Prof. Dr. Kamarudin Hussin, Omar A.K.A. Abdulkareem, Mohd Mustafa Al Bakri Abdullah, Assoc. Prof. Dr. Khairul Nizar Ismail, Assoc. Prof. Che Mohd Ruzaidi Ghazali, Mohammad Tamizi Selimin, Muhammad Faheem B. Mohd Tahir.** High Fire-Resistance Lightweight Geopolymer Concrete. *Malaysian Technology Expo MTE 2013. Kuala Lumpur, Malaysia. 21-23 Feb 2013. Silver Medal.*
- **Mohd Mustafa Al Bakri Abdullah, Omar A.K.A. Abdulkareem, Prof. Dr. Kamarudin Hussin, Assoc. Prof. Dr. Khairul Nizar Ismail, Assoc. Prof. Che Mohd Ruzaidi Ghazali, Muhammad Faheem B. Mohd Tahir.** High Fire-Resistance Lightweight Geopolymer Concrete. *International Warsaw Invention Show IWIS 2013, Warsaw, Poland. 8-10 Oct 2013. Gold Medal.*